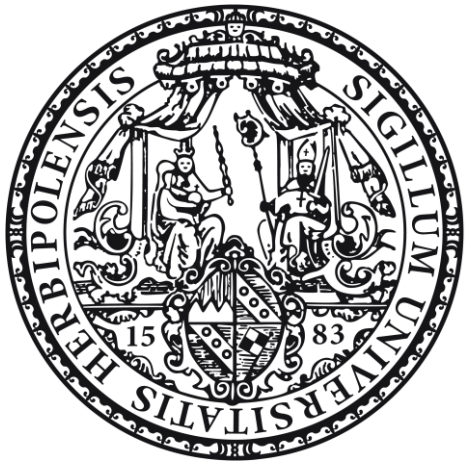

Detection of ligand dependent Frizzled conformational changes

Nachweis von Liganden-abhängigen Frizzled Konformationsänderungen

Doctoral thesis for a doctoral degree
at the Graduate School of Life Sciences,
Julius-Maximilians-Universität Würzburg,
Section: Biomedicine

submitted by

María Consuelo Alonso Cañizal

from Sevilla (Spain)

Würzburg 2018

Submitted on: …….

Members of the *Promotionskomitee*:

Chairperson: Prof. Dr. Georg Gasteiger

Primary Supervisor: Prof. Dr. Carsten Hoffmann

Supervisor (Second): Prof. Dr. med. Tobias Langenhan

Supervisor (Third): Prof. Dr. Gunnar Schulte

Date of Public Defense: …….

Date of Receipt of Certificates: …….

Affidavit

I hereby confirm that my thesis entitled "Detection of ligand dependent Frizzled conformational changes" is the result of my own work. I did not receive any help or support from commercial consultants. All sources and / or materials applied are listed and specified in the thesis.

Furthermore, I confirm that this thesis has not yet been submitted as part of another examination process neither in identical nor in similar form.

Place, Date Signature

Eidesstattliche Erklärung

Hiermit erkläre ich an Eides statt, die Dissertation „Nachweis von Liganden-abhängigen Frizzled Konformationsänderungen" eigenständig, d.h. insbesondere selbständig und ohne Hilfe eines kommerziellen Promotionsberaters, angefertigt und keine anderen als die von mir angegebenen Quellen und Hilfsmittel verwendet zu haben.

Ich erkläre außerdem, dass die Dissertation weder in gleicher noch in ähnlicher Form bereits in einem anderen Prüfungsverfahren vorgelegen hat.

Ort, Datum Unterschrift

“Science has great beauty. A scientist in his laboratory is not a mere technician: he is also a child confronting natural phenomena that impress him as though they were fairy tales.”

Marie Curie

Content

List of Figures

List of Tables

Summary

Frizzled (FZD) are highly conserved receptors that belong to class F of the G protein-coupled receptor (GPCR) superfamily. They are involved in a great variety of processes during embryonic development, organogenesis, and adult tissue homeostasis. In particular, FZD_5 is an important therapeutic target due to its involvement in several pathologies, such as tumorigenesis. Nevertheless, little is known regarding the activation of FZD receptors and the signal initiation, and their GPCR nature has been debated. In order to investigate the activation mechanism of these receptors, FRET (Förster Resonance Energy Transfer)-based biosensors for FZD_5 have been developed and characterized. A cyan fluorescent protein (CFP) was fused to the C-terminus of the receptor and the specific FlAsH-binding sequence (CCPGCC) was inserted within the 2^{nd} or the 3^{rd} intracellular loop. Single-cell FRET experiments performed using one of these sensors, V5-mFZD_5-FlAsH436-CFP, reported structural rearrangements in FZD_5 upon stimulation with the endogenous ligand WNT-5A. These movements are similar to those observed in other GPCRs using the same technique, which suggests an activation mechanism for FZD reminiscent of GPCRs. Furthermore, stimulation of the FZD_5 FRET-based sensor with various recombinant WNT proteins in a microplate FRET reader allowed to obtain concentration-response curves for several ligands, being possible to distinguish between full and partial agonists. This technology allowed to address the selectivity between WNTs and FZD_5 using a full-length receptor in living cells. In addition, G protein FRET-based sensors revealed that WNT-5A specifically induced $G\alpha_q$ activation mediated by FZD_5, but not $G\alpha_i$ activation. Other WNT proteins were also able to induce $G\alpha_q$ activation, but with lower efficacy than WNT-5A. In addition, a dual DAG/calcium sensor further showed that WNT-5A stimulation led to the activation of the $G\alpha_q$-dependent signaling pathway mediated by FZD_5, which outcome was the activation of Protein Kinase C (PKC) and the release of intracellular calcium. Altogether, these data provide evidence that the activation process of FZD_5 resembles the general characteristics of class A and B GPCR activation, and this receptor also mediates the activation of the heterotrimeric $G\alpha_q$ protein and its downstream signaling pathway. In addition, the FZD_5 receptor FRET-based sensor provides a valuable tool to characterize the pharmacological properties of WNTs and other potential ligands for this receptor.

Zusammenfassung

Frizzled (FZD) sind hochkonservierte Rezeptoren welche zur Klasse F der G- Protein-gekoppelte Rezeptor Superfamilie gehören. Diese haben wichtige Funktionen in verschiedenen physiologischen Prozessen wie zum Beispiel Embryonalentwicklung, Organogenese und adulte Gewebe-homöostase. FZD_5 ist aufgrund seiner Beteiligung an verschiedenen pathologischen Prozessen wie der Tumorgenese ein wichtiges therapeutisches Ziel. Jedoch ist über die Aktivierung und Signalauslösung der FZD Rezeptoren sehr wenig bekannt und deren GPCR Eigenschaften sind umstritten. Um den Aktivierungsmechanismus dieser Rezeptoren zu untersuchen, wurden FRET (Förster Resonance Energy Transfer)-basierte FZD_5 Biosensoren entwickelt und charakterisiert. Ein cyan fluoreszierendes Protein (CFP) wurde an den C-Terminus des Rezeptors fusioniert und die FlAsH-bindende Sequenz (CCPGCC) wurde im 2. oder 3. intrazellulären Loop eingefügt. Einzel-zell FRET Versuche mit dem Sensor V5-mFZD_5-FlAsH436-CFP haben gezeigt, dass Stimulation mit dem endogenen Ligand WNT-5A zur FZD_5 Konformationsänderungen führt. Diese Konformationsänderungen sind ähnlich wie bei anderen GPCRs, was darauf hinweist, dass der FZD Aktivierungsmechanismus vergleichbar mit dem von GPCRs ist. Außerdem wurde der FZD_5 FRET-basierter Sensor mit verschiedenen rekombinierten WNT Proteinen stimuliert und mit einem FRET-Platten Reader gemessen, was die Erstellung von Konzentrations - Wirkungskurven und die Unterscheidung zwischen Voll- und Partialagonisten ermöglichte. Diese Methode erlaubte es, die Selektivität zwischen WNTs und FZD_5 mittels des Volllängenrezeptors in lebenden Zellen zu untersuchen. Zudem haben G-Protein FRET-basierte Sensoren gezeigt, dass WNT-5A die FZD_5 vermittelte $G\alpha_q$ Aktivierung jedoch nicht die $G\alpha_i$ Aktivierung spezifisch induziert. Andere WNT Proteine können auch die $G\alpha_q$ Aktivierung induzieren aber mit geringerer Effizienz als WNT-5A. Ein doppelter DAG/Calcium Sensor hat zudem gezeigt, dass WNT-5A Stimulation zu einer durch FZD_5 vermittelten Aktivierung der $G\alpha_q$-abhängigen Signaltransduktionkaskade führt, was zur Aktivierung der Protein Kinase C (PKC) und zur Freisetzung intrazellulären Calciums führt. Zusammenfassend wurde in der vorliegenden Arbeit die Ähnlichkeit des FZD_5 Rezeptors zur Klasse A und B der GPCRs bezüglich allgemeinen Eigenschaften und Aktivierung verdeutlicht. Zudem vermittelt dieser Rezeptor die Aktivierung der $G\alpha_q$-abhängigen Signaltransduktionkaskade. Ein FZD_5 Rezeptor FRET-basierter Sensor stellt ein wertvolles Werkzeug zur pharmakologischen Charakterisierung der WNTs und anderer potentiellen FZD_5 Liganden dar.

1. Introduction

1.1. Brief history

1.1.1. Discovery of WNTs

In the second half of 20th century, intensive research in cancer had led to the discovery of several viral oncogenes and their precursors, which were called proto-oncogenes (Nusse and Varnus, 2012). This term refers to any cellular gene that has the potential to cause cancer, which could happen, for instance, by mutations or by insertion of oncogenic retroviruses.

The mouse mammary tumor virus (MMTV) is a murine retrovirus involved in the development of breast cancer. A systematic analysis looking for insertion sites of the MMTV in the genome led to the identification of the gene *int1*, a proto-oncogene that was activated by MMTV in many tumors (Nusse and Varnus, 1982). After its discovery, however, it proved to be quite difficult to determine the function of the protein and its mechanism of action, as well as generating antibodies to detect it or identifying its cellular receptor and components of the pathway (Nusse and Varnus, 2012). It was known, however, that *int1* was expressed only during embryogenesis and that it was highly conserved in evolution. In 1987, a homologue of *int1* was found in the genome of *Drosophila melanogaster* and was named *Dint1* (Rijsewijk et al., 1987). This gene turned out to be identical to *Wingless*, a segment polarity gene involved in development (Cabrera et al., 1987). *Wingless* had been identified years before for its role in pattern specification during gastrulation. Its name derived from the phenotype that results from mutations in the gene: the cells responsible of producing an adult wing led to the formation of a thoracic notum instead (Swarup and Verheyen, 2012; Cabrera et al., 1987). *Wingless* (*wg*) was involved in various steps of development in different tissues. Further studies showed that *int1* was also involved in embryonic axis formation in *Xenopus Laevis*; therefore it was also important in vertebrate development (McMahon and Moon, 1989).

Later discoveries of other mammalian genes related to *int-1*, all potential secreted polypeptides, led to the characterization of the WNT family (Nusse et al., 1991). The name WNT was proposed as an acronym from the combination of *wingless* and *int-1*. Subsequently, *int-1* was renamed as *WNT-1*. During the following years, many studies identified components of the WNT pathway in vertebrates, such as the APC (Adenomatous Polyposis Coli) protein or

β-catenin, which was a homologue of *Armadillo*, another segment polarity gene in Drosophila. Gradually, GSK3 (glycogen synthase kinase 3), DVL (Dishevelled) and Axin were identified, and the signaling pathway began to develop (Nusse and Varnus, 2012).

1.1.2. Receptors for WNT proteins

Back in 1944, Calvin Bridges and Katherine Brehme reviewed many different mutants of *Drosophila melanogaster* (Bridges and Brehme, 1944). One particular mutation in a locus produced irregular and curly hairs in comparison to the *wild-type* (wt) fly, and irregular bristles on thorax, wings and feet. Consequently, this locus was called *Frizzled*. Years later, the product of the *Frizzled* locus was found to be an essential protein for polarity patterns in several tissues, both transmitting and interpreting the polarity signal (Vinson and Adler, 1987). This gene actually led to a seven-transmembrane protein whose extracellular and intracellular domains allowed it to achieve both cellular functions (Vinson et al., 1989; Krasnow and Adler, 1994). The structure of the protein was also reminiscent of GPCRs (Schulte, 2010).

The fact that Frizzled could interact with Dishevelled in Drosophila (Krasnow et al., 1995), a known member of the Wingless pathway (Perrimon and Mahowald, 1987), finally led to the discovery of a *Frizzled* homologue in the human genome. From that, a family of several Frizzled could be identified, and its interaction with WNTs was described. In 1996, Frizzled was officially recognized as WNT receptor (Nusse and Varnus, 2012; Bhanot et al., 1996). A few years later, the protein Arrow was identified in Drosophila as a co-receptor for WNT. *Arrow* was another segment polarity gene that belonged to the Low density lipoprotein receptor-Related Protein (LRP) family (Wehrli et al., 2000). In addition, other receptors for WNT include the trans-membrane tyrosine kinases of the ROR and RYK families (van Amerongen R et al., 2008).

In 2005, the International Union of Pharmacology (IUPHAR) included 10 Frizzled (FZD_{1-10}) and one Smoothened (SMO) receptors as a separate class F within the GPCR superfamily (Foord et al., 2005). The classification considered the 7-transmembrane (7TM) structure of the receptors, with an extracellular N-terminus and an intracellular C-terminus; the sequence similarity to the Secretin receptors of class B, including conserved cysteines in the extracellular loops; and the fact that coupling to G proteins had been suggested for some of them (Lagerström and Schiöth, 2008; Malbon, 2004).

1.2. WNT-FZD signaling

The discovery of WNT proteins and FZD receptors led to the emergence of an extensive and complex field of research. Since then, several cellular pathways have been described, which are involved in different biological processes during development, tissue homeostasis and stem cell maintenance and regulation. In mammals, 19 WNT proteins and 10 FZDs are known, but the interaction between ligands and receptors is intricate, and could differ depending on tissue localization, or the presence of specific extracellular and intracellular partners, which could drive the activation of certain downstream signaling pathways (**Fig. 1**). In the next sections, an overview of the main components of the pathways that will be mentioned throughout this thesis (1.2.1) and the most well established signaling cascades (1.2.2) is provided.

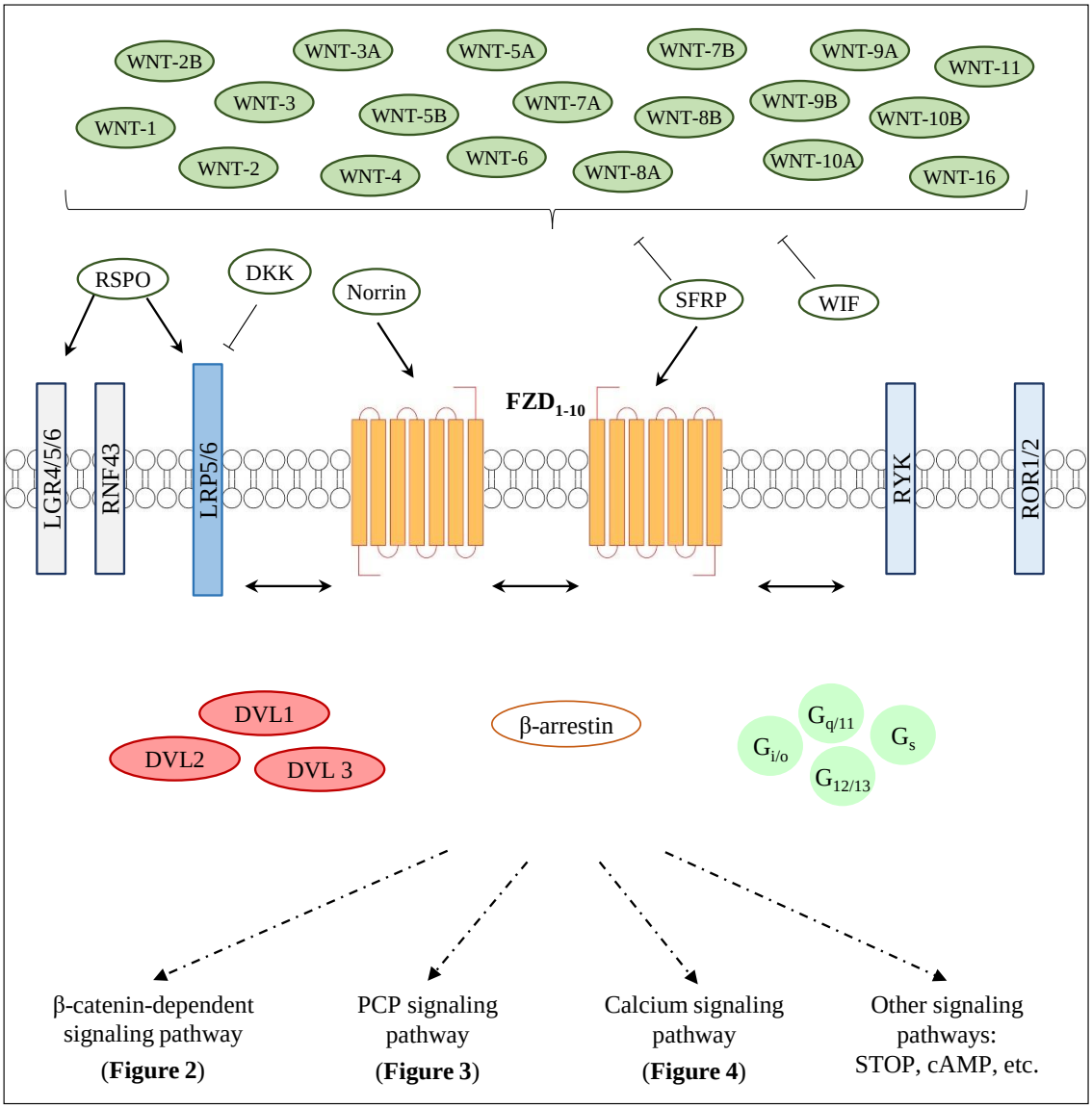

Figure 1. Overview of the main WNT signaling components.

1.2.1. Main components of the pathways

1.2.1.1. WNT proteins

WNTs are secreted lipoglycoproteins that act as morphogens. They are highly conserved in animals, although they are not present in plants, fungi or unicellular organisms (Holstein, 2012). WNTs present two main posttranslational modifications: acylation and glycosylation. During their transit through the endoplasmic reticulum, WNTs are acylated by Porcupine, which adds palmitoleic acid groups. Then, in the Golgi, WNTs associate with Wls/Evi, which transport them to the plasma membrane. They are later released to the extracellular space, where they can travel variable distances and exhibit signaling activity to other cells, acting in a paracrine or autocrine manner. These modifications make WNTs highly hydrophobic proteins and, in fact, detergents are needed for purification and *in vitro* maintenance (Grainger and Willert, 2018; Foulquier et al., 2018; Nusse and Clevers, 2017). The first active purified WNT was the mouse WNT-3A (Willert et al., 2003), followed by WNT-5A (Schulte et al., 2005).

Crystallization of Xenopus WNT-8 in complex with the cysteine-rich domain (CRD) of mouse FZD_8 showed that the structure of WNTs is formed by two distinct domains that are reminiscent of a 'hand'. This assembling allows WNTs to interact with two different binding sites in the receptor. The N-terminus of WNT is considered the 'thumb' and carries a palmitoleic acid group, stablishing lipid-mediated contacts with the CRD; the C-terminal domain, which would be the 'finger', binds the CRD through protein interactions. Although there is a high degree of conservation in the amino acids of the finger region, slight differences may influence so that WNTs have preferences for some FZDs-CRDs and interact with the receptors with different binding affinities. The fact that WNTs can activate tyrosine receptors, such as ROR2, which also has a CRD, and FZD with or without LRP5/6, suggests that the binding between WNT and FZD might be enough to induce receptor activation. Moreover, FZD activation may also occur due to WNT-induced receptor dimerization (Janda et al., 2012).

WNTs can be classified by their ability to induce secondary body axis formation in Xenopus. WNT-1/-3A/-7A/-7B/-8 are considered to induce that phenotype and, thus, to activate the β-catenin signaling pathway. On the contrary, WNT-4/-5A/-5B/-6/-11 have been shown to induce PCP (Planar Cell Polarity) signaling, and WNT-5A/-11 also induce intracellular calcium (Ca^{2+}) release (Foulquier et al., 2018; De A, 2011; Kohn and Moon, 2005).

1.2.1.2. Cellular receptors

FZDs are the main receptors for the WNT family. Their structure and functions will be described in detailed in section 1.3.2. In addition, WNTs can also activate the tyrosine kinase receptors RYK and ROR1/2 (Green et al., 2014). These single transmembrane domain receptors are generally involved in canonical and non-canonical signaling pathways, respectively. LRP5/6 are also single transmembrane domain receptors that act as co-receptors with FZD to activate β-catenin signaling pathway (**Fig. 1 and 2**). In addition, WNTs can bind to components of the extracellular matrix (ECM), such as Glypicans. At some level, they act as receptors or co-receptors, competing with FZDs. These interactions influence WNT concentration at the cell surface, as well as allow the diffusion of the ligand and the creation of WNT gradients (Filmus et al., 2015; Capurro et al., 2014; Schulte, 2010).

1.2.1.3. Dishevelled

Dishevelled is thought to play a central role in all FZD-mediated signaling pathways (**Fig. 1**). It receives, integrates and propagates the information, leading to the activation of one or other signaling cascade. In mammals, three isoforms have been described: DVL1, DVL2 and DVL3.

DVL proteins have three conserved domains: an N-terminal DIX, a central PDZ, and a C-terminal DEP domain. The DIX domain mediates polymerization of DVL and interaction with Axin, cooperating in signalosome assembling. The PDZ (atypical postsynaptic density 95/disc-large/zona occludens-1) domain mediates interaction with other proteins which have a PDZ-binding domain, like FZD receptors. The DEP (Dishevelled, Egl-10, Pleckstrin) domain also allows interaction with other proteins, such as DAAM1 (Dishevelled-associated activator of morphogenesis 1). Additionally, DVL presents a basic region located between DIX and PDZ that consists of conserved serine and threonine residues, and a proline-rich region situated between PDZ and DEP (Sharma et al., 2018).

DVL can interact with FZD receptors at three different motifs, one located in the C-terminus and the other two in the 3rd intracellular loop (ICL-3) of the receptor. The PDZ domain of DVL is thought to interact only with the C-terminus of FZD, while the DIX domain does not bind directly to the receptor. The DEP domain can interact with the three motifs in the receptor, but also with negatively charged lipids in the membrane in order to stabilize the interaction (Tauriello et al., 2012).

1.2.2. WNT-FZD signaling pathways

The interaction between WNTs and FZDs can lead to the activation of diverse signaling pathways. Traditionally, they have been classified as canonical (β-catenin-dependent) and non-canonical (β-catenin-independent). This last group is broad and complex, and among others, it includes the PCP, calcium, and STOP pathways.

1.2.2.1. β-catenin-dependent signaling pathway

The WNT/β-catenin-dependent signaling pathway is an evolutionary conserved communication system that regulates different aspects during embryonic development and adult tissue homeostasis. It is involved in several functions, such as cell fate determination, differentiation, stem cell renewal, and tumorigenesis (Steinhart and Angers, 2018; Nusse and Clevers, 2017).

In the absence of WNTs (**Fig. 2,** left panel), the levels of β-catenin in the cytoplasm are low due to the existence of a 'destruction complex', also called 'Axin degradosome' (Gammons and Bienz, 2018). This complex is constitutively active and it comprises the kinases GSK3α/β and CK1α (casein kinase 1α), plus Axin and APC tumor suppressor, both of them acting as scaffolding proteins. Axin homo-polymerizes through its DIX domains, generating filaments that allow the assembly of the other members of the complex. APC also interacts with Axin and itself. Both proteins facilitate the serine/threonine phosphorylation of β-catenin at its N-terminus by the kinases, which leads to the release of β-catenin from the complex. Subsequently, β-catenin is recruited by the E3 ubiquitin ligase β-Trcp. Ubiquitination of β-catenin targets it for proteasomal degradation (Steinhart and Angers, 2018; Foulquier et al., 2018; Yu and Virshup, 2014; Niehrs, 2012). In the nucleus, Groucho/TLE is associated with the nuclear transcription factor LEF/TCF (lymphoid enhancer-binding factor/T cell-specific), which represses the expression of target genes (Gammons and Bienz, 2018).

In addition, in the absence of WNTs, DVL is likely bound to FZD receptor as a monomer through its DEP domain and mediates the association of FZD to RNF43/ZNRF3 (Gammons and Bienz, 2018). These E3 ubiquitin ligases are target genes of the pathway; therefore, by targeting FZD for endocytosis and degradation, they act as negative feedback regulators. RNF43 is also a co-receptor of LGR4/5/6 (**Fig. 1**). Binding of the R-spondin secreted proteins (RSPO1-4) to LGR4/5 and RNF43/ZNRF3 decreases the activity of the ligases and thus increases the presence of FZD in the membrane (Yu and Virshup, 2014).

In the presence of WNT proteins (**Fig. 2,** right panel), WNT favors the dimerization between FZD receptor and the LRP5/6 co-receptor, by binding both and bringing them closer together. Consequently, there is an increased concentration of DVL close to the membrane that leads to homo-polymerization of DVL through its DIX domains, which also increases its avidity for Axin. Therefore, the 'degradosome' is recruited to the membrane and Axin stablishes hetero-polymers with DVL via their DIX domains. At the same time, GSK3 and other kinases phosphorylate LRP5/6 at its C-terminus. Later binding of GSK3 to the phosphorylated tail of LRP5/6 inhibits the kinase and brings Axin closer to LRP5/6. The fine molecular mechanisms of this process are still not fully understood. This series of events leads to the formation of a 'WNT signalosome' (WNT-FZD-LRP5/6-DVL-Axin complex), which inhibits the destruction complex and leads to the accumulation of β-catenin in the cytoplasm. Further dimerization of DVL through its DEP domain causes the dissociation of DVL from FZD (Steinhart and Angers, 2018; Gammons and Bienz, 2018; Nusse and Clevers, 2017).

Increasing levels of β-catenin in the cytoplasm leads to the translocation of the protein to the nucleus, where it is captured by the scaffold protein BCL9/Legless. That leads to the reorganization of a complex called 'WNT enhanceosome' (Gammons and Bienz, 2018), which also includes a chromatin-binding protein called Pygo, TCF/LEF, ChiLS and Groucho/TLE. As a consequence, LEF/TCF becomes a transcriptional activator of β-catenin target genes. Some of these genes include regulators of the pathway, genes involved in cell cycle or in stem cell regulation.

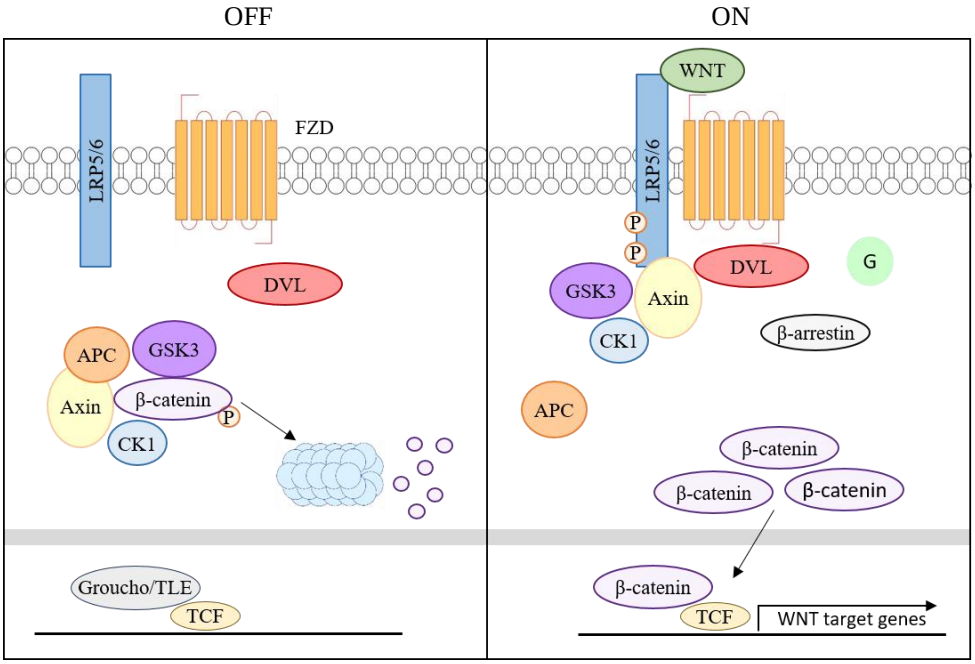

Figure 2. WNT/FZD-mediated β-catenin-dependent signaling pathway.

1.2.2.2. PCP signaling pathway

Frizzled was first identified due to a mutation in a Drosophila locus. This protein belonged to an evolutionary conserved pathway that controlled cell migration and tissue polarity. In order to generate structures and tissues, cells move and organize according to the information that they receive, regarding for instance position in an epithelial plane or apical-basal polarity. The planar cell polarity refers to the cellular orientation, primarily in epithelial or mesenchymal cells, and it regulates many processes during development. It is a β-catenin-independent pathway and one of the most studied non-canonical signaling routes (Humphries and Mlodzik, 2018; Komiya and Habas, 2008; Seifert and Mlodzik, 2007). Dysregulations in the pathway have been linked to tumor progression and angiogenesis (Wang, 2009).

The PCP pathway comprises six essential proteins, organized in two complexes that localize in opposite sides of the cell. On one hand, the FZD receptor, Celsr (Flamingo in Drosophila), and the cytoplasmic proteins DVL and Inversin/Diversin (Diego in Drosophila). On the other hand, the transmembrane proteins Van Gogh-like 1 and 2 (Vangl1/2; Strabismus in Drosophila) and Celsr, and the cytoplasmic protein Prickle. Vangl1 is able to interact with a FZD receptor from an adjacent cell, stabilizing both complexes. In addition, components of the complexes within one cell inhibit each other, contributing to the spatial separation (Foulquier et al., 2018; Seifert and Mlodzik, 2007).

Within the FZD-DVL complex (**Fig. 3**), the interaction between DVL and DAAM1 leads to the activation of the small GTPases Rho and Cdc42, as well as the Rho-associated kinase (ROCK), which ultimately induces actin polymerization and cytoskeletal reorganization (Komiya and Habas, 2008). In addition, DVL can also interact and activate Rac1, which leads to the phosphorylation and activation of the c-JUN-N-terminal kinase (JNK), and the JNK/p38-type MAP kinase pathway. Subsequently, transcription factors, such as c-Jun, are activated (Foulquier et al., 2018; Yang and Mlodzik, 2015).

The role of WNTs in PCP signaling is still not fully understood, although they are thought to modulate the interaction between FZD and Vangl1 and, therefore, altering the balance between the two complexes. Binding of WNT to its receptor would lead to the internalization of the complex and the activation of the signaling cascade.

FZD_3 and FZD_6 have been described to participate in PCP signaling. Besides them, other receptors for PCP might include ROR1/2, RYK or PTK7. Some of the ligands that have been found to activate the pathways are WNT-4, WNT-5A, WNT-5B or WNT-11 (Foulquier et al., 2018; Komiya and Habas, 2008; Katoh, 2005). Other regulators of the pathway include CK1ε or the heterotrimeric $G\alpha_o$ protein (Seifert and Mlodzik, 2007). In addition, protein kinase A (PKA) has been shown to act as a negative regulator of the pathway, by interacting and inhibiting RhoA.

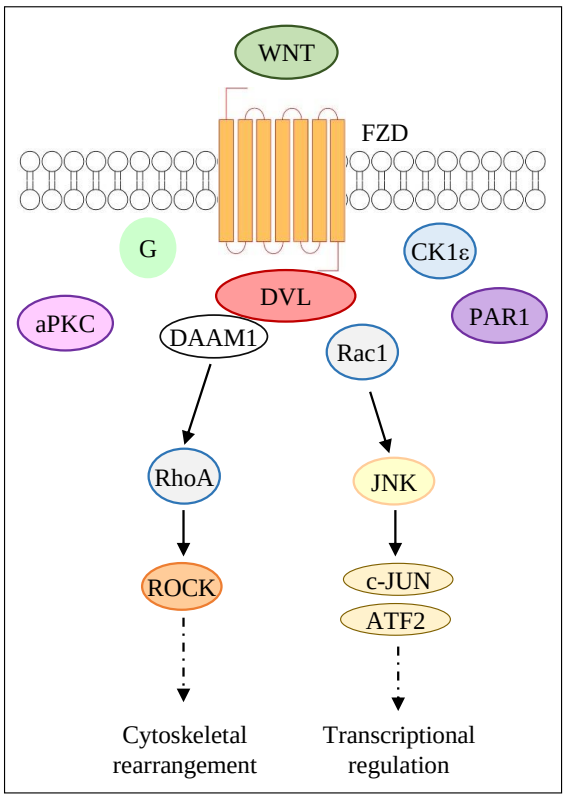

Figure 3. WNT/FZD-mediated PCP signaling pathway.

1.2.2.3. Calcium signaling pathway

In 1997, embryogenesis studies in Zebrafish revealed that Xenopus WNT-5A might induce or modulate the intracellular calcium signaling pathway (Slusarski et al., 1997a); additionally, overexpression of some FZD receptors mediated intracellular calcium release in a G protein-dependent manner (Slusarski et al., 1997b). A couple of years later, it was shown that certain combinations of WNT and FZD, such as co-expression of rat FZD_2 and Xenopus WNT-5A, led to the translocation of PKC to the plasma membrane; PKC activation was probably dependent on G proteins and independent of β-catenin (Sheldahl et al., 1999). In addition, some FZDs and WNTs, which had been reported to induce calcium release and PKC activation, were also able to activate the calcium/calmodulin-dependent protein kinase II (CaMKII) in Xenopus embryos. This activation was pertussis toxin (PTX)-sensitive and occurred several minutes after receptor activation (Kühl et al., 2000a).

Interestingly, WNT proteins that were known to induce the β-catenin-dependent signaling pathway did not seem to induce intracellular calcium release, whereas those WNTs that activated PKC and CaMKII did not stabilize β-catenin. Both pathways also showed antagonistic effects over each other. Moreover, WNTs induced different cellular responses depending on the FZD receptor (Kühl et al., 2000a). In view of all of this, the WNT-dependent calcium pathway was described as the first non-canonical WNT signaling route in vertebrates (Kühl et al., 2000b). At that time, G proteins were suspected to be required, although no direct interaction between Frizzled and G proteins had been shown.

The signaling cascade starts with the binding between WNT and FZD (**Fig. 4**), although other receptors, like ROR1/2, have been described to activate the pathway. The active receptor induces the activation of Phospholipase C (PLC), which in many GPCRs occurs upon the dissociation of the heterotrimeric $G\alpha_q$ protein. PLC catalyzes the hydrolysis of phosphatidylinositol 4,5-bisphosphate (PIP_2) into the second messengers diacylglycerol (DAG) and inositol trisphosphate (IP_3). While DAG remains in the plasma membrane, IP_3 mediates the release of calcium from the endoplasmic reticulum. Calcium and DAG collaborate to activate PKC, which translocates to the membrane to bind DAG. In addition, calcium and calmodulin activate CaMKII. Finally, PKC, CaMKII, and calcium lead to the activation of several nuclear transcription factors, such as NFkB, CREB or NFAT (De, 2011; Kohn and Moon, 2005).

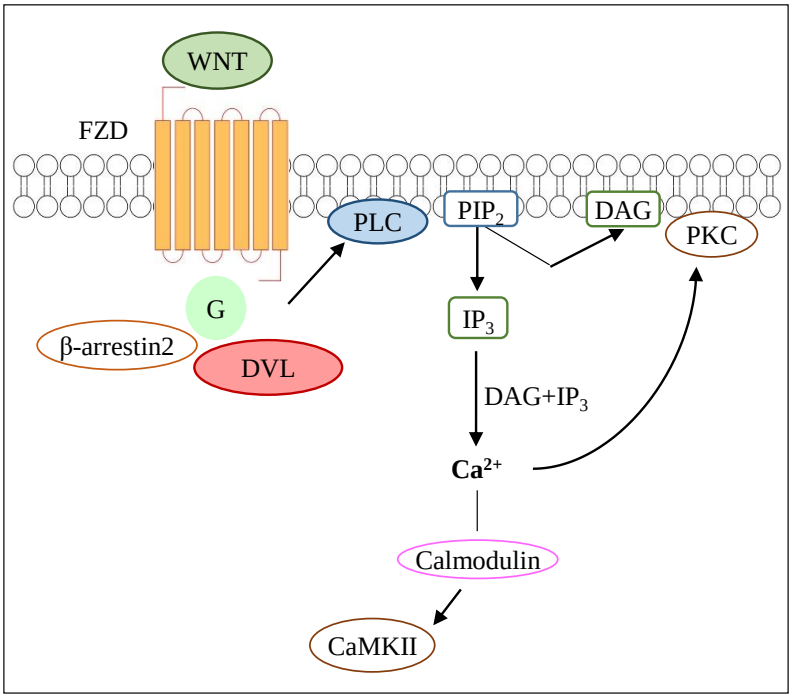

Figure 4. WNT/FZD-mediated calcium signaling pathway.

WNT/Ca^{2+} signaling regulates cell adhesion and cell movements (Kühl et al., 2000b). Additionally, it modulates different aspects during development, including convergent extension movement, body plan specification and formation of organs (De, 2011; Kohn and Moon, 2005). In fact, some of the functions partially overlap with PCP signaling, and sometimes both pathways are activated by the same WNTs and FZDs (Seitz et al., 2014). DVL, which was known to play a role in both β-catenin and PCP pathways, was also suggested to participate in Ca^{2+} signaling (Sheldahl et al., 2003).

Furthermore, another intracellular effector shared by the three signaling cascades is β-arrestin2. Despite its role in GPCR desensitization, β-arrestin2 is a positive regulator of WNT signaling. In WNT/Ca^{2+} pathway, it is thought to interact and form a complex with DVL and Gβ subunit, contributing to signal transduction (Seitz et al., 2014). Since β-arrestin2 can interact with all three isoforms of DVL, it appears that the composition of the complex may influence the activation of different WNT signaling routes (Gentzel et al., 2015).

1.2.3. WNT-FZD selectivity and specificity

The selectivity between WNTs and FZDs is one of the main open questions in the field and it has not been fully addressed, although it is beginning to be understood (Dijksterhuis et al., 2014). As previously mentioned, WNTs are hydrophobic proteins, which further complicates to investigate WNT-FZD affinity and specificity. While WNT-1/-3/-3A/-7A/-7B/-8A/-8B/-10A/-10B have been shown to induce β-catenin-dependent signaling in combination with certain receptors, WNT-4/-5A/-5B/-6/-11 are traditionally considered non-canonical ligands, as detailed in the previous section (1.2.1.1).

In 2010, for instance, the relative affinity of the interaction between certain WNTs and the CRD of FZD_5 and FZD_{10} was measured by using an ELISA-based technique (Carmon et al., 2010). Purified WNT-3A was able to interact with CRD-FZD_5 (K_d=83.7nM) and induced β-catenin activation (EC_{50}=5nM), as measured by the TopFlash assay. WNT-5A was not determined to bind CRD-FZD_5 nor to activate the β-catenin signaling pathway.

The binding affinities of several recombinant WNT proteins to various FZDs were further investigated by means of using bio-layer interferometry, employing only the CRDs and not the complete receptors (Dijksterhuis et al., 2015). These experiments suggested that WNT binds FZD with high affinity. Regarding FZD_5, WNT-3A and WNT-5A showed strong binding (K_D<10nM) to the CRD of the receptor, whereas WNT-4 and WNT-5B only exhibited intermediate binding (K_D: 10-40nM). Steady state was reached for 200nM WNT, the maximal measured concentration, in approx. 500 seconds. Focusing on WNT-5A, this ligand only showed strong binding to the CRD of $FZD_{5/8}$. WNT-3A displayed strong or intermediate binding to all the tested CRD-FZD, and activated β-catenin-dependent pathway via $FZD_{4/5/7/8}$.

Recently, using CRISPR/Cas9 technology and genetic rescue experiments, a map of certain WNT-FZD interactions was published (Voloshanenko et al., 2017), and it showed that not all the tested WNTs were able to induce β-catenin signaling via all the receptors. Interestingly, the apparent selectivity between WNT and FZD might be linked to the phylogenetic relation of the receptors. WNT-3 and WNT-3A induced β-catenin-dependent signaling through $FZD_{1/2/7}$, whereas WNT-7A did so only via FZD_5, and WNT-7B through FZD_5 and FZD_8. These two last receptors seem to be the most variable, being able to bind more different ligands. In particular, WNT-1/-7B/-8A/-8B/-9B/-10A were shown to induce canonical signaling via FZD_5 and FZD_8, and WNT-3A/-7A via FZD_5 but not FZD_8. WNT-9A was not found to signal through FZD_5.

1.3. Frizzled as G protein-coupled receptors

FZDs were recognized as WNT receptors in 1996 and incorporated into the GPCR superfamily in 2005, although their GPCR nature has been questioned since then. Over the last years, research has also focus on understanding the relation and similarities between FZDs and other well-known GPCRs, as well as investigating G protein activation mediated by FZDs, and connecting this role with the traditional WNT-mediated signaling pathways. The focus of this project is the FZD_5 receptor, regarding its activation mechanism and its ability to mediate G protein activation and signaling. Therefore, the next sections provide an overview of the GPCR family, its signaling mechanisms, and the FZD receptors.

1.3.1. GPCR superfamily

G protein-coupled receptors constitute the largest family of membrane proteins in the human genome, with more than 800 receptors described to date (Lagerström and Schiöth, 2008; IUPHAR/BPS Guide to Pharmacology). In 1994, Kolakowski developed a database (GPCRdb) in order to collect all the information regarding these receptors and introduced a novel A-F classification based on sequence homology. From that, several nomenclature systems have been published. One of the most used nowadays is the GRAFS classification system, which organizes the GPCRs into five main families: Rhodopsin (class A), Secretin (class B), Glutamate (class C), Adhesion, and Frizzled/Taste2 (Fredriksson et al., 2003).

GPCRs can be found in almost every organ of the body and they respond to a great variety of stimuli, modulating various signaling pathways and cellular responses. Consequently, they are also involved in a multitude of disorders and thus constitute important pharmaceutical targets. Nowadays, almost 40% of FDA approved drugs target GPCRs (Sriram and Insel, 2018; Hauser et al., 2017).

In order to be classified as a GPCR, a receptor should fulfill two conditions. On one hand, to have seven membrane-spanning domains. All GPCRs have in common their structure, consisting of a single protein, with an extracellular N-terminus, an intracellular C-terminus, seven-transmembrane domains, three extracellular (ECL) and three intracellular (ICL) loops. On the other hand, the ability to interact with and activate G proteins. Although many of these receptors mediate signal transduction through G protein activation, G protein coupling has not been described for all of them (Fredriksson et al., 2003).

1.3.1.1. GPCR activation mechanism and signaling outcome

Generally, upon ligand binding, the GPCR undergoes conformational changes that lead to rearrangements in the intracellular domains. These movements allow the engagement and activation of signaling effectors, which leads to the subsequent activation of downstream signaling pathways, whether G protein-dependent or independent (*i.e.* mediated by β-arrestins or by G protein-coupled receptor kinases (GRKs); Hilger et al., 2018; Lohse et al., 2014; Kobilka, 2007). Distinct ligands have the ability to stabilize different conformational states in the receptor, thus modulating receptor activity. Ligands that are able to induce the maximal signaling response are named full agonists, whereas partial agonists only induce a submaximal response, and inverse agonists decrease the basal activity (Kauk and Hoffmann, 2018; Galandrin et al., 2007).

Some of the main intracellular effectors of GPCRs are G proteins, which are formed by three subunits: Gα, Gβ, and Gγ. Depending on the Gα subunit, four major families have been described in humans: G_s, $G_{q/11}$, $G_{i/o}$, and $G_{12/13}$. In the inactive state, GDP-bound Gα forms a heterotrimer with Gβγ. Receptor activation induces the engagement of the inactive heterotrimeric protein, which leads to GDP release. As a consequence, GTP binds to the 'empty' Gα subunit, which undergoes conformational changes that ultimately lead to the dissociation of Gα and Gβγ. Separately, both subunits regulate different signaling cascades. Last, GTP is hydrolyzed to GDP by Gα, which then re-associates with Gβγ (Hilger et al., 2018; Mahoney and Sunahara, 2016; Oldham and Hamm, 2008).

Regarding the signaling pathways, $G\alpha_s$ activates adenylyl cyclase (AC), which in turn stimulates cAMP production, leading to the activation of PKA. $G\alpha_i$ has the opposite effect, by inhibiting the production of cAMP. Moreover, $G\alpha_i$ protein is PTX-sensitive; therefore, detecting PTX-sensitive G-proteins has become a useful readout to investigate G protein activation, as mentioned in section 1.2.2.3 for WNTs/FZDs. $G\alpha_q$ induces the activation of PLC, which ultimately leads to calcium release and PKC activation (**Fig. 4**). $G\alpha_{12/13}$ regulates signaling of Rho GTPases. Furthermore, Gβγ subunits can recruit GRKs and modulate other signaling effectors, such as AC, PLC, or calcium and potassium channels (Milligan and Kostenis, 2006).

1.3.1.2. Overview of GPCR subfamilies

- **Rhodopsin-like receptors**

The IUPHAR currently includes 719 receptors within the rhodopsin family, which corresponds to almost 90% of all human GPCRs (IUPHAR/BPS Guide to Pharmacology). That makes class A the largest group within the GPCR superfamily, and it is also highly heterogeneous, including receptors involved in olfaction, vision or taste. These receptors have been found not only as monomers, but also forming oligomers. Variability can be found in the structure but also regarding the ligand, from small molecules to peptides or photons. However, most receptors have in common a short N- and C- termini (Lagerström and Schiöth, 2008). For many of these receptors, the ligands bind in a cavity between the transmembrane regions and the extracellular loops (Fredriksson et al., 2003). Some of these receptors have been associated with very fast processes. For instance, the α- and β-adrenergic, A_{2A}-adenosine and muscarinic receptors are activated in about 50ms (Lohse et al., 2012).

A representative member of this family is Rhodopsin, which was also the first crystallized GPCR (Palczewski et al., 2000). Following this structure, and subsequent studies, a novel mechanism of receptor activation was proposed, by which ligand binding induces the rearrangement of the transmembrane helices, especially TM6, allowing the interaction with G protein, β-arrestin and GRK (Hilger et al., 2018; Lohse et al., 2014).

- **Secretin-like receptors**

Class B, originally considered as family B1, comprises 15 receptors in humans, including the Secretin, Glucagon and Glucagon-like, and Parathyroid hormone (PTH) receptors. Due to their involvement in a large number of diseases, they are of great pharmaceutical interest. They have in common a long N-terminus and a short C-terminus. While the sequence of the N-terminus varies between receptors, all of them stablish cysteine bridges between the cysteines in the first and second extracellular loops and the N-terminus. Furthermore, family B receptors can be found forming homomers and heteromers (de Graaf et al., 2017; Roed et al., 2012; Lagerström and Schiöth, 2008).

All class B receptors respond to peptide hormones, in general short or medium-size peptides, through a binding mechanism called ‘two-domain model’. The first step in this model, by which the C-terminus of the ligand binds to the N-terminal domain of the receptor, determines the

affinity and specificity of the binding. In the second step, the N-terminal region of the ligand interacts with the core domain of the receptor, which leads to receptor activation (Roed et al., 2012; Castro et al., 2005). This binding mechanism, different from many class A receptors, results in slower kinetics. For instance, the PTHR was determined to be activated within one second (Castro et al., 2005; Vilardaga et al., 2003).

Interestingly, the PTHR presents a PDZ recognition sequence (KSxxxW) in its C-terminus, similar to the one found in FZD receptors (Romero et al., 2010). This motif allows the interaction between PTHR and DVL, and the subsequent activation of β-catenin independently of WNTs. Therefore, it is important to note that besides FZD, other GPCRs can recruit DVL and activate β-catenin-dependent signaling pathway.

- **Glutamate receptors**

Class C is formed by 22 receptors, which among others include the metabotropic glutamate, the $GABA_B$, the calcium-sensing, and the sweet and umami taste receptors (Roed et al., 2012; Lagerström and Schiöth, 2008). Both the metabotropic glutamate and the $GABA_B$ receptors are found in the central neural system (CNS) and therefore constitute an important therapeutic target (Chun et al., 2012). Most members of the family have a large N-terminus, which contains a Venus flytrap (VFT) module. It involves two domains, creating a cavity where the ligand binds and induces receptor activation. Even though binding occurs only to the N-terminus, allosteric ligands are thought to interact with the transmembrane domains of the receptors. Additionally, and similarly to FZD receptors, the N-terminal region also contain a CRD, which connects the VFT to the transmembrane domains. In contrast to other GPCRs, receptors from class C form constitutive dimers and their activation mechanism is unique (Chun et al., 2012; Lagerström and Schiöth, 2008; Pin et al., 2004).

- **Adhesion receptors**

Originally considered as part of the class B, as B2 subfamily, the adhesion class constitutes the second largest family of GPCRs, with 33 members in humans that are organized in nine subfamilies. These receptors are evolutionary conserved and most of them have in common a long N- and C-termini, and a GAIN domain that includes a proteolytic motif (GPS). The large N-terminal tail allows interactions with components of the matrix and with other cells. Although they are thought to bind extracellular matrix molecules, the endogenous ligand is unknown for

many of them. Similarly to other GPCRs, they have cysteine residues in the extracellular loops 1 and 2 (Hamann et al., 2015; Langenhan et al., 2013; Lagerström and Schiöth, 2008). Some members of this family are implicated in planar cell polarity, such as Celsr1, which is associated with FZD receptors and DVL (Langenhan et al., 2013).

- **Frizzled/Taste2**

The fifth class of GPCRs can be subdivided into two groups. On one hand, the Taste2 receptors, which in humans include 25 bitter taste receptors, although many are still orphans. On the other hand, a second group composed of ten Frizzled receptors ($FZD_{1–10}$) and one SMO (Lagerström and Schiöth, 2008). FZD and SMO share the common structure of other GPCRs, consisting of 7TM domains, as well as one extracellular N-terminal and one intracellular C-terminal domains. FZD can be subdivided into four families: FZD_1, FZD_2 and FZD_7; FZD_5 and FZD_8; FZD_4, FZD_9 and FZD_{10}; FZD_3 and FZD_6 (Schulte, 2010).

1.3.2. FZD receptors

1.3.2.1. Sequence and structure

FZDs have a large N-terminus, which contains a signal peptide and a CRD similar to the class C GPCRs (**Fig. 5**). This region is considered the orthosteric site of these receptors and is the main responsible for ligand binding, although it is still not clear if it is involved in signal transduction. Moreover, it is also unknown how the bound ligand leads to receptor activation. Besides the CRD, there might be other binding sites in the extracellular loops. The CRD is highly conserved, and in fact most of the cysteines are also found in the SMO receptor, which underlines the idea that the CRD has other functions besides binding the ligand (Schulte, 2010; Lagerström and Schiöth, 2008; Schulte and Bryja, 2007). Additionally, the CRD is also involved in receptor dimerization.

The main interaction partners of FZD are the WNT proteins, although other molecules have been described to bind these receptors or their co-receptors (**Fig. 1**), such as RSPOs, the soluble Frizzled-related proteins (sFRPs), and Norrin, which specifically interacts with FZD_4 (Lagerström and Schiöth, 2008; Schulte and Bryja, 2007).

FZDs share several domains with other GPCRs, for example, cysteines in the 1st and 2nd extracellular loops, or charged residues in the 3rd intracellular loop that are important for

coupling to G proteins. However, they also lack other relevant motifs for this function. In addition, some FZDs may form a helix VIII in the C-terminus, which has been linked to G protein coupling. In the C-terminus, the KTxxxW sequence is conserved in all FZDs but not in SMO. This motif is a PDZ-binding sequence, which allows the interaction with proteins with a PDZ domain, especially DVL (Schulte, 2010; Schulte and Bryja, 2007). As previously mentioned, this sequence can be found in other GPCRs, such as the PTH receptor.

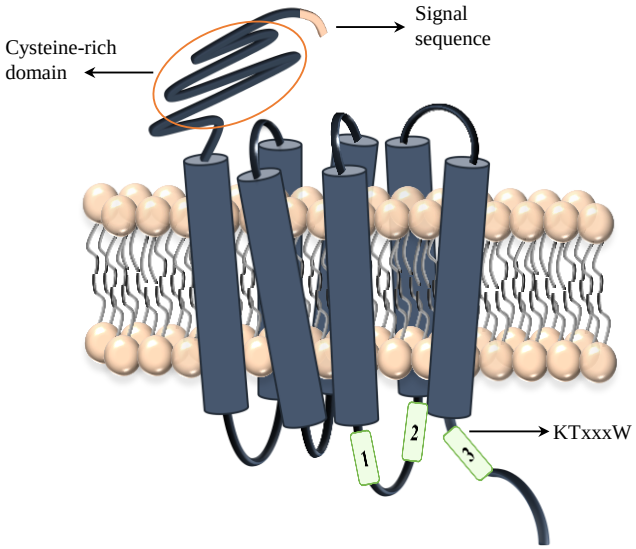

Figure 5. General FZD_5 receptor structure. The protein has 7TM domains. The CRD is highlighted in the N-terminus with an orange circle. The three motifs of interaction with DVL in the C-terminus and ICL-3 are shown in green. The conserved sequence KTxxxW is found in the C-terminus.

1.3.2.2. FZD receptors oligomerization

Similarly to other GPCRs, FZDs can form homo- and hetero-dimers (**Fig. 1**). Several signaling pathways require the interaction of FZD with co-receptors, such as LRP5/6 in β-catenin-dependent signaling (Angers and Moon, 2009). FZDs are thought to dimerize via their transmembrane domains or their CRDs. In fact, FZD-FZD interactions are thought to be enough to induce activation of β-catenin signaling in the absence of WNTs (Schulte, 2010).

Currently, the stoichiometry of the ligand-receptor complex is unknown. A widespread hypothesis suggests a 1:2 model, where binding of one WNT molecule would promote FZD receptor dimerization through their CRDs (Nile et al., 2017). In addition, dimerization of FZD might lead to the formation of high-order oligomers. This model was suggested for FZD_5, FZD_7 and FZD_8. The crystal structure of the CRD of FZD_4 supported this 1:2 stoichiometry and

revealed higher-order complexes. WNT-5A induced FZD_4 dimerization, and subsequent oligomerization, by binding two CRDs (DeBruine et al., 2017). FZD_6 has been shown to form constitutive homodimers in the inactive state, which dissociate upon WNT stimulation (Petersen et al., 2017).

FZD receptor dimerization appears to be important, not only for assembling of components of the pathways, but also for signaling. Therefore, it emerges as a potential factor to be considered in Frizzled pharmacology (Wang et al., 2018; Zhang et al., 2018; Ferré, 2015). A better knowledge of the stoichiometry of the complexes, the association or dissociation of receptors upon ligand binding, or the conformational rearrangements that FZDs and CRDs could undergo upon dimerization, would contribute to understand the activation process of FZD and the selective activation of signaling pathways.

1.3.2.3. Crystal structures: SMO vs FZD_4

The SMO receptor belongs to the Frizzled family and it is an important component of the Hedgehog signaling pathway. Similarly to FZD, SMO contains a CRD. Crystallization of the SMO receptor revealed a 7TM structure, a short helix VIII located parallel to the membrane, and long extracellular loops. In general, although the sequence similarity between SMO and class A GPCRs is quite low, the overall 3D structure of SMO is highly conserved. An important difference refers to the conserved prolines in helices V, VI and VII of class A, which are involved in receptor activation and the movement of helix VI. These prolines are missing in SMO, but several glycines in the same helices could provide flexibility and contribute to conformational changes upon receptor activation (Wang et al., 2013). Another crystal structure of SMO bound to the antagonist Vismodegib revealed that, upon binding of the compound to the transmembrane domains (TMD), the receptor undergoes a conformational change that involves a movement of helix VI, and leads to a reorganization in the structure of the CRD (Byrne et al., 2016). Furthermore, binding of cholesterol induces a movement in the CRD that leads to structural rearrangements in the receptor, which includes the extracellular part of helix VI and the ECL-3. Overall, the activation mechanism appears to be different from other GPCRs (Zhang et al., 2017). However, the recent structure of the sterol-activated SMO shows a reorientation of the CRD upon ligand binding that, through allosteric communication, induces a conformational change in the TMD reminiscent of class A and B GPCR activation (Huang et al., 2018).

The structure of the transmembrane domains of FZD_4 was solved in a ligand-free state and it also lacked the CRD. Similarly to SMO, the structure of FZD_4 revealed 7TM helices, as well as a short helix VIII packed parallel to the membrane. This helix VIII contains the conserved sequence KTxxxW for interaction with PDZ proteins, such as DVL. The extension of the helix VI is shorter than the one found in SMO. In addition, this helix VI remains packed and stable in a close conformation, which could prevent the conserved movement observed in other GPCRs upon activation. In contrast, two bends in helix VII may be involved in receptor activation (Yang et al., 2018).

In addition, the hinge region and the extracellular loops of FZD_4 are quite compact, much more than in class B and C GPCRs. Moreover, the transmembrane pocked of FZD_4 is tight, and no cavity exists between helices III, VI and VII, which suggests that FZD_4 cannot accommodate ligands in the traditional transmembrane binding pocket or allosteric modulators in the said cavity. Besides being too narrow, the transmembrane binding pocked is also quite hydrophilic due to the presence of polar residues, which would negatively affect the binding affinity of a ligand. It is then possible that the nature of the pocket has hindered the design of drug molecules so far (Zhang et al., 2018; Yang et al., 2018).

Altogether, there seem to be some marked differences between SMO, and thus other known crystallized GPCRs, and FZD_4 regarding ligand binding and activation mechanism. It is still unclear how WNT induces FZD activation, whether WNT binds only to the CRD and that leads to a conformational change in that region, like in class C GPCRs, or there might be also an interaction with the extracellular regions of the receptor, like in class B. Since the FZD_4 receptor was crystallized in an inactive, ligand-free state, it is possible that WNT-induced activation would produce a rearrangement that opens the receptor at its transmembrane regions, and would thus facilitate the interaction with intracellular partners.

1.3.2.4. FZD receptors and G proteins

G protein activation mediated by FZD receptors was suggested for the first time when WNT-5A was found to induce calcium signaling in embryos (Slusarski et al., 1997a), as detailed in section 1.2.2.3. Evidence of G protein activation linked to FZD has accumulated through the years and has been recently reviewed (Wright and Schulte, 2018). Nevertheless, little is known about the selectivity between FZD and G proteins, and it is still not clear whether all the receptors of the family can in fact couple to G proteins.

Lately, the use of microscopy techniques have reported activation of G proteins mediated by overexpressed FZD receptors in living cells. For instance, FZD_6 has been shown to be pre-coupled to $G\alpha_{i1}$ and $G\alpha_q$, but not $G\alpha_{o/s/12}$. Stimulation with the ligand WNT-5A induced the dissociation of the complex. Interestingly, the interaction between the receptor and the G protein was dependent on the expression levels of DVL. Therefore, DVL is thought to play a dual role, regulating the FZD_6-G protein interaction at endogenous levels, but inhibiting it at high or low concentrations (Kilander et al., 2014). In contrast, FZD_4 forms an inactive complex with $G\alpha_{12/13}$, but not with $G\alpha_{s/i/o/q}$, and this process is independent of the intracellular levels of DVL. Upon stimulation with WNT-3A/-5A/-7A/-10B, FZD_4-$G\alpha_{12/13}$ dissociates and regulates RhoGEF proteins (Arthofer et al., 2016). Meanwhile, FZD_{10} is able to form an inactive complex with $G\alpha_{13}$ but not with $G\alpha_{12}$ or $G\alpha_{s/i/o/q}$. This process does not require DVL, although high levels of this protein negatively affects the interaction. Stimulation with WNT-5A and WNT-7A, but not WNT-3A, induces $G\alpha_{13}$ activation and YAP/TAZ signaling (Hot et al., 2017).

1.3.2.5. FZD_5 receptor

FZD_5 is expressed in several tissues during development and regulates diverse cellular functions. For instance, it is involved in synaptogenesis in the hippocampus (Sahores et al., 2010), in neural development (Slater et al., 2013) and in inflammatory responses (Blumenthal et al., 2006). In addition, FZD_5 is a potential therapeutic target in tumorigenesis. Up-regulation of this receptor has been implicated in several types of cancer, such as breast cancer, renal cell carcinoma, or pancreatic ductal adenocarcinoma cells (Zeng et al., 2018; Steinhart et al., 2017). Furthermore, the axis WNT-5A/FZD_5 is also implicated in Alzheimer's disease and rheumatoid arthritis (Dijksterhuis et al., 2014). Interestingly, WNT-5A exhibits anti-tumor effects mediated by FZD_5 in prostate cancer (Thiele et al., 2018).

FZD_5 is a 585 amino acids length receptor that belongs to the same subfamily than FZD_8, with which shares 70% identity. These two receptors appear to be quite promiscuous, being able to interact with many different WNT proteins. Particularly, FZD_5 has been described to interact with WNT-1/-2/-3/-3A/-5A/-7A/-7B/-8A/-8B/-9B/-10A/-10B/-11 in different contexts, as discussed in section 1.2.3 (Voloshanenko et al., 2017; Dijksterhuis et al., 2015). These interactions may lead to the activation of various signaling pathways. The two best described ligands for FZD_5 are WNT-3A and WNT-5A. While the first one is linked to β-catenin dependent signaling, WNT-5A has been found to be implicated in both canonical and non-canonical cascades. WNT-5A/FZD_5 induced axis duplication in Xenopus (Ishikawa et al., 2001; He X et al., 1997), a phenotype associated with canonical signaling, but also PKC activation (Weeraratna et al., 2002) and CaMKII signaling (Chen et al., 2015). Moreover, FZD_5 has been suggested to induce G protein activation, although direct proof is still missing.

Generally, in many GPCRs, the interfaces for β-arrestin (Kang et al., 2015) and G protein (Carpenten et al., 2016) binding are found in ICL-2, ICL-3 and the C-terminus. To some extent, these areas of interaction appear to be conserved in FZD receptors. Moreover, the ICL-3 and the C-terminus of FZD_5 are described binding sites for DVL (**Fig. 5**; Tauriello et al., 2012), and some residues in ICL-1 and ICL-2 are also thought to contribute to this binding (Gammons et al., 2016). Therefore, there appears to be an overlapping between the contact areas of FZD_5 with DVL and G proteins, which suggests that FZD_5 could not bind the two proteins simultaneously.

Altogether, FZD_5 arises as an interesting pharmacological target. In order to better understand its GPCR nature, its selectivity for WNTs and its interaction with G proteins, FRET technology will be employed, which has been successfully used before to investigate other GPCRs. Therefore, FRET is described in detail in the following section (1.4).

1.4. Förster Resonance Energy Transfer

In living organisms, the spatio-temporal control of protein complexes regulates the activation and deactivation of different signaling cascades. In order to investigate protein-protein interactions and molecular proximity in living cells, several technologies have been developed, which include Fluorescence Correlation Spectroscopy (FCS; Briddon et al., 2018), Bioluminescence Resonance Energy Transfer (BRET; Stoddart et al., 2018) or fluorescence imaging techniques, such as Förster Resonance Energy Transfer (FRET; Kauk and Hoffmann, 2018) or Fluorescence Recovery After Photobleaching (FRAP; Veerapathiran and Wohland, 2018).

1.4.1. FRET microscopy

FRET is a non-radiative technique that normally involves two fluorescent molecules, a donor and an acceptor, that are found relatively close to each other, generally between 1 and 10nm (10-100Å). When the donor is in an excited electronic state, it transfers energy to the acceptor through long-range dipole-dipole interactions (**Fig. 6**). Therefore, several requirements must be fulfilled in order for FRET to occur: first, the distance between the fluorophores should be less than 100Å; second, the dipole moments of both molecules should have a relative orientation towards each other, being FRET higher if the orientation is parallel; and third, the donor emission spectrum should overlap with the acceptor excitation spectrum (Kremers, Piston, and Davidson, 2018; Lohse et al., 2012).

The existence of energy transfer between the fluorophores can be demonstrated by quenching of the acceptor fluorescence, which leads to an increase in the donor fluorescence emission. This concept is called FRET efficiency (E), and it can be determined by using the following formula: $E = 1/[1 + (r/R_0)^6]$, being r the distance between the two fluorophores, and R_0 the distance where FRET efficiency is 50%. This optimal value R_0, also known as 'Föster distance', can be determined for any pair of fluorophores, although it is normally around 4-6nm. If the two fluorophores are relatively far from each other or two close, r would be much higher or lower than R_0, and thus the FRET efficiency will be low or high. In practice, this may result in the absence or existence of FRET between the fluorophores, so exploring optimal positions for the two fluorophores and determining the FRET efficiency would be a first step in FRET applications (Kremers, Piston, and Davidson, 2018; Stumpf and Hoffmann, 2016; Jares-Erijman and Jovin, 2003). Therefore, FRET efficiency has been determined for the FZD_5 FRET-based biosensors developed in this project.

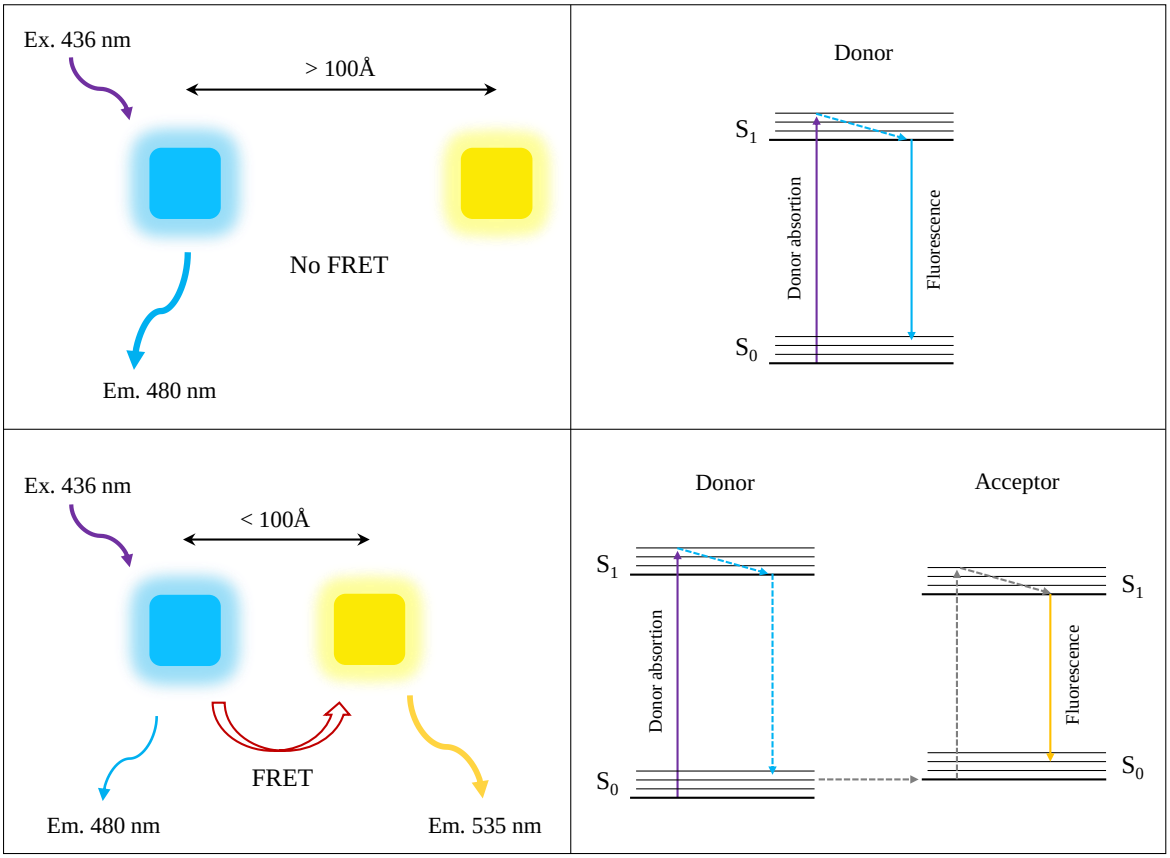

Figure 6. Fundaments of FRET. An excited donor fluorophore is able to transfer energy to an acceptor fluorophore if there is an overlapping between the spectra, and the distance between the fluorophores and the orientation of the dipole moments are adequate.

FRET technique can be used in live-cell experiments by using different approaches, such as: 1. FLIM, which detects the donor lifetime; 2. acceptor photobleaching, which is also used for determining the FRET efficiency, as previously mentioned; 3. spectral imaging, where the spectral profile of both molecules is measured; 4. sensitized emission. This last approach consists of exciting the donor at its optimal wavelength and collecting the emission fluorescence of both fluorophores by using specific filters. Since there is an overlapping between the spectra of the fluorophores, it is important to correct the measured FRET signal for bleed-through, cross excitation, and leakage of the donor fluorescence into the acceptor detection channel (Kremers, Piston and Davidson, 2018; Lohse et al., 2012).

Nowadays, many different FRET pairs have been described, and the most common involves the cyan and yellow fluorescent proteins (ECFP-EYFP). Some variants have been introduced along the years, like using TFP or Cerulean instead of CFP, or Venus instead of YFP. In addition, other pairs include green or red proteins, such as green fluorescent protein

(EGFP)-mCherry, Venus-mCherry or Venus-tdTomato (Kremers, Piston and Davidson, 2018). Nevertheless, one disadvantage of the fluorescent proteins is their size, of around 30KDa. Insertion of one or two fluorophores in a protein could thus alter its structure or function. An alternative is the use of smaller fluorophores (Tian et al., 2017), such as FlAsH (Fluorescein Arsenical Hairpin) or ReAsH (Resorufin Arsenical Hairpin). In particular, FlAsH is a compound of 700Da that specifically binds the six amino acid sequence CCPGCC. FlAsH becomes fluorescent when attached to its binding-motif, exhibiting similar properties to YFP. It can be used in combination with CFP or its derivatives to perform dynamic FRET experiments (Hoffmann et al., 2005).

1.4.2. FRET-based sensors to investigate GPCR activation and signaling

FRET microscopy is one of the most used techniques for investigating GPCR activation and signaling. It can be used to monitor conformational changes within one protein, by introducing a pair of fluorophores in the same molecule (so called biosensor; **Fig. 7**), or to measure protein-protein interactions, such as receptor oligomerization, by fusing each fluorophore to a different molecule. Therefore, FRET has helped to understand the interactions between ligand-receptor, receptor-G protein, and receptor-β-arrestin, as well as to determine the kinetics of receptor and G protein activation and deactivation, or to investigate the formation of second messengers, such as cAMP (Vilardaga et al., 2013; Lohse et al., 2012; Nikolaev et al., 2004).

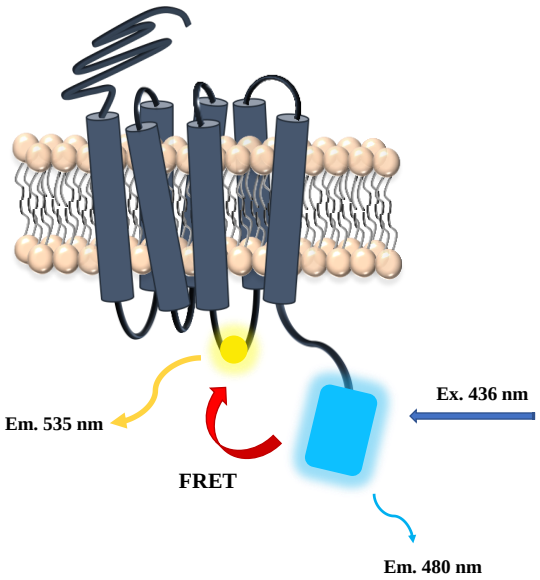

Figure 7. FZD_5 receptor FRET-based biosensor. CFP was fused at the end of the C-terminus and the FlAsH-binding motif was inserted either in ICL-2 or ICL-3. Ligand-induced conformational changes would alter the relative distance between the fluorophores and thus lead to a change in FRET.

The first GPCR FRET-based sensors were published in 2003 (Vilardaga et al., 2003) for two receptors, the α_{2A}-adrenergic receptor and the PTHR. These sensors allowed to monitor for the first time activation of these receptors in living cells. The pair of fluorophores CFP and YFP were inserted into the C-terminus and the third intracellular loop of each receptor, although considerable optimization was needed in order to find the best positions for both fluorophores. In 2016, FRET-based sensors for 18 different GPCRs had been published, which belong to class A, B and C (Stumpf and Hoffmann, 2016). At that time, no FRET-based sensors for FZD receptors had been published. These sensors make possible to monitor dynamic movements of a receptor and determine the activation kinetics. In addition, they also provide information about full and partial agonists, which stabilize different states when bound to their receptor (Kauk and Hoffmann, 2018; Vilardaga et al., 2009). Biosensors that report intramolecular conformational changes also exist for β-arrestins (Nuber et al., 2016), and for G proteins, in which the fluorophores are tagged to the Gα and Gβγ subunits (**Fig. 8**; Adjobo-Hermans et al., 2011; Bünemann et al., 2003).

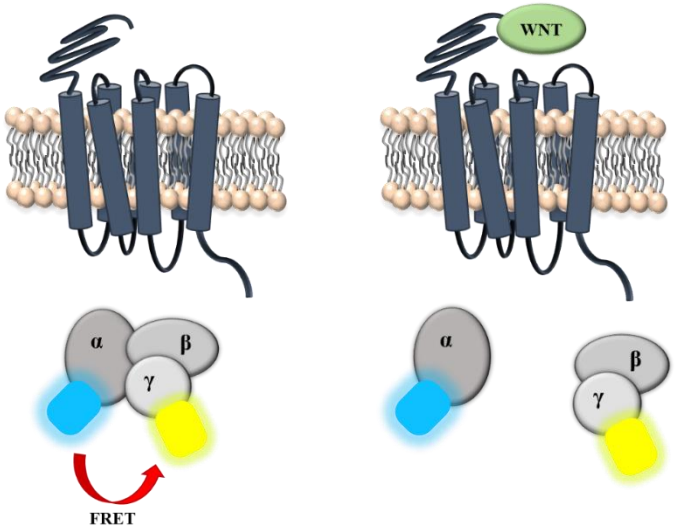

Figure 8. G protein FRET-based sensor. Upon activation, the receptor mediates the dissociation between Gα and Gβγ subunits, leading to a decrease in the FRET signal.

In order to investigate the activation process of FZD_5 receptor, FRET-based biosensors for this receptor have been developed within the scope of this project (**Fig. 7**). In addition, FRET-based sensors for G proteins (**Fig. 8**) have been also used in this project to further investigate G protein activation mediated by FZD_5.

2. Motivation

WNTs and FZDs are part of an evolutionary conserved mechanism that regulates many processes involved in embryonic development, regulation of adult stem cells and tissue homeostasis. Dysregulations in these signaling pathways are linked to important human pathologies, such as tumorigenesis, neurodegenerative diseases or cardiovascular disorders. Therefore, it is crucial to understand how cells receive WNT signals and relay this information. Furthermore, investigating the pharmacological properties of FZD receptors becomes essential in order to improve the development of drugs targeting these receptors. Several questions still remain open regarding WNT-FZD specificity, ligand affinity, or FZD-G protein interaction.

Crystal structures of receptors provide information about the molecular mechanisms implicated in ligand binding and receptor activation. Nevertheless, structures do not allow to investigate dynamic events, like the conformational movements that the receptor undergoes upon ligand binding and how it transmits the information to intracellular partners. Therefore, FRET technology will be employed to investigate the mechanisms of FZD receptor and G protein activation by various WNT proteins, with focus on FZD_5 receptor.

The main goals of this PhD project include:

- Development and characterization of FZD_5 receptor FRET-based biosensors.
- Investigate the conformational changes that the FZD_5 receptor undergoes upon activation.
- Optimize a procedure that allows screening of ligands.
- Explore ligand-receptor specificity, and ligand- and concentration-dependent changes in receptor conformation.
- Characterize the signaling behavior of WNTs with regard to FZD_5 by using FRET-based sensors for G proteins.
- Investigate the specific activation of the $G\alpha_q$-mediated PLC signaling pathway by means of using a dual DAG/calcium sensor.

3. Materials and Methods

3.1. Materials

3.1.1. DNA

DNA	Vector	Information	Source	Bacterial resistance
Mouse, V5-mFZD$_5$	pcDNA3.4	V5-tagged at the N-terminus	Madelon Maurice (UMC, Utrecht)	Ampicillin
Mouse, V5-mFZD$_5$-CFP	pcDNA3	ECFP fused at the end of the C-terminus of the receptor	This thesis	Ampicillin
Mouse, V5-mFZD$_5$-FlAsH436-CFP	pcDNA3	ECFP at the end of the C-terminus of the receptor. FlAsH-binding sequence inserted within ICL-3 between Gly436 and Gly437	This thesis	Ampicillin
Mouse, V5-mFZD$_5$-FlAsH439-CFP	pcDNA3	ECFP at the end of the C-terminus of the receptor. FlAsH-binding sequence inserted within ICL-3 between Lys439 and Thr440	This thesis	Ampicillin
Mouse, V5-mFZD$_5$-FlAsH436	pcDNA3.4	FlAsH-binding sequence inserted within ICL-3 between Gly436 and Gly437	This thesis	Ampicillin
Mouse, V5-mFZD$_5$-FlAsH439	pcDNA3.4	FlAsH-binding sequence inserted within ICL-3 between Lys439 and Thr440	This thesis	Ampicillin
Mouse, V5-mFZD$_5$-FlAsH349-CFP	pcDNA3	ECFP at the end of the C-terminus of the receptor. FlAsH-binding sequence inserted within ICL-2 between Gly349 and Asn350	This thesis	Ampicillin
Mouse, V5-mFZD$_5$-FlAsH354-CFP	pcDNA3	ECFP at the end of the C-terminus of the receptor. FlAsH-binding sequence inserted within ICL-2 between Ala354 and Gly355	This thesis	Ampicillin
Mouse, V5-mFZD$_5$-mCherry	pmCherry-N1	mCherry at the end of the C-terminus of the receptor	This thesis	Kanamycin
Mouse, V5-mFZD$_5$-GFP	pcDNA3	EGFP fused at the end of the C-terminus of the receptor	This thesis	Ampicillin
Mouse, V5-mFZD$_5$-YFP	pcDNA3	EYFP fused at the end of the C-terminus of the receptor	This thesis	Ampicillin
pcDNA (control)	pcDNA3		Vítězslav Bryja (MU, Brno)	Ampicillin
FLAG-DVL1			Gunnar Schulte (KI, Stockholm)	Ampicillin
HA-DVL2			Gunnar Schulte (KI, Stockholm)	Ampicillin
GFP-DVL2			Gunnar Schulte (KI, Stockholm)	Kanamycin
GFP-DVL3	pEGFP		Vítězslav Bryja (MU, Brno)	Kanamycin
Downward DAG2 + R-GECO	pUB2.1		Tewson et al., 2012	Ampicillin

DNA	Vector	Information	Source	Bacterial resistance
Human, M_3AChR-CFP	pcDNA3	ECFP fused at the end of the C-terminus of the receptor	Hoffmann et al., 2012	Ampicillin
Human, M_1AChR-CFP	pcDNA3	ECFP fused at the end of the C-terminus of the receptor	Meserer et al., 2017	Ampicillin
Human, M_1AChR-FlAsH-CFP	pcDNA3		Meserer et al., 2017	Ampicillin
$G\alpha_q$				Ampicillin
$G\beta_1$	pcMV			Ampicillin
$G\gamma_2$				Kanamycin
Gi protein trimers ($G\alpha_{i1}$, $G\alpha_{i2}$ and $G\alpha_{i3}$)	Clontech-style N1	pGβ_1-2A- cp173Venus -Gγ_2-IRES-Gα_i-mTurquoise2-Δ9	van Unen et al., 2016	Kanamycin
$G\alpha_q$ protein trimer		$G\alpha_q$-mTqΔ6 + $G\beta_1$ + cpVenus-$G\gamma_2$	Adjobo-Hermans et al., 2011	Kanamycin

3.1.2. PCR primers

DNA	Description	Primers
V5-mFZD$_5$-CFP	Deletion of the STOP codon TAA	Forward: 5'- ATC TGG TGG GTC ATC CTG TC-3' Reverse: 5'-CTG ATG TCT AGA TAC GTG CGA CAG GGA CAC TTG-3'
V5-mFZD$_5$-FlAsH436-CFP	Insertion of FlAsH-binding motif in ICL-3	Forward-1: 5'-TGT TGC CCG GGC TGC TGT GGC ACT AAG ACG GAC AAG CTA-3' Forward-2: 5'-AGC GTC ATC AAG CAG GGT TGT TGC CCG GGC TGC TGT G-3' Forward-3: 5'-TCA CTC TTC CGC ATC CGG AGC GTC ATC AAG CAG GGT TGT-3' Reverse: 5'-CTG ATG TCT AGA TAC GTG CGA CAG GGA CAC TTG-3'
V5-mFZD$_5$-FlAsH439-CFP	Insertion of FlAsH-binding motif in ICL-3	Forward-1: 5'-TGT TGC CCG GGC TGC TGT ACG GAC AAG CTA GAG AAG CTC-3' Forward-2: 5'-AAG CAG GGT GGC ACT AAG TGT TGC CCG GGC TGC TGT ACG-3' Forward-3: 5'-CGC ATC CGG AGC GTC ATC AAG CAG GGT GGC ACT AAG TGT-3' Reverse: 5'-CTC ACT CTA GAT ACG TGC GAC AG-3'
V5-mFZD$_5$-FlAsH349-CFP	Insertion of FlAsH-binding motif in ICL-2	Forward: 5'-GGC ATG AAG TGG GGC TGT TGC CCG GGC TGC TGT AAT GAA GCC ATC GCA-3' Reverse: 5'-TGC GAT GGC TTC ATT ACA GCA GCC CGG GCA ACA GCC CCA CTT CAT GCC-3'
V5-mFZD$_5$-FlAsH354-CFP	Insertion of FlAsH-binding motif in ICL-2	Forward: 5'-AAT GAA GCC ATC GCA TGT TGC CCG GGC TGC TGT GGT TAT GCA CAG TAC-3' Reverse: 5'-GTA CTG TGC ATA ACC ACA GCA GCC CGG GCA ACA TGC GAT GGC TTC ATT-3'
V5-mFZD$_5$-mCherry	Insertion of a BglII site	Forward: 5'-CAG TAA GCT TAG ATC TAC CAT GGT CCC GTG CAC GCT G-3' Reverse: 5'-GTG CGC ACC TTG TTG TAG AG-3'
	Insertion of an AgeI site	Forward: 5'-CAG TGT CAA GTC CAT TAC GG-3' Reverse: 5'-AGC AGT ACC GGT TGT ACG TGC GAC AGG GAC ACT TG-3'

Name	Description	Primers
GPO	Mycoplasma PCR	5'-ACT CCT ACG GGA GGC AGC AGT-3'
MGSO	Mycoplasma PCR	5'-TGC ACC ATC TGT CAC TCT GTT AAC CTC -3'

* Sequencing of DNA and development of primers for cloning were done by Eurofins Genomics.

3.1.3. Cell lines

Cell line	Description
HEK 293	
HEK 293 T	
HEK 293 V5-mFZD$_5$-CFP	Homogeneous stable cell line expressing the receptor construct V5-mFZD$_5$-CFP
HEK 293 V5-mFZD$_5$-FlAsH436-CFP	Homogeneous stable cell line expressing the receptor FRET sensor V5-mFZD$_5$-FlAsH436-CFP
HEK 293 V5-mFZD$_5$-FlAsH439-CFP	Heterogeneous stable cell line expressing the receptor FRET sensor V5-mFZD$_5$-FlAsH439-CFP
HEK 293 Downward DAG2/R-GECO	Homogeneous stable cell line expressing the dual DAG/calcium sensor
HEK 293 V5-mFZD$_5$-CFP + Downward DAG2/R-GECO	Homogeneous stable cell line co-expressing the dual DAG/calcium sensor and the receptor V5-mFZD$_5$-CFP
HEK 293 M$_3$AChR-CFP + Downward DAG2/R-GECO	Homogeneous stable cell line co-expressing the dual DAG/calcium sensor and the receptor M$_3$AChR-CFP
HEK 293 DVL KO	Knock-out cell line for all three Dishevelled protein isoforms (from Gunnar Schulte, KI, Stockholm)

3.1.4. Software

Software	Supplier	Version
Adobe (Reader / Acrobat / Illustrator)	Adobe	CS6
Biovoxxel-ImageJ (Fiji Windows 64Bit)		
Clampex / Clampfit	Molecular Devices, LLC	10.3
ClustalX2	Clustal	2.1
Gen5™ Data Analysis	BioTek	
GraphPad	Prism	7
Leica AF	Leica	Leica AF
Microsoft Office	Microsoft	2013
OriginPro (64Bit)	OriginLab Corporation	9.0.0
Serial Cloner		2.6.1

3.1.5. Consumables

Bacteria	Supplier
E. coli DH5α	Invitrogen

Enzymes and related reagents	Supplier
Nucleotides	New England Biolabs
Pfu polymerase and Pfu polymerase buffer	Promega
Restriction enzymes and buffers	New England Biolabs
T4 DNA Ligase and Ligase buffer	New England Biolabs
Taq polymerase and Taq polymerase buffer	New England Biolabs
QuikChange Lightning Site-Directed Mutagenesis Kit	Agilent Technologies

Ligands	Size	Reference	Lot
Recombinant Mouse Wnt-2b Protein	25µg	R&D 3900-WN-025	DCWK0316111 DCWK0418021
Recombinant Mouse Wnt-3a Protein	10µg	R&D 1324-WN-010	HTR11316041 HTR11117111
Recombinant Human/Mouse Wnt-5a Protein	10µg	R&D 645-WN-010	MCR4916121 MCR4917121
Recombinant Mouse Wnt-5b Protein	25µg	R&D 3006-WN-025	SCI1416121
Recombinant Mouse Wnt-8a Protein	10µg	R&D 8419-WN-010	DDTZ0515111
Recombinant Mouse Wnt-9a Protein	25µg	R&D 8148-WN-025	DDDM0517081
Recombinant Mouse Wnt-9b Protein	25µg	R&D 3669-WN-025	SKP2914101
Recombinant Mouse Wnt-10b Protein	10µg	R&D 2110-WN-010	TTU2515081
Recombinant Mouse Wnt-16b Protein	25µg	R&D 9148-WN-025	DFPI0316081
Recombinant Mouse WIF-1 Protein, CF	50µg	R&D 135-WF-050	DQJ0515081
Carbachol		Alfa Aesar	
Control- and WNT-5A-conditioned medium		Vítězslav Bryja (Brno)	

Expendable materials	Supplier	Cat. No. / Ref.
6-well plates	Sarstedt	83.3920
12-well plates	Sarstedt	83.3921
24-well plates	Sarstedt	83.3922
96-well plates	Sarstedt	83.3924
100mm plates	Sarstedt	83.3902
150mm plates	Sarstedt	83.3903
"Attofluor" Cell chamber	Molecular Probes	
Black 96-well BRAND-plates, flat bottom cellGrade	Brand	781968
Cell culture flask 25cm^2		
Cryo-Tubes	Nunc/ThermoScientific	375418 / 368632
Eppendorf Research Plus , 8-channel, variable 1-10µl / 10-100µl / 30-300µl	Eppendorf	3125000010 / 3125000036 / 3125000052
Eppendorf Xplorer plus, 8-channel, variable, 5-100µl	Eppendorf	4861 000.783
Falcon tubes (15ml, 50ml)	Becton Dickinson	
Gloves – SensiCare Ice / Peha-soft nitrile	Medline / Hartmann	486802 / 942207
Neubauer chamber		
Parafilm M	Bemis	PM-996
PCR tubes (0.5 ml)	Eppendorf	
Pipettes (P2.5, P10, P100, P1000)	Eppendorf	
Pipettes tips	SurPhob biozym	VT 0270/0230/0200/0240
Protein LoBind Tubes 1.5ml	Eppendorf	022431081
Round glass coverslips 13mm		
Round glass coverslips 24mm	Hartenstein	0111640
Safe-Lock Tubes 1.5ml	Eppendorf	0030120.086
Syringe filtration unit Filtropur S0.2	Sarstedt	83.1826.001
WillCo-dish® 40mm glass bottom dishes	WillCo Wells	GWST-5040/1.5-0.5
µ-Slide 8 wells	Ibidi	

Commercial kits	Supplier	Cat. No. / Ref.
DNA Gel Extraction Kit	Millipore	LSKGEL050
Effectene® Transfection Reagent	Qiagen	301427
Lipofectamine® 2000 Transfection Reagent		
Modified TAE Buffer Concentrate (50X)	Millipore	CS201628 500mL
NucleoBond® Xtra Midi	Macherey-Nagel	740410.50

Buffers and reagents	Composition
Gel loading dye	0.1M EDTA, 50% glycerin, 0.1% bromophenol
Imaging Buffer	10mM HEPES, 140mM NaCl, 5.4mM KCl, 1mM $MgCl_2$, 2mM $CaCl_2$ (pH 7.3)
KCM buffer 5X	500mM KCl, 150mM $CaCl_2$, 250mM $MgCl_2$
Labeling Buffer	10mM HEPES, 150mM NaCl, 25mM KCl, 2mM $MgCl_2$, 4mM $CaCl_2$, 10mM Glucose (pH 7.3)
LB medium	80g Pepton, 50g yeast extract, 25g NaCl, water up to 5L
LB medium with antibiotic	0.08 g/L ampicillin or 0.05g/L kanamycin
LB medium with agar	10g/L agar
Milk buffer	5% milk powder into TBST buffer 1X
PBTA	PBS, 3% BSA, 0,25% Triton, 0,01 % NaN_3
Running buffer 1X	10% running buffer 10X, 1% SDS (10%), dH_2O
SOC medium	2g Tryptone, 0.5g yeast extract, 0.05g NaCl, 1mL $MgCl_2$ (1M), 1mL $MgSO_4$ (1M), 1mL Glucose (2M), water up to 100mL
Transfer buffer	20% transfer buffer 5X (Biorad), 20% ethanol (95%), 60% dH_2O
TBST buffer 10X	60.5g Tris, 200g NaCl, 35ml HCl, dH_2O up to 2.5L (pH 7.6)
TBST buffer 1X	10% TBST buffer 10X, 0.05% Tween20, dH_2O

Reagents for cell culture	Supplier	Cat. No. / Ref.
Dulbecco's modified Eagle's medium (DMEM) 4.5g/L glucose	PanBiotech Gibco	P04-03600 500mL 21969-035 500mL
Dulbecco's Phosphate Buffered Saline (DPBS)	Gibco	14190-094 500mL
Fetal Bovine Serum (FBS)	Biochrom	S0115 500mL
L-Glutamine (200mM)	PanBiotech	P04-80100 100mL
Penicillin/Streptomycin	Gibco	15140-122 100mL
Poly-D-Lysine (100mg)	MP Biomedicals	150175
Trypsin/EDTA	PanBiotech	P10-023100 100mL

Chemicals	Supplier	Cat. No. / Ref.
Agar	Applichem	A0949
Agarose, peqGOLD Universal	peqLAB	35-1020
Ampicillin	Sigma-Aldrich	A9518-25g
Antibody, Cy3 anti-mouse	Jackson ImmunoResearch Laboratories	
Antibody, enzyme-conjugated anti-rabbit		
Antibody, mouse anti-FLAG M2	Sigma-Aldrich	
Antibody, rabbit anti-DVL2	Cell Signaling Technology	
BAL (2,3-dimercapto-1-propanol)	Fluka / Sigma-Aldrich	38520 / 54046
Bromophenol blue	Applichem	A23310025
BSA, albumin fraction V (pH 7.0)	Applichem	A1391
$CaCl_2$	Merck	102382
DAPI		
DMSO (Dimethyl sulfoxide)	Sigma	D4540 100mL
DNA-ladders (100bp/1kbp)	New England Biolabs	N3231S / N3231L

Chemicals	Supplier	Cat. No. / Ref.
ECL, Western Blotting Substrate	Bio-Rad	
EDT (1,2-Ethanedithiol)	Sigma	02390 25mL
EDTA	Roth	X986.2
Ethanol 100%	Sigma-Aldrich	32205-2.5L
Ethanol 70%	T.H. Geyer	2202
FlAsH	Dr. E. Heller (custom synthesis)	
Gel, precast 7.5% acrylamide	Bio-Rad	
Geneticin (G-418) Sulphate	Gibco – Life Technologies	11811-031
Glucose	Applichem	A0883
Glycerol gelatin	Sigma-Aldrich	
H_2O_2 30%	Applichem	A0626
HCl		
HDGreen plus DNA stain	Intas science imaging	ISII-HDGreen Plus
HEPES	Sigma-Aldrich	H3375
Immersion oil for microscopy	Applichem	A0699
Ionomycin calcium salt	Sigma-Aldrich	I3909
Isopropanol	Sigma-Aldrich	33539 2.5L-M
Kanamycin	Roth	T832.3
KCl	Applichem	A2939
LGK-974 (Porcupine inhibitor)	Cayman Chemical	14072
Methanol	Sigma-Aldrich	32213.05L-M
$MgCl_2$	Applichem	1036
$MgSO_4$	Applichem	A4101
Midori green DNA staining		
Milk powder		
NaCl	Applichem	131659
NaOH	Applichem	A1551
Phorbol 12,13-dibutyrate (PdBU)	Sigma-Aldrich	P1269
Peptone	Applichem	
PFA		
PVDF membranes		
Running buffer 10X	Bio-Rad	
SDS		
Terralin	Schulke	23184-A
Transfer buffer 5X	Bio-Rad	
Tris		
Tryptone	Applichem	A1553
Tween20	BioRad	170-6531
Yeast extract	Applichem	A1552

3.2. Methods

3.2.1. Description of plasmids and sensors

The mouse V5-mFZD$_5$ receptor in pcDNA3.4 was a gift from Madelon Maurice (Utrecht). This gene was used as a basis to design four FRET-based biosensors. In addition, the receptor was fused to different fluorophores: CFP, GFP, YFP or mCherry. The development of these constructs is described in the following section (3.2.2).

In order to investigate the activation of G proteins mediated by FZD$_5$ in response to WNTs, FRET sensors for the Gα_{i1}, Gα_{i2}, Gα_{i3}, and Gα_q isoforms were used. Each sensor comprises a single plasmid encoding the three subunits of the protein: Gα_q or Gα_i bound to mTurquoise, untagged Gβ_1, and Gγ_2 fused to cpVenus (van Unen et al., 2016; Adjobo-Hermans et al., 2011). Upon ligand stimulation, the activation of the G protein leads to the dissociation between Gα and G$\beta\gamma$ subunits, producing a decrease in the FRET signal.

To evaluate the specific activation of the Gα_q-PLC pathway, a dual fluorescence probe (downward DAG2/R-GECO) developed by Montana Molecular was employed (Tewson et al., 2012), which allows the simultaneous detection of DAG and calcium. This probe is composed of two independent sensors cloned on both sides of a 2A peptide sequence. The DAG sensor consists of a cpGFP fused to the C1 domain of a PKC; the second sensor is a red-shifted fluorescent calcium indicator (R-GECO). Upon receptor activation, binding of calcium induces a conformational change in R-GECO, which leads to an increase in the red fluorescence. Simultaneously, the DAG sensor is translocated to the membrane to bind diacylglycerol, causing a decrease in the green fluorescence. This dual sensor has been successfully employed with the M$_1$AChR (Meserer et al., 2017; Agnetta et al., 2017).

3.2.2. Design of FZD$_5$ receptor constructs

To generate the construct V5-mFZD$_5$-CFP, the STOP codon TAA was deleted from the V5-mFZD$_5$ gene by standard Polymerase Chain Reaction (PCR) using the following primers: 5'- ATC TGG TGG GTC ATC CTG TC-3' (forward) and 5'-CTG ATG TCT AGA TAC GTG CGA CAG GGA CAC TTG-3' (reverse); the construct was later sub-cloned into a CFP-pcDNA3 vector between HindIII and XbaI sites.

In order to create FZD_5 FRET-based receptor sensors, the FlAsH-binding sequence 5'-TGT TGC CCG GGC TGC TGT-3' (CCPGCC, one-letter amino acid code) was inserted within the 3rd intracellular loop of V5-mFZD_5-CFP by standard overlapping PCRs. The sequence was introduced between the amino acids Gly436 and Gly437 for the sensor V5-mFZD_5-FlAsH436-CFP, using the following forward primers (1-3): 5'-TGT TGC CCG GGC TGC TGT GGC ACT AAG ACG GAC AAG CTA-3', 5'-AGC GTC ATC AAG CAG GGT TGT TGC CCG GGC TGC TGT G-3' and 5'-TCA CTC TTC CGC ATC CGG AGC GTC ATC AAG CAG GGT TGT-3' and the following reverse primer: 5'-CTG ATG TCT AGA TAC GTG CGA CAG GGA CAC TTG-3'. For the sensor V5-mFZD_5-FlAsH439-CFP, the following forward primers (1-3): 5'-TGT TGC CCG GGC TGC TGT ACG GAC AAG CTA GAG AAG CTC-3', 5'-AAG CAG GGT GGC ACT AAG TGT TGC CCG GGC TGC TGT ACG-3' and 5'-CGC ATC CGG AGC GTC ATC AAG CAG GGT GGC ACT AAG TGT-3' and the following reverse primer: 5'-CTC ACT CTA GAT ACG TGC GAC AG-3' were used to introduce the motif between Lys439 and Thr440. The region containing the FlAsH-binding motif was inserted back into the V5-mFZD_5 plasmid between the restriction sites HindIII and BstXI in order to generate the constructs without CFP.

In addition, two more sensors were created by inserting the FlAsH-binding sequence 5' TGT TGC CCG GGC TGC TGT 3' within the 2nd intracellular loop of V5-mFZD_5-CFP by means of using the QuikChange Lightning Site-Directed Mutagenesis Kit. The motif was introduced between the amino acids Gly349 and Asn350 for the sensor V5-mFZD_5-FlAsH349-CFP using the following primers: 5'-GGC ATG AAG TGG GGC TGT TGC CCG GGC TGC TGT AAT GAA GCC ATC GCA-3' (forward) and 5'-TGC GAT GGC TTC ATT ACA GCA GCC CGG GCA ACA GCC CCA CTT CAT GCC-3' (reverse), and between Ala354 and Gly355 to create the sensor V5-mFZD_5-FlAsH354-CFP, with the following primers: 5'-AAT GAA GCC ATC GCA TGT TGC CCG GGC TGC TGT GGT TAT GCA CAG TAC-3' (forward) and 5'-GTA CTG TGC ATA ACC ACA GCA GCC CGG GCA ACA TGC GAT GGC TTC ATT-3' (reverse).

Additionally, V5-mFZD_5 was cloned into YFP-pcDNA3 and GFP-pcDNA3 vectors between HindIII and XbaI sites to generate the constructs V5-mFZD_5-YFP and V5-mFZD_5-GFP, respectively. Last, and in order to obtain a receptor with the red fluorophore mCherry, two new restriction sites were added in the gene V5-mFZD_5-CFP. A BglII site was placed behind the HindIII site using the following primers: 5'-CAG TAA GCT TAG ATC TAC CAT GGT CCC GTG CAC GCT G-3' (forward) and 5'-GTG CGC ACC TTG TTG TAG AG-3' (reverse). An

AgeI site was cloned in front of the XbaI restriction site, at the end of the gene, using the following primers: 5'-CAG TGT CAA GTC CAT TAC GG-3' (forward) and 5'-AGC AGT ACC GGT TGT ACG TGC GAC AGG GAC ACT TG-3' (reverse). After that, the new V5-mFZD$_5$ was sub-cloned into pmCherry-N1 vector between the restriction sites BglII and AgeI.

3.2.3. Methods for cloning and DNA amplification

3.2.3.1. Polymerase Chain Reaction

In general, the following procedure was followed for standard PCRs:

PCR reaction	Cycling Parameters
10µl DNA template (10ng/µl) 72µl ddH_2O 10µl buffer Pfu (10X) 2µl dNTPs (10mM) 2.5µl forward primer (20pmol/µl) 2.5µl reverse primer (20pmol/µl) 1µl Pfu polymerase	Step 1: 94°C 3 minutes Step 2: 94°C 30 seconds Step 3: 55°C 1 minute } 30 cycles Step 4: 72°C 2 minutes Step 5: 72°C 5 minutes Step 6: 4°C

Gel 1% agarose was prepared by dissolving 1g agarose in 100ml of modified TAE Buffer (1X). Once the PCR protocols were finished, 2-3µl of DNA loading dye were added to each sample and an electrophoresis was performed using 1% agarose gel with 0.01% Midori green or HDGreen plus staining. The desired DNA band was extracted from the gel and purified for ligation.

For PCRs performed with the QuikChange Lightning Site-Directed Mutagenesis Kit, the following protocol was followed:

PCR reaction	Cycling Parameters
5µl 10X reaction buffer 1µl DNA template (50ng) 1.25µl primer 1 (125ng) 1.25µl primer 2 (125ng) 1µl dNTP mix 1.5µl QuickSolution reagent 39µl ddH_2O 1µl QuickChange Lightning Enzyme	Step 1: 95°C 2 minutes Step 2: 95°C 20 seconds Step 3: 60°C 10 seconds } 68 cycles Step 4: 68°C 7 minutes Step 5: 68°C 5 minutes Step 6: 4°C

The manufacturer's protocol was followed for the subsequent steps.

3.2.3.2. Restriction analysis

In general, DNA digestion was performed by incubating the following reaction for 1 hour at 37°C: 1µl DNA (1µg/µl) + 1µl of each enzyme + 1µl buffer + ddH_2O (up to 20µl)

For digestion of PCR products prior to a ligation procedure, or plasmids that were used as vectors, the following reactions were incubated for 2 hours at 37°C:

- DNA (41µl PCR product) + 2µl of each enzyme + 5µl buffer
- 5µg of DNA (plasmid for vector) + 2µl of each enzyme + 5µl buffer + ddH_2O (up to 50µl)

Once the restriction analysis was finished, 3µl of DNA loading dye were added to each sample. An electrophoresis was performed using 1% agarose gel with 0.01% staining, as previously described. The desired DNA bands were extracted from the gel and purified for ligation.

3.2.3.3. Ligations

In general, ligations were performed by incubating the following reaction at 16°C overnight. The selected insert:vector ratio was 3:1 or 5:1.

Ligation reaction	Control reaction
20ng DNA vector 3X or 5X DNA insert 2µl 10X ligase buffer 1µl T4 DNA ligase ddH_2O (up to 20µl)	20ng DNA vector - 2µl 10X ligase buffer 1µl T4 DNA ligase ddH_2O (up to 20µl)

3.2.3.4. DNA amplification and extraction

DNA was amplified by means of bacterial transformation (E. coli DH5α). For general amplification of plasmids, 0.5µg DNA were used as template. For ligation products, transformation was done the following day by using the whole volume of the ligation reaction as template.

First, DNA was mixed with 100µl KCM buffer (1X) in a 1.5ml tube and incubated for 10 minutes on ice. Next, 100µl of competent bacteria were added to the mix, which was incubated for 20 additional minutes on ice, followed by 10 minutes at room temperature (RT). After that time, 1ml LB medium without antibiotics was added to the tube and the mix was incubated for 1 hour at 37°C and 400rpm. Tubes were then centrifuged 5 minutes at 4000g and 800µl supernatant were discarded. Last, the pellet was re-suspended in the remaining volume, and

100µl bacteria were plated in 100mm LB plates containing the adequate antibiotic (ampicillin or kanamycin). Plates were incubated overnight at 37°C. The following day, individual colonies were picked by using pipette tips. Each selected colony was placed in an Erlenmeyer flask containing 200ml LB medium supplemented with the adequate antibiotic. Flasks were incubated overnight at 37°C with agitation.

The following day, bacterial culture medium was centrifuged for 20 minutes at 4°C and 5000rpm. DNA extraction was done by using the NucleoBond Xtra Midi kit, following the manufacturer's instructions. Briefly, supernatant was first discarded and the pellet was re-suspended in 8ml Resuspension Buffer (RES), supplemented with RNaseA. Next, 8ml Lysis Buffer (LYS) was added to the mix, for 5 minutes at RT. Cell lysis was stopped by addition of 8ml Neutralization Buffer (NEU). The whole volume was then loaded onto the filter of a NucleoBond Xtra Column, which was previously equilibrated by adding 12ml of Equilibration Buffer (EQU). Once the column was empty, the filter was washed by adding 5ml of Equilibration Buffer (EQU). Next, the filter was removed and the column was washed again by adding 8ml Washing Buffer (WASH). Last, the column was placed inside a 50ml Falcon tube and 5ml of Elution Buffer (ELU) were applied to elute the plasmid DNA.

In order to precipitate the DNA, the column was discarded and 3.5ml isopropanol were added to the Falcon tube. The mix was centrifuged for 30 minutes at 4°C. Supernatant was then removed, 2ml of 70% ethanol were added for washing the DNA and the tube was centrifuged again for 10 minutes at 4°C. After that, ethanol was completely removed and the pellet was allowed to dry at RT. Last, DNA was reconstituted in 100µl ddH_2O.

3.2.3.5. DNA quantification

DNA concentration was determined by means of using a Nanodrop. Afterward, DNA was diluted in the appropriate amount of ddH_2O in order to achieve a final concentration of 1µg/µl. A DNA aliquot was placed at -20°C for medium- and long-term storage, and another aliquot was kept at 4°C for daily experiments.

3.2.4. Cell culture

HEK293 and HEK293T cells were cultured in DMEM, with 4.5g/l glucose and 0.11g/l sodium pyruvate, supplemented with 10% FBS, 1% penicillin/streptomycin and 1% L-glutamine in a humidified 7% CO_2 incubator at 37°C. Cells were normally passaged every 2–3 days. To do so, cells were first washed with 2ml DPBS, and 1ml of Trypsin/EDTA was used to detach the cells; then, cells were re-suspended in 5ml of fresh medium and the appropriate volume of cells was expanded into a new 100mm plate with 10ml of fresh medium. All the previous steps took place at a laminar air flow hood, under sterile conditions.

3.2.4.1. Mycoplasma test

Cells were tested for mycoplasma contamination every 2-3 weeks by means of using specific PCR primers. To prepare the sample, 100µl of cell culture supernatant were taken into an Eppendorf tube, boiled 5 minutes at 95°C and then centrifuged 1 minute at 13000rpm. After that, 2µl of supernatant were used as DNA template in the following PCR reaction:

PCR reaction	Cycling Parameters
2.5µl 10X buffer 2.5µl dNTPs (2mM) 1µl $MgCl_2$ (50mM) 0.25µl primer GPO (50pM) 0.25µl primer MGSO (50pM) 0.2µl Taq polymerase 25µl ddH_2O	Step 1: 95°C 5 minutes Step 2: 95°C 20 seconds Step 3: 60°C 30 seconds Step 4: 72°C 1 minute (30 cycles) Step 5: 72°C 5 minutes Step 6: 4°C

Presence of mycoplasma was detected as a 720bp band in 1% agarose gel with 0.01% Midori green or HDGreen plus staining. Sequences of the primers GPO and MGSO can be found in section 3.1.2.

3.2.4.2. Freezing and thawing cells

In order to preserve the cells for medium- and long-term, cell culture medium described in section 3.2.4 was supplemented with 10% DMSO and 10% FBS to generate a freezing medium. Cells at 90-95% confluency in a 100mm plate were washed with 2ml DPBS, detached with 1ml of Trypsin/EDTA and then re-suspended in 5ml of freezing medium. Cells were placed in cryo-tubes and frozen at -20°C. Tubes were moved to -80°C 4-5 hours later.

To thaw cells, cryo-tubes stored at -80°C were placed in a 37°C water bath for a few minutes. Cells were then transferred to a 100mm plate with 10ml of regular cell culture medium. Medium was replaced 3-4 hours later.

3.2.4.3. Generation of stable cell lines

In order to create stable cell lines, HEK293 cells were seeded into 100mm plates and transfected four hours later using the Effectene reagent, according to the manufacturer's instructions. For cells expressing the FZD_5 receptor constructs, cells were transfected with 3µg of DNA per plate: V5-mFZD_5-CFP, V5-mFZD_5-FlAsH436-CFP or V5-mFZD_5-FlAsH439-CFP. For calcium experiments, cells were co-transfected with 4.2µg of the dual DAG/Ca^{2+} sensor and 3µg of the receptor, either V5-mFZD_5-CFP or the muscarinic acetylcholine receptor 3 tagged with CFP (M_3AChR-CFP). For control experiments or for those which involved the M_1AChR, stable cells were generated by transfecting only 4.2µg of the dual DAG/Ca^{2+} sensor. Culture medium was replaced 16-18 hours after transfection. Forty-eight hours after seeding and for a period of 2-3 weeks, culture medium was replaced every day with medium supplemented with 500µg/ml Geneticin (G-418) in order to select cells transfected with the plasmids. After that time, individual colonies were selected and characterized using confocal microscopy. Positive homogeneous cells expressing the desired construct were maintained in DMEM containing 200µg/ml of G-418. In the case of HEK293 cells expressing V5-mFZD_5-FlAsH439-CFP, after selection for two weeks with G-418, cells were split and maintained in medium with 200µg/ml of G-418, to obtain heterogeneous stable cells.

3.2.5. Ligand binding

Non-transfected HEK293 cells and HEK293 cells stably expressing the receptors V5-mFZD_5-CFP or V5-mFZD_5-FlAsH436-CFP were seeded in 25cm^2 flasks 72 hours before the experiments. Medium was exchange 24h later and empty cells were transfected with 1µg/flask of V5-mFZD_5 using Lipofectamine 2000, according to the manufacturer's instructions. The day after, cells were immobilized onto pre-activated ConA LNB chips and incubated overnight inside the Attana Cell 200 machine. Experiments were performed the next morning using a specific peptide provided by the company Pepscan (PEP P2F06) and following the procedure optimized by Attana. Data were fit by the Attana software to a 2:1 kinetics, heterogeneous ligand model.

3.2.6. Immunoblotting

Empty HEK293 cells and HEK293 cells stably expressing the receptors V5-mFZD$_5$-CFP or V5-mFZD$_5$-FlAsH436-CFP were seeded onto 24-well plates, at a density of 100000 cells/well. Medium was changed 18h later and cells were stimulated for 2 hours at 37°C with either normal DMEM or medium supplemented with WNTs, to achieve a final concentration in the wells of 300ng/ml. After that time, cells were harvested with lysis buffer, sonicated and boiled at 95°C for 5 minutes. Precast gels, 7.5% acrylamide, were assembled into a vertical electrophoresis tank, which was next filled with running buffer 1X. For each condition, 10µl of cells were loaded into the gel. As control for protein weight, 3.5µl ladder buffer was also loaded in the gel. Electrophoresis was done at 250V for 30 minutes.

PVDF membranes were activated by incubating them with methanol for one minute. After washing the membranes with transfer buffer, the proteins were transferred from the gels to the membranes by using a semi-dry botting method, in a transfer system from Bio-Rad ('mixed' program, 7 minutes). After that, the gels were discarded and the membranes were blocked by incubation with milk buffer for 30 minutes at RT. Next, membranes were placed in 50ml falcon tubes and incubated overnight with primary antibody anti-DVL2 (dilution 1:1000, in milk buffer), at 4°C with shaking. The next day, the membranes were taken out of the tubes, washed three times with TBST for 10 minutes at RT and then incubated in new 50ml falcons with an enzyme-conjugated secondary antibody anti-rabbit (dilution 1:5000, in milk buffer) for 1h at RT, with shaking. Last, the membranes were washed three times with TBST for 10 minutes at RT and then revealed by incubating them with ECL substrate for 4 minutes. Revelation of the membranes was done in the Bio-Rad developing machine.

3.2.7. Immunocytochemistry

Round 13mm glass coverslips were placed in 24-well plates and coated with 0.1% gelatin (400µl/well). After 30 minutes, gelatin was removed and the coverslips were left to dry at RT. One hour later, empty HEK293 cells and HEK293 cells stably expressing the receptors V5-mFZD$_5$-CFP or V5-mFZD$_5$-FlAsH436-CFP were seeded onto the coverslips, 100000 cells/well. Cells were transfected 24h later with 100ng/well of DVL1-FLAG using Lipofectamine 2000. Additionally, half of the wells containing empty cells were also transfected with the V5-mFZD$_5$ receptor. The following day, cells were fixed by incubating them with 300µl/well PBS containing 4% paraformaldehyde. After that, cells were washed

three times with PBS and then blocked for 40 minutes with 300µl/well PBTA. Cells were incubated overnight at 4°C with 200µl/well of primary antibody, mouse anti-FLAG M2 (1:500) diluted in PBTA. The next day, cells were washed twice with PBS and then incubated in the dark for 40 minutes at RT with the secondary antibody, Cy3 anti-mouse (1:500) diluted in PBS. After washing with PBS three times, cells were incubated 5 minutes with DAPI in the dark at RT. Last, cells were washed twice with PBS and once with dH_2O. Coverslips were mounted with glycerol gelatin onto glass slides and stored in the fridge. The fixed samples were analyzed using confocal microscopy, as detailed in the next section (3.2.8).

3.2.8. Confocal Microscopy Analysis

To investigate the cellular expression and localization of the new FZD_5 receptor constructs, as well as FZD_5-induced DVL recruitment to the membrane, and the activation of PLC pathway using the dual DAG/Ca^{2+} sensor, confocal analysis of the cells was performed using a Leica SP8 microscope, equipped with four detection channels, with a 63x water objective.

3.2.8.1. Preparation of cells

Round 24mm glass coverslips were placed in six-well plates and coated with 200µl of poly-D-lysine (1 mg/ml) for 20 minutes at RT. After that time, coverslips were washed with 1ml DPBS and HEK293 cells were seeded onto them. Four to five hours later, cells were transfected using Effectene, according to the manufacturer's instructions. Cell culture medium was replaced 16-18h later and experiments were performed 24 hours after that. To investigate the cellular expression of the constructs, 500ng of each receptor were transfected per well. For FZD_5-mediated DVL recruitment assays, cells were co-transfected with 150ng of GFP-DVL and 450ng of pcDNA or the corresponding receptor construct.

For calcium experiments, HEK293 cells stably co-expressing the dual DAG/Ca^{2+} sensor and the desired receptor construct, either V5-mFZD_5-CFP or M_3AChR-CFP, were seeded onto round 24mm cover slips previously placed in 6-well plates and pre-coated with poly-D-lysine. Culture medium was replaced 4-5h later and analysis of the cells was done 48h after seeding the cells. For experiments involving the V5-mFZD_5 receptor, cells were incubated overnight with the Porcupine inhibitor LGK-974 prior the experiments, at a final concentration of 0.1µM. For control experiments without receptor, stable cells expressing only the dual DAG/Ca^{2+} sensor were seeded onto the coverslips and the same procedure followed.

In experiments regarding the M_1ACh receptor, the stable cells expressing the DAG/Ca^{2+} sensor were transfected 3-4 hours later with 500ng/well of the construct M_1AChR-CFP. Cell culture medium was exchanged 16-18 h later and analysis of the cells was done 48h after transfection.

To reduce the assay volume, calcium experiments were also performed in Ibidi µ-slide 8well plates. Wells were coated with 300µl poly-D-lysine for 30 minutes at RT and then washed with DPBS. HEK293 cells stably co-expressing the dual DAG/Ca^{2+} sensor and the desired receptor construct, either V5-mFZD$_5$-CFP or M_3AChR-CFP, were seeded onto the wells. Analysis of the cells was done the following day. If the cells expressed the V5-mFZD$_5$-CFP receptor, cells were incubated overnight with the Porcupine inhibitor LGK-974 prior the experiments.

3.2.8.2. Confocal Microscopy: experimental procedure

The day of the experiments, coverslips with the cells were mounted using an Attofluor holder and cells were maintained in imaging buffer. CFP was excited using a diode laser at 442nm laser line and fluorescence intensities were detected from 460 to 500 nm. GFP was excited using an Argon laser (30% intensity) at 488nm laser line and detected at 510-560nm. R-GECO was excited at 562nm laser line and emission was detected from 600 to 700 nm. In general, images were acquired using 512×512 resolution, 400Hz, line average 3 and frame accumulation 2.

In calcium experiments, CFP was only used to localize cells expressing the receptor V5-mFZD$_5$-CFP, M_3AChR-CFP, or M_1AChR-CFP, but not for measurements. Images were taken as a time series using 512×512 resolution and 400Hz, line average 1 and frame accumulation 1, with an acquisition time of 1.29 seconds. For experiments with the FZD$_5$ receptor, cells were maintained in 200µl of normal cell culture medium (DMEM), then stimulated with additional 600µl of WNT-5A- or control-conditioned medium right before the measurement started, and monitored for additional 30 minutes. For experiments with the muscarinic receptors, cells were maintained in 900µl imaging buffer. After 15 seconds, 100µl of the ligand Carbachol were added to the cells, to achieve a final concentration in the holder of 100µM. The cellular response was monitored for 5 additional minutes.

For experiments done using the Ibidi µ-slide 8well plates, cells were maintained in 250µl of imaging buffer. 50µl of the ligand were added a few seconds after the recording started and the same procedure followed.

Confocal analysis of the fixed samples was done using a 63x oil-immersion objective. DAPI was excited using a Diode 405 laser at 405nm laser line and fluorescence intensities were detected at 431-480nm. Cy3 was excited using a DPSS laser at 561nm laser line and detected at 590-679nm. Images were acquired using 1024×1024 resolution, 400Hz, line average 8.

Data were acquired using the Leica software and then analyzed using the Leica Application Suite X (LAS X). For further analysis, Origin software and GraphPad Prism 7 were used.

3.2.9. FlAsH labeling

The labeling was done following the generalized procedure published in Nature protocols (Hoffmann et al., 2010). Fresh labeling buffer was stored at 4°C and glucose was added shortly before using, to achieve a final concentration of 1.8 g/l. Transfected or stable cells were washed once with labeling buffer and then incubated at 37°C for 1 hour with the same buffer supplemented with 1µM FlAsH and 12.5µM 1,2-ethanedithiol (EDT). After that time and in order to reduce non-specific labeling, cells were rinsed once with labeling buffer and incubated at 37°C for 10 min with this same buffer containing 250µM EDT. Finally, cells were washed again twice with labeling buffer and maintained in DMEM prior to measurements. When the FlAsH labeling was performed in 96-well plates, cells were instead maintained in 90µl/well imaging buffer supplemented with 0.1% BSA.

FlAsH labeling was performed in 6-well plates, Will-Co dishes and 96-well plates, depending on the experiment. A scheme with a detailed protocol is shown in the next page.

FlAsH labeling protocol:

- **Step 1: preparation**
  - n = 1 + number of wells from a 6-well plate
  - 1 x 6-well plate (6 wells) ≈ 4 x WillCo-dishes

- Prepare 3 eppendorf tubes (1.5ml):

  - Buffer 2.1: 1ml DMSO + 2.1µl EDT
  - Buffer 42: 1ml DMSO + 42µl EDT
  - FlAsH: (‘n’ x 1µl FlAsH) + (‘n’ x 1µl buffer 2.1)
- Incubate for 5 minutes at RT

- Labeling buffer: add glucose (final concentration 1.8g/l)
- Prepare 2 falcon tubes:
  - FlAsH buffer: 2 x ‘n’ ml labeling buffer (+glucose) + FlAsH eppendorf
  - Washing buffer: 25ml labeling buffer (+glucose) + 12.5µl buffer 42

- **Step 2: FlAsH labeling, general procedure**
  - 6-well plate: 2ml/well
  - WillCo-dish: 3ml/plate

Wash with labeling buffer (1X)

⇩

Incubation for 1 hour at 37°C with ‘FlAsH buffer’

⇩

Wash with labeling buffer (1X)

⇩

Incubation for 10 minutes at 37°C with washing buffer

⇩

Wash with labeling buffer (2X)

⇩

Maintain cells in DMEM+++

10-15 minutes at 37°C prior experiment

3.2.10. FRET Microscopy

3.2.10.1. Microscope set-up for single-cell FRET experiments

FRET measurements were performed on a Zeiss inverted microscope (Axiovert200), equipped with an oil immersion 63x objective lens and a dual-emission photometric system (Till Photonics). Cells expressing the desire DNA construct were excited at 436 ± 10 nm using a frequency of 10 Hz with 40ms illumination time out of a total of 100ms. Emission of the donor, CFP or mTurquoise (480 ± 20 nm), emission of the acceptor, FlAsH or cpVenus (535 ± 15 nm), and the FRET ratio (FlAsH/CFP or cpVenus/mTurquoise) were monitored simultaneously over time. Fluorescence signals were detected by photodiodes and digitalized using an analogue-digital converter (Digidata 1440A, Axon Instruments). Fluorescence intensities data were acquired using Clampex software. The acceptor emission was corrected for each experiment by directly exciting at 490nm with 10ms illumination time out of a total of 100ms. When required, the emission ratio was additionally corrected for donor bleed-through and photo-bleaching. Data were analyzed using Origin software.

3.2.10.2. Determination of FRET efficiency

Fluorescence imaging of FZD_5 FRET sensors was performed as previously described (Jost et al., 2008; Hoffmann et al., 2005). HEK293 cells were seeded onto round 24mm coverslips previously coated with poly-D-lysine, as described in section 3.2.8.1. Cells were transfected 4-5h later using Effectene with 500ng of the corresponding receptor sensor per well, or co-transfected with 300ng of V5-mFZD_5-CFP and 300ng of V5-mFZD_5-FlAsH for control experiments. Cell culture medium was replaced 16–18h later. Experiments were conducted the following day.

Coverslips with the cells were mounted using an Attofluor holder and the cells were maintained in 999µl of imaging buffer. Approx. 20-30 seconds after the recording started, 1µl of 2,3-dimercapto-1-propanol (BAL) was added to the cells, to achieve a final concentration in the holder of 5mM. The compound BAL removes FlAsH from its binding motif in the receptor, which results in a dequenching of CFP fluorescence. The CFP recovery, FlAsH fluorescence, and FRET ratio (FlAsH/CFP) were monitored over time. To calculate the FRET efficiency, the minimum and maximum values of CFP were introduced into the following equation: (CFP*max*-CFP*min*)/CFP*max*∗100.

3.2.10.3. BioPen® microfluidic system

The BioPen microfluidic system (Fluicell) was employed to deliver the ligands in single-cell FRET experiments (Ainla et al., 2012; Ainla et al., 2010). This novel perfusion system allows to expose individual cells to the ligand solution without affecting the neighboring cells. The pipette can contain up to four different solutions, with an exchange time between them of sub-seconds. Moreover, a recirculation system inside the pipette allows to collect the applied solution, avoiding contamination of the medium with the ligand. Thus, measuring several cells per experiment from a single plate is possible using this system. In addition, only 30µl are needed per solution. That is an important advantage considering that the recombinant WNT proteins are difficult to handle and their commercial cost is high.

3.2.10.4. Receptor activation in single-cells

In order to investigate the activation of the FZD_5 receptor in real time, WillCo-dish® 40mm glass bottom dishes were coated with 1ml poly-D-lysine for 30 minutes at RT and then washed with DPBS. HEK293 cells stably expressing the receptor sensor V5-FZD_5-FlAsH436-CFP were seeded onto these plates. The culture medium was replaced 16-18 hours later, and cells were incubated overnight with the Porcupine inhibitor LGK-974, at a final concentration in the medium of 0.1µM. FlAsH labeling of the receptor sensors was performed the next day, 48h after seeding the cells, and the WillCo-dish with the labelled cells was placed on the inverted microscope. During measurements, cells were maintained in imaging buffer and the BioPen® microfluidic system was used to deliver the ligands. The recombinant protein WNT-5A was diluted in imaging buffer containing 0.1% BSA. FRET experiments were performed as described in the previous section (3.2.10.1).

3.2.10.5. Activation of $G\alpha_q$ protein in single-cells

HEK293 cells were seeded onto 40mm WillCo-dishes pre-coated with poly-D-lysine and transfected 4 hours later with 600ng of V5-mFZD_5 receptor and 200ng of the corresponding G protein FRET-sensor, using Effectene. Culture medium was replaced 16-18 hours later and cells were incubated overnight with the Porcupine inhibitor LGK-974, at a final concentration in the cells of 0.1µM. FRET measurements were performed the following day, 48h after seeding the cells, which were maintained in imaging buffer.

Recombinant protein WNT-5A was dissolved in imaging buffer containing 0.1% BSA and the BioPen® microfluidic system was used to deliver the ligand. FRET experiments were performed as previously described (section 3.2.10.1).

3.2.11. Microplate reader

In order to perform screenings by using different WNTs, FZD_5 receptor conformational changes and G protein activation were investigated by using a microplate reader from BioTek: Synergy™ Neo2 Multi-Mode Microplate Reader. Experiments were done using the Gen5™ Data Analysis Software. Cells were excited at 420/50 nm (Biotek CFP/YFP filter, code 1035013) and emission was detected at 485/20 and 540/25 nm (Biotek CFP/YFP filter, code 1035043).

3.2.11.1. Receptor activation

Stable cells expressing the receptor sensor V5-FZD_5-FlAsH436-CFP or V5-FZD_5-FlAsH439-CFP were expanded in 100mm plates and 72h later 40000 cells/well were placed in black 96-well BRAND-plates. These plates were previously coated with 100µl/well of poly-D-lysine for 30 minutes at RT and then washed with 200µl/well of sterile PBS. FlAsH labeling was done 24h after seeding the cells in the 96-well plates and cells were later maintained at 37°C in 90µl imaging buffer containing 0.1% BSA. Analysis of the cells was done using the Synergy Neo2 microplate reader, as described above. Recombinant WNT proteins (10µl) were added to the cells 4-5 minutes after the reading started, to reach the desired final concentration of ligand in each well, which is indicated in the concentration-response curves. Changes in fluorescence were recorded for additional 10-15 minutes.

3.2.11.2. Activation of $G\alpha_q$ protein

HEK293 T or HEK293 DVL KO cells were expanded in 100mm plates. Forty-eight hours later, when 60-70% confluence was reached, cell culture medium was exchanged and cells were transfected with 1.8µg of the V5-mFZD_5 receptor or pcDNA3, and 600ng of the corresponding G protein-FRET sensor, using Effectene. For DVL over-expression experiments, cells were also transfected with 600ng HA-DVL2. Twenty-four hours after transfection, black 96-well plates were coated with 100µl/well of poly-D-lysine for 30 min, washed with 200µl/well of

sterile PBS, and 30000 cells were seeded per well. Analysis of the cells was done 24h later using the Synergy Neo2 microplate reader, as previously described. During measurements, cells were maintained at 37°C in 90µl imaging buffer containing 0.1% BSA. Recombinant WNT proteins were diluted in imaging buffer containing 0.1% BSA and 10µl were added to the cells five minutes after the reading started, to reach the desired final concentration of ligand in each well, which is indicated in the concentration-response curves. Fluorescence changes were recorded for additional 15-20 minutes.

For control experiments of the receptor FRET sensor, HEK293T cells were co-transfected with the $G\alpha_q$ FRET-sensor and the receptor with the FlAsH-binding motif, either V5-mFZD$_5$-FlAsH436 or V5-mFZD$_5$-FlAsH439, in the same ratio as before, and the same procedure followed.

Two schemes with detailed protocols for measuring receptor and G protein activation in a microplate FRET reader are shown in the following pages.

- **Measuring receptor activation in 96-well plates:**

V5-mFZD$_5$-FlAsH-CFP stable cells.
1x100mm plate, cell confluency 90-100%

96-well plate: 100µl/well poly-D-lysine for 30 minutes at RT

⇩

Washing: 200µl/well PBS

⇩

Place 40000 cells/well

⇩ 24 hours

- Prepare buffer 2.1 and 42 as indicated in the general procedure.
- For 1 x 96-well plate:
  - Eppendorf-FlAsH: 6µl FlAsH + 6µl buffer 2.1
  - FlAsH buffer: 12 ml labeling buffer (+glucose) + Eppendorf-FlAsH
  - Washing buffer: 12ml labeling buffer (+glucose) + 6µl buffer 42

Washing: 200µl/well labeling buffer (1X)

⇩

Incubation for 1 hour at 37°C with 100µl/well 'FlAsH buffer'

⇩

Washing: 200µl/well labeling buffer (1X)

⇩

Incubation for 10 minutes at 37°C with 100µl/well washing buffer

⇩

Washing: 200µl/well labeling buffer (2X)

⇩

90µl/well imaging buffer 0.1% BSA

⇩

10-15 minutes at 37°C prior experiment

⇩

Place the plate inside the plate reader

⇩

Reading protocol. 4 columns per experiment (*e.g.* A2-H5)

Procedure details:

1. Set temperature: preheat at 37°C
2. Kinetic:
Runtime 0:04:00 (HH:MM:SS), Interval 0:00:30, 9 Reads
3. Plate out: add ligands (10µl/well)
4. Shake: 1 second
5. Set temperature: preheat at 37°C
6. Delay: 1 second
7. Kinetic:
Runtime 0:10:38 (HH:MM:SS), Interval 0:00:13, 50 Reads

- **Measuring G protein activation in 96-well plates:**

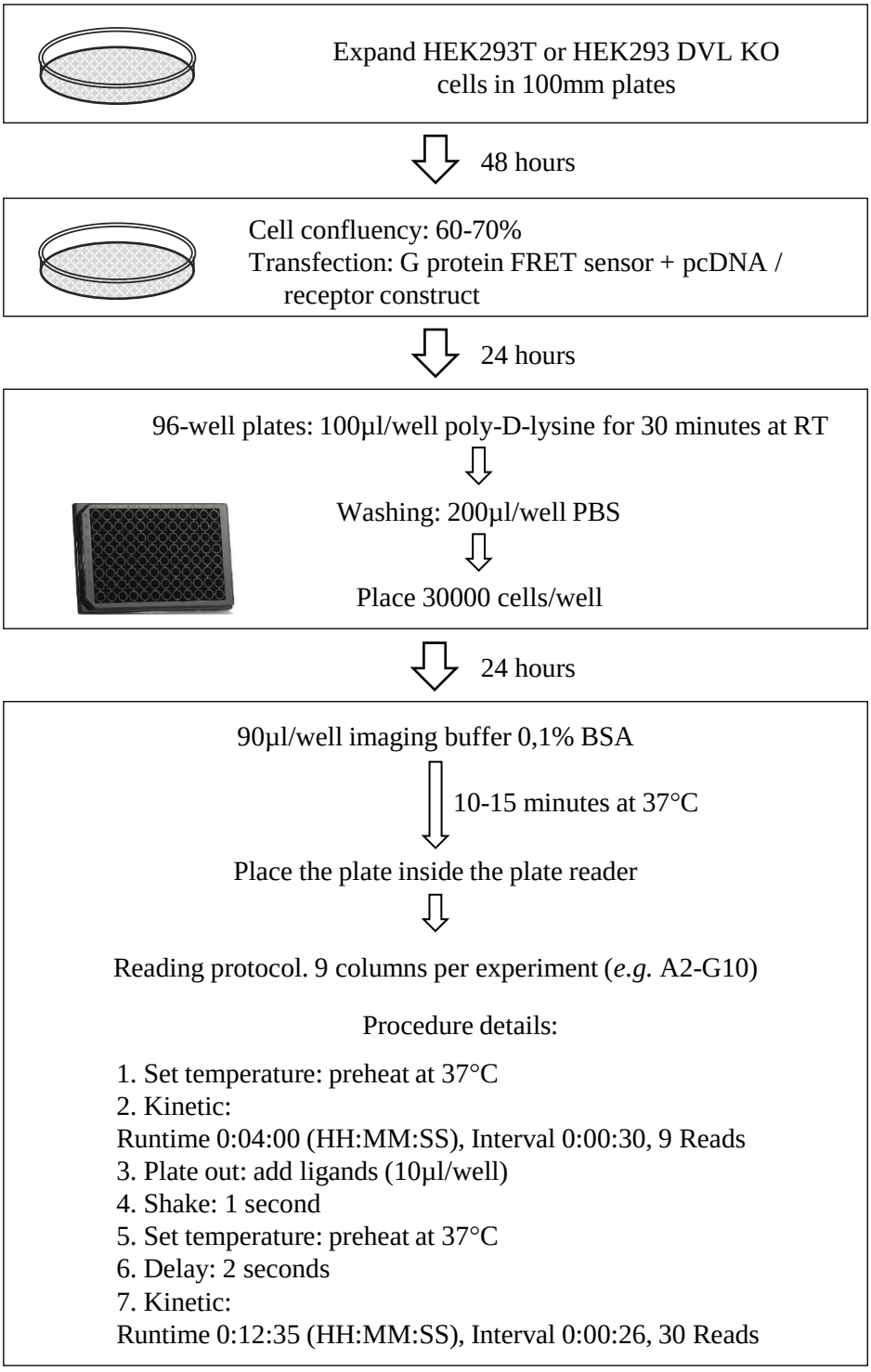

3.2.11.3. $G\alpha_q$ titration

Stable cells expressing the V5-FZD_5-FlAsH436-CFP receptor sensor were expanded in 60mm plates. Twenty-four hours later, when 60-70% confluency was reached, cells were transfected with 100ng of the $G\beta_1$ subunit, 40ng of $G\gamma_2$ and increasing concentrations of $G\alpha_q$: 0, 10, 25, 50, 100, 150, 300, 400 or 500ng per plate. Variable concentrations of pcDNA were used to balance the total amount of DNA per plate. 24h after transfection, 30000 cells/well were seeded in black 96-well plates. FlAsH labeling of the cells was performed one day later and cells were then maintained in 100µl imaging buffer containing 0.1% BSA. Basal fluorescence of the cells was recorded for 5 to 10 minutes by using a Synergy Neo2 microplate reader, as previously described.

3.2.11.4. Data analysis

The Gen5™ Data Analysis Software was employed to design and perform the experiments. The reading protocol is detailed in the two previous schemes. Once the procedure was finished, data were exported as excel file, which included 3 tables: basal 420/50, 485/20; basal 420/50, 540/25; and FRET ratio. Data from the third table 'FRET ratio' were selected for analysis.

In the first place, to determine the FRET change produced by each concentration of ligand, the averages were calculated for the values before (F_{before}) and right after (F_{after}) ligand addition. The ratio (F_{ligand}) was then calculated as F_{after}/F_{before}. Next, the FRET change was corrected for the signal obtained in vehicle-treated cells. In order to do so, the ratio obtained for each concentration of the ligand (F_{ligand}) was divided to the one obtained for the buffer (F_{buffer}): F_{ligand}/F_{buffer}. Finally, data were analyzed and fit to a dose-response curve with variable slope (four parameters) using the software GraphPad Prism 7.

4. Results

4.1. FZD_5 receptor undergoes conformational changes upon activation, as detected by using FRET-based biosensors.

4.1.1. Design of FZD_5 receptor constructs

A mouse FZD_5 receptor containing a V5 tag in the N-terminal tail was used to generate four FRET-based biosensors. The constructs were created by inserting the FlAsH-binding motif (CCPGCC, 1 letter amino acid code) within the 2nd or the 3rd intracellular loop of the receptor, and by fusing a CFP to the C-terminal tail of FZD_5.

The mouse FZD_5 protein sequence from Uniprot (code Q9EQD0) was used as reference to identify positions of insertion for the FlAsH-binding sequence. Particularly, the positions in ICL-3 were selected also considering the motifs of interaction with DVL (Tauriello et al., 2012). Regarding ICL-2, the six amino acid motif was introduced between Gly349 and Asn350 for the sensor V5-FZD_5-FlAsH349-CFP and between Ala354 and Gly355 to create the sensor V5-FZD_5-FlAsH354-CFP. Regarding ICL-3, the motif was inserted between Gly436 and Gly437 to generate the sensor V5-mFZD_5-FlAsH436-CFP or between the Lys439 and Thr440 for the sensor V5-mFZD_5-FlAsH439-CFP. A sketch of the receptor structure and the position of the fluorophores is depicted in **figure 9**.

Additionally, three more constructs were produced by fusing the green or yellow fluorescent protein, or the red fluorophore mCherry to the C-terminus of the FZD_5 receptor. For the purpose of a smoother discussion, the original V5-mFZD_5 receptor construct will be considered as 'wild-type' throughout this thesis.

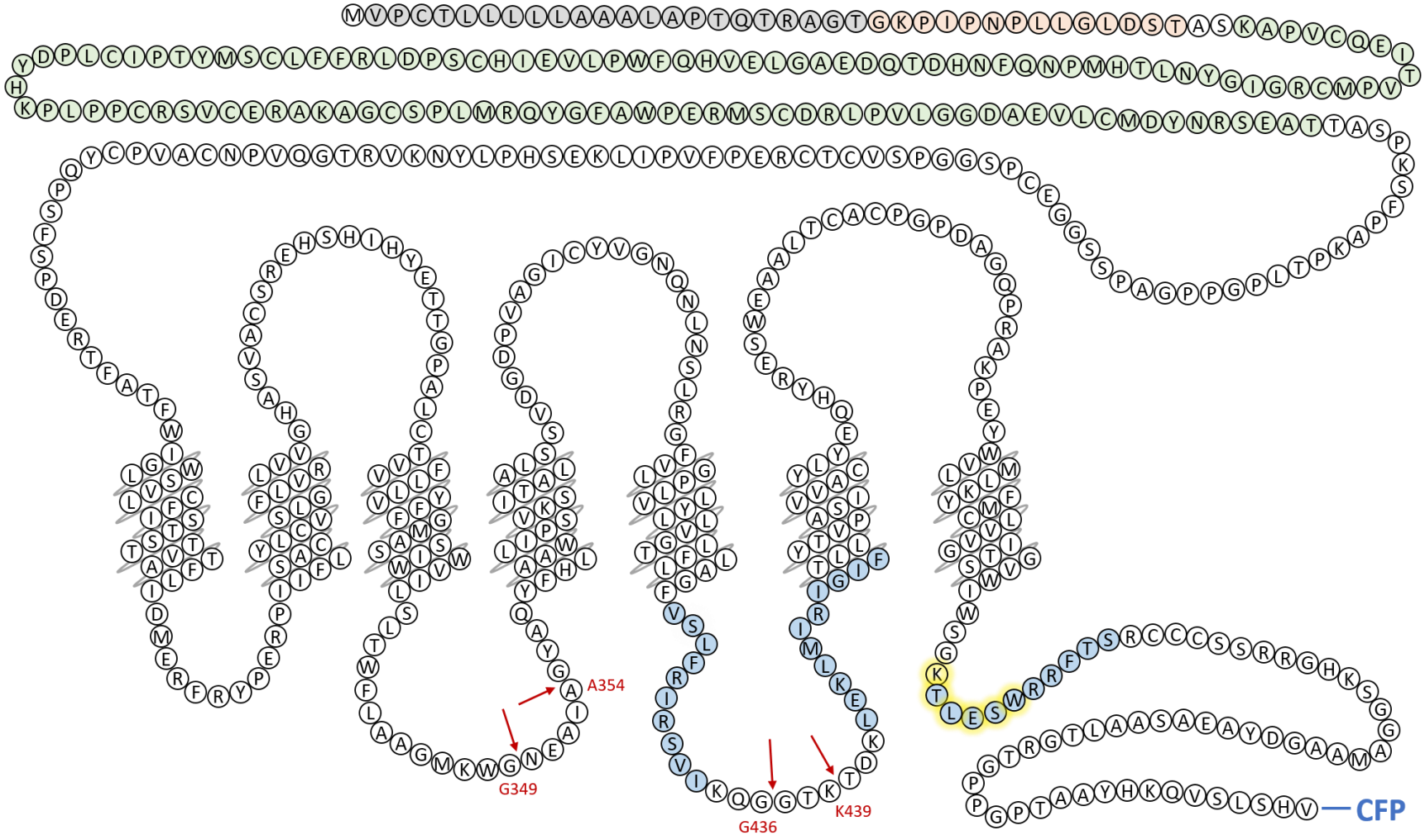
A354
G349
G436
K439
CFP

Figure 9. Mouse FZD_5 receptor sequence.

Sketch depicting the amino acids sequence of the mouse FZD_5 receptor employed in this thesis. Information about transmembrane domains, extra- and intra-cellular loops, and N- and C-terminal tails was obtained from Uniprot (code Q9EQD0). The predicted helix VIII is not shown as such. In the N-terminus of the receptor, the 22 amino acids belonging to the signal peptide appear as grey, the V5 tag (14 amino acids) is shown as orange circles and in green, the putative cysteine-rich domain (ncbi, cd07460). The amino acids illustrated as blue circles in the C-terminus and in the ICL-3 represent the 3 motifs of interaction with DVL (Tauriello et al., 2012). The sequence KTLESW, highlighted in the C-terminus, corresponds to the conserved domain involved in binding to PDZ motif. To generate the construct V5-mFZD_5-CFP, the STOP codon of the receptor was deleted and CFP was fused at the end of the C-terminus. The red arrows indicate the insertion sites of the FlAsH-binding motif (CCPGCC, 1 letter amino acid code), within ICL-2 or ICL-3: between G349 and N350 for the sensor V5-mFZD_5-FlAsH349-CFP; between A354 and G355 for the sensor V5-mFZD_5-FlAsH354-CFP; between G436 and G437 for the sensor V5-mFZD_5-FlAsH436-CFP; between K439 and T440 for the sensor V5-mFZD_5-FlAsH439-CFP.

4.1.2. Characterization of the FZD_5 FRET-based biosensors

4.1.2.1. Cellular localization

The cellular localization of all FZD_5 constructs was analyzed by confocal microscopy. All the receptors containing the individual fluorophores CFP, GFP, YFP or mCherry localized to the plasma membrane, as well as the two receptor sensors containing the FlAsH-binding motif within ICL-3 (**Fig. 10A, D-H**). On the contrary, the two sensors with the FlAsH-binding sequence within ICL-2 were found in the intracellular compartments (**Fig. 10B-C**), indicating that the insertion of the six amino acids in these positions affected the structure of the receptors and thus hampered the translocation of the sensors to the plasma membrane. Since a proper folding of the receptor and a membrane localization are necessary requirements to perform FRET analysis, the sensors V5-FZD_5-FlAsH349-CFP and V5-FZD_5-FlAsH354-CFP were not considered for further experiments.

Figure 10. Cellular localization of FZD_5 constructs.

Confocal images of representative cells overexpressing the different FZD_5 receptor constructs. Scale bars represent 10µm. All the receptors tagged with a fluorescent protein at the end of their C-terminal tail showed membrane localization: V5-mFZD_5-CFP **(A)**, V5-mFZD_5-mCherry **(F)**, V5-mFZD_5-GFP **(G)** or V5-mFZD_5-YFP **(H)**. In contrast, the two receptor sensors with the FlAsH-binding motif inserted within ICL-2, V5-mFZD_5-FlAsH349-CFP **(B)** and V5-mFZD_5-FlAsH354-CFP **(C)**, were not expressed in the plasma membrane, but mostly in the intracellular membranes. On the contrary, the two sensors with the FlAsH-binding sequence within ICL-3, V5-mFZD_5-FlAsH436-CFP **(D)** and V5-mFZD_5-FlAsH439-CFP **(E)**, were localized to the plasma membrane.

A

V5-mFZD$_5$-CFP

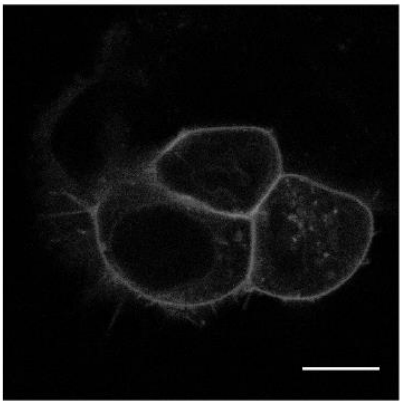

B

V5-mFZD$_5$-FlAsH349-CFP

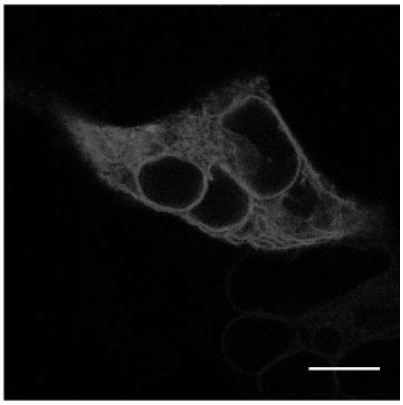

C

V5-mFZD$_5$-FlAsH354-CFP

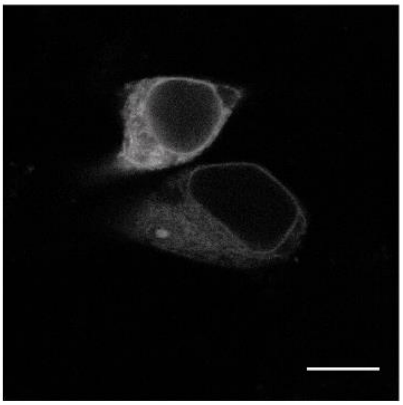

D

V5-mFZD$_5$-FlAsH436-CFP

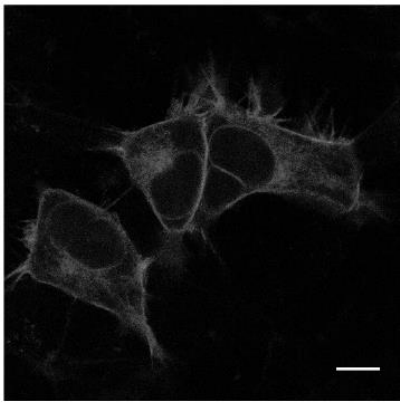

E

V5-mFZD$_5$-FlAsH439-CFP

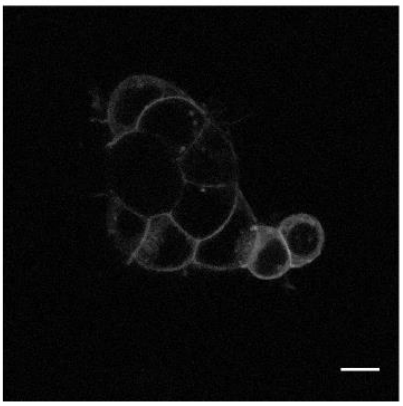

F

V5-mFZD$_5$-mCherryN1

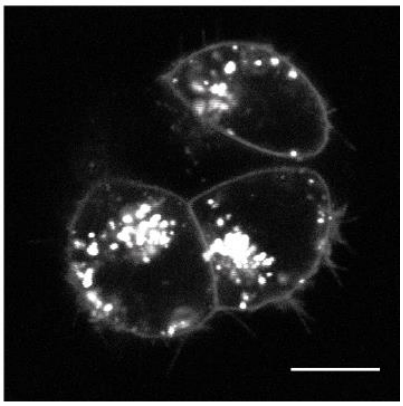

G

V5-mFZD$_5$-GFP

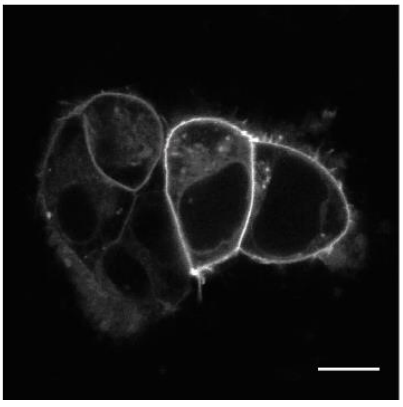

H

V5-mFZD$_5$-YFP

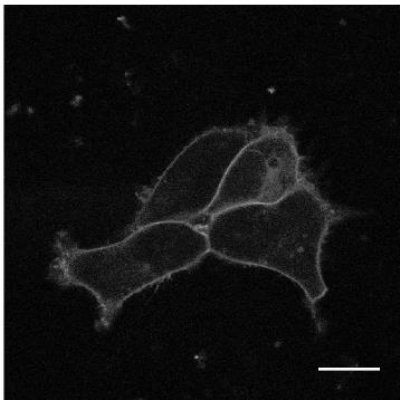

4.1.2.2. Ligand binding

Ligand binding properties of the receptor constructs were studied by means of using Attana Cell™200 Quartz Crystal Microbalance (QCM) technology (Clausen et al., 2016; Aastrup et al., 2014). One specific peptide (P2F06) generated by Pepscan, which acted as an antagonist, was used at different concentrations to perform kinetic analysis. The resulting data were fitted using a 2:1 kinetics model (heterogeneous ligand model) using the Attana software, which returned the parameters for each receptor tested (**Fig. 11A-C**). No difference in the ligand binding and affinity was observed between the different analyzed receptors (**Fig. 11D**), which suggests that neither insertion of the CCPGCC motif in ICL-3 nor CFP insertion in the C-terminus altered the binding properties of the FZD_5 constructs.

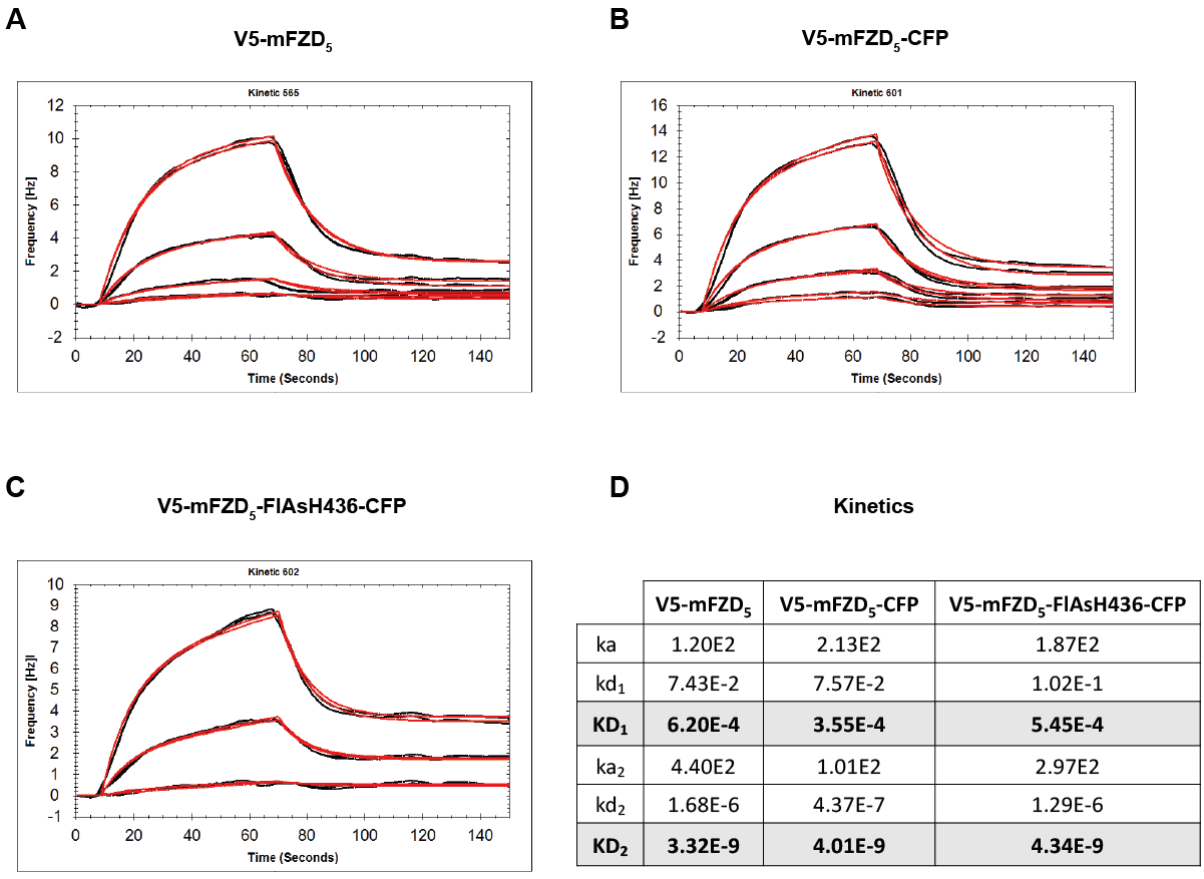

	V5-mFZD$_5$	V5-mFZD$_5$-CFP	V5-mFZD$_5$-FlAsH436-CFP
ka	1.20E2	2.13E2	1.87E2
kd$_1$	7.43E-2	7.57E-2	1.02E-1
KD$_1$	**6.20E-4**	**3.55E-4**	**5.45E-4**
ka$_2$	4.40E2	1.01E2	2.97E2
kd$_2$	1.68E-6	4.37E-7	1.29E-6
KD$_2$	**3.32E-9**	**4.01E-9**	**4.34E-9**

Figure 11. Ligand binding.

Attana Cell™200 QCM technology was used to determine the ligand binding properties of the receptor constructs. HEK293 cells transiently overexpressing the receptor V5-mFZD$_5$ **(A)** or stable cells expressing the constructs V5-mFZD$_5$-CFP **(B)** or V5-mFZD$_5$-FlAsH436-CFP **(C)** were immobilized

onto ConA LNB chips and introduced inside the Attana Cell 200 machine. The ligand, an antagonistic peptide (P2F06) developed by Pepscan, was injected into the machine and kinetics of the interaction were measured. The first part of the graphics represents the binding of the ligand to the receptor that occurred while the peptide was being injected, while the second part of the curves (decrease after 70 seconds) indicates the dissociation of the complex. Data were corrected for non-transfected HEK293 cells and fitted by using a 2:1 kinetics model using the Attana software, to determine the kinetic rate constants (k_a and k_d). The affinity (K_D) was calculated as a ratio k_d/k_a. No difference in binding affinities was observed for the three receptor constructs **(D)**.

4.1.2.3. Basal energy transfer

Since both receptor sensors V5-mFZD$_5$-FlAsH436-CFP and V5-mFZD$_5$-FlAsH439-CFP localized to the plasma membrane and their ligand-binding site showed similar properties to the wild-type receptor, the basal energy transfer between the fluorophores CFP and FlAsH was analyzed. In order to do that, the FRET efficiency of the two receptor constructs was determined by using the compound 'British anti-Lewisite' (BAL: 2,3-dimercapto-1-propanol), a molecule with high affinity for arsenicals (Hoffmann et al., 2010; Jost et al., 2008; Hoffmann et al., 2005). Addition of 5mM BAL removes FlAsH from its binding site in the receptor, producing a dequenching in CFP fluorescence. HEK293 cells expressing the receptor sensor V5-mFZD$_5$-FlAsH436-CFP or V5-mFZD$_5$-FlAsH439-CFP were labeled with FlAsH before the measurement, and BAL was added to the cells 20-30 seconds after the measurement started (**Fig. 12A, C**). FRET efficiency was calculated using the following formula: (ECFP*max*-ECFP*min*)/ECFP*max*∗100, considering CFP minimum and maximum values. No significant difference was observed between the two sensors, which both exhibited basal intramolecular FRET, with a FRET efficiency of 6.42±0.81% for V5-mFZD$_5$-FlAsH436-CFP and 6.16±0.97% for V5-mFZD$_5$-FlAsH439-CFP (**Fig. 12E**). No basal intermolecular FRET was observed when the individual constructs V5-mFZD$_5$-FlAsH436 or V5-mFZD$_5$-FlAsH439 were co-expressed with V5-mFZD$_5$-CFP in HEK293 cells (**Fig. 12B, D**), which indicates that the aforementioned signals come from within one receptor and there is not energy transfer between the fluorophores of adjacent receptors, or from the potential existence of dimers.

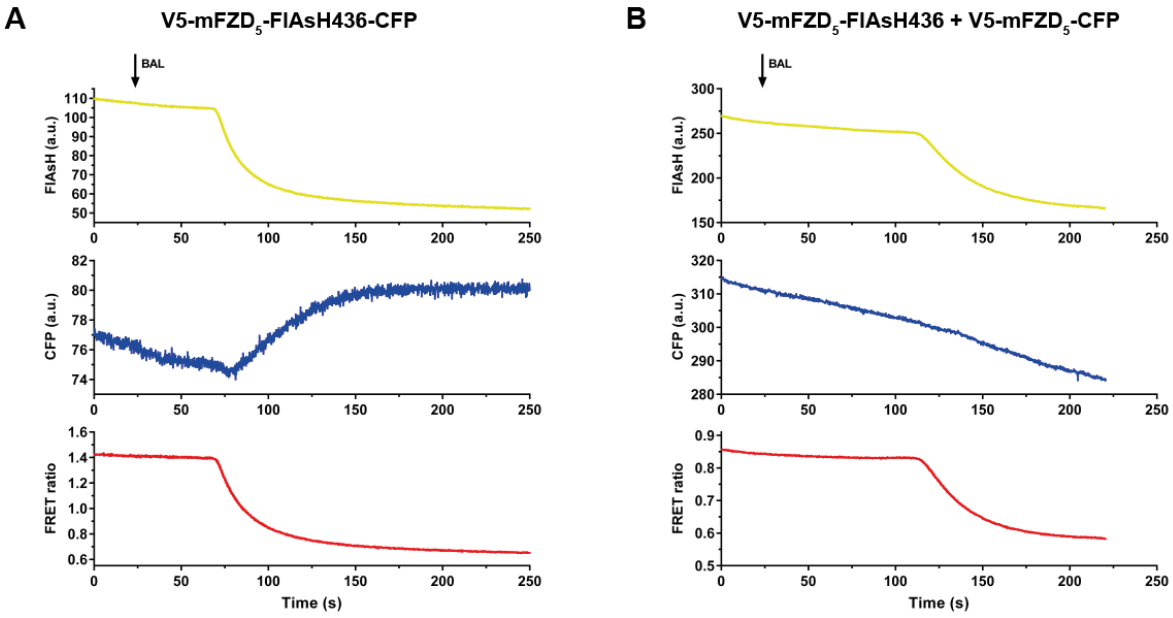
A
V5-mFZD5-FlAsH436-CFP
BAL
FlAsH (a.u.)
CFP (a.u.)
FRET ratio
Time (s)
B
V5-mFZD5-FlAsH436 + V5-mFZD5-CFP
BAL
FlAsH (a.u.)
CFP (a.u.)
FRET ratio
Time (s)

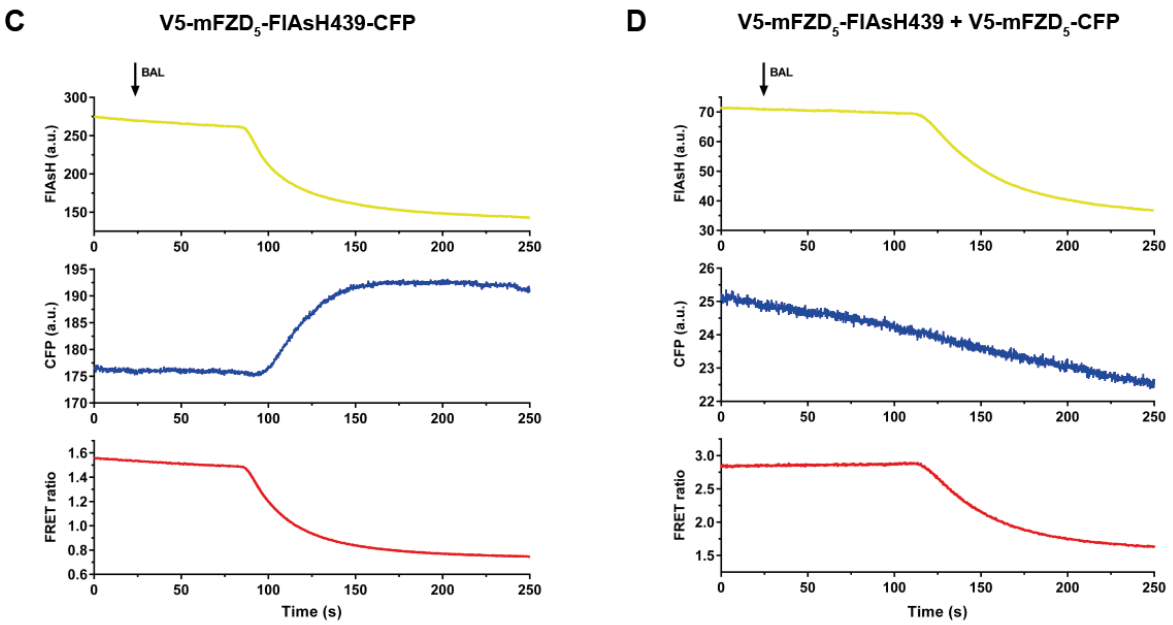
C
V5-mFZD5-FlAsH439-CFP
BAL
FlAsH (a.u.)
CFP (a.u.)
FRET ratio
Time (s)
D
V5-mFZD5-FlAsH439 + V5-mFZD5-CFP
BAL
FlAsH (a.u.)
CFP (a.u.)
FRET ratio
Time (s)

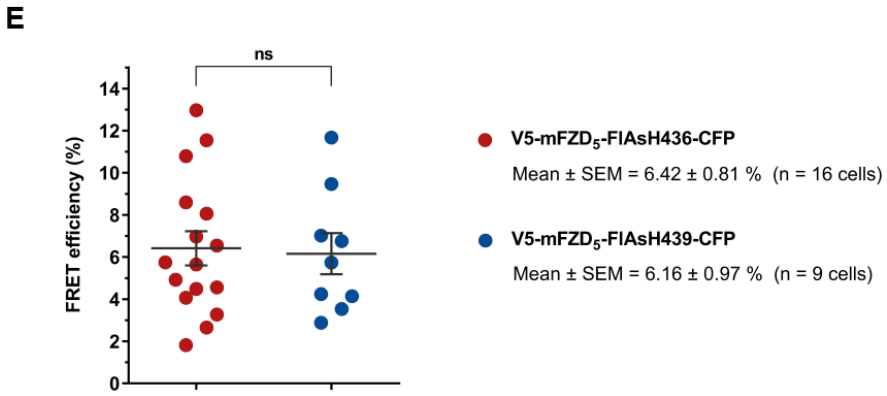
E
ns
FRET efficiency (%)
V5-mFZD5-FlAsH436-CFP
Mean ± SEM = 6.42 ± 0.81 % (n = 16 cells)
V5-mFZD5-FlAsH439-CFP
Mean ± SEM = 6.16 ± 0.97 % (n = 9 cells)

Figure 12. Determination of basal energy transfer.

FRET efficiency was determined by adding the compound BAL (2,3-dimercapto-1-propanol) to HEK293 cells overexpressing the corresponding receptor FRET sensor, V5-mFZD$_5$-FlAsH436-CFP **(A)** or V5-mFZD$_5$-FlAsH439-CFP **(C)**. BAL displaces FlAsH from its binding site in the receptor, which leads to a decrease in the acceptor fluorescence and, consequently, a recovery in CFP emission. This increase in CFP fluorescence can be observed for both FRET sensors, which indicates basal intramolecular FRET. No basal intermolecular FRET was detected when HEK293 cells co-expressed the receptor V5-mFZD$_5$-CFP with the individual constructs V5-mFZD$_5$-FlAsH436 **(B)** or V5-mFZD$_5$-FlAsH439 **(D)**. Graphics **(A-D)** correspond to representative experiments and show raw data for CFP and FlAsH emission, being FRET determined as FlAsH/CFP ratio. FRET efficiency was calculated using the following equation: (CFP*max*-CFP*min*)/CFP*max**100. **(E)** Data from individual experiments were determined for V5-mFZD$_5$-FlAsH436-CFP (n=16 cells) and for V5-mFZD$_5$-FlAsH439-CFP (n=9 cells). Data are shown as a dot scatter plot, represented as mean ± SEM. No significant difference in FRET efficiency was detected for the two receptor sensors. ns: non-significant (two-tailed unpaired t test). This material has been published in: Wright and Alonso-Cañizal et al., 2018.

4.1.2.4. FZD$_5$-induced DVL phosphorylation and recruitment

DVL is an essential component of the WNT signaling pathways that participates in both, canonical and non-canonical signaling. DVL can bind at different positions in the C-terminus and in the ICL-3 of the FZD$_5$ receptor (Tauriello et al., 2012), so the question arose if the insertion of the fluorophores could affect the interaction between the FZD$_5$ constructs and DVL. In order to investigate that possibility, HEK293 cells stably expressing the receptors V5-mFZD$_5$-CFP or V5-mFZD$_5$-FlAsH436-CFP were stimulated with the recombinant ligand WNT-3A or WNT-5A (**Fig. 13A**). CK1ε has been shown to bind and to phosphorylate DVL upon stimulation with WNTs, which leads to the emergence of a new population of phosphorylated DVL protein (Bryja et al., 2007; González-Sancho et al., 2004). In the case of V5-mFZD$_5$-CFP, upon ligand stimulation, the phosphorylation of DVL resulted in a reduction of its electrophoretic mobility that could not be observed for V5-mFZD$_5$-FlAsH436-CFP. This suggests that the insertion of the FlAsH-binding sequence within ICL-3 interferes with the interaction between FZD$_5$ and DVL.

To further evaluate these results, the ability of the different receptor constructs to mediate DVL recruitment to the plasma membrane was analyzed (**Fig. 13B**). DVL can be found in the cell in a punctate or even appearance, depending on CK1ε or the WNT protein. However, when a FZD receptor is overexpressed in the same cell, DVL relocates to the membrane in the absence of ligand (Bernatík et al., 2014; Bryja et al., 2007). Therefore, the distinctive distribution patterns allow to investigate the recruitment of DVL induced by FZD_5. As expected from the previous data, cells expressing either the wild-type FZD_5 or the receptor with CFP showed FLAG-DVL1 localization to the plasma membrane. On the contrary, V5-mFZD_5-FlAsH436-CFP was not capable of inducing this phenotype. A similar result was observed when cells were transfected with GFP-DVL2. Neither V5-mFZD_5-FlAsH436-CFP nor V5-mFZD_5-FlAsH439-CFP were able to induce DVL2 recruitment to the plasma membrane. Interestingly, when GFP-DVL3 was co-expressed in cells with the different receptors, it was mainly found in the intracellular compartments, in punctate appearance. Not even the wild-type receptor could induce the recruitment of this protein, which might suggest that DVL3 biology is slightly different to DVL1 and DVL2 with regards to FZD_5 receptor. However, DVL3 has been shown before to be recruited by FZD_5 (Bernatík et al., 2014), which would open the possibility that the structure or function of the DVL3 protein used for these experiments is disturbed, maybe because of the insertion of the GFP. Quantification of the DVL2 distribution is shown in **figure 13C**. No difference was observed for the two FZD_5 receptor sensors, being none of them able to induce DVL recruitment to the plasma membrane.

Altogether, the characterization of the FZD_5 receptor FRET-based sensors indicate that they can be used to investigate the conformational movements that occur in the receptor upon ligand stimulation. From this point on, all FRET experiments regarding receptor activation have been performed in HEK293 cells stably expressing either the probe V5-mFZD_5-FlAsH436-CFP or V5-mFZD_5-FlAsH439-CFP.

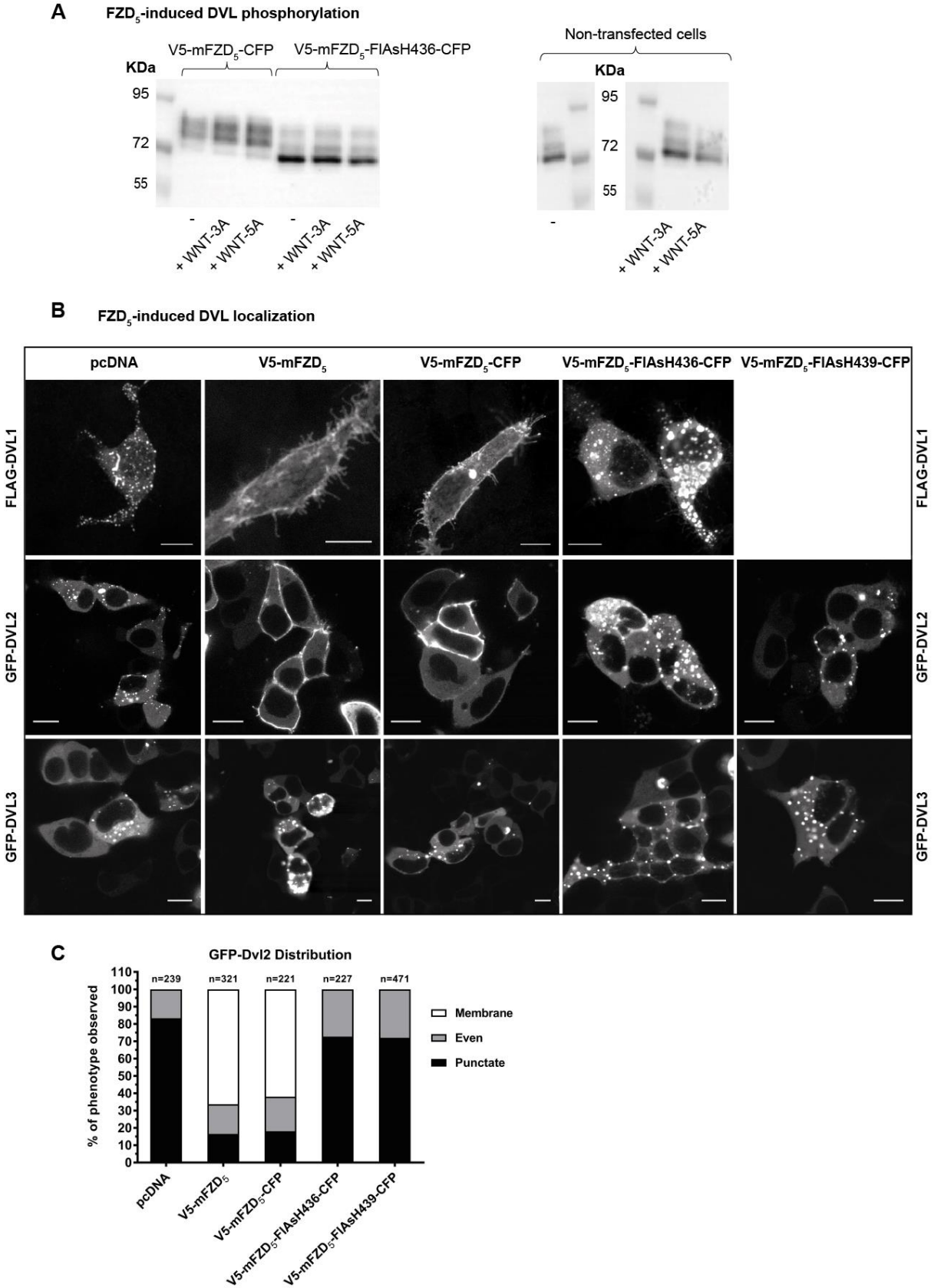
A
FZD5-induced DVL phosphorylation
V5-mFZD5-CFP
V5-mFZD5-FlAsH436-CFP
KDa
95
72
55
-
+ WNT-3A
+ WNT-5A
-
+ WNT-3A
+ WNT-5A
Non-transfected cells
KDa
95
72
55
-
+ WNT-3A
+ WNT-5A
B
FZD5-induced DVL localization
pcDNA
V5-mFZD5
V5-mFZD5-CFP
V5-mFZD5-FlAsH436-CFP
V5-mFZD5-FlAsH439-CFP
FLAG-DVL1
GFP-DVL2
GFP-DVL3
C
GFP-Dvl2 Distribution
% of phenotype observed
n=239
n=321
n=221
n=227
n=471
Membrane
Even
Punctate
pcDNA
V5-mFZD5
V5-mFZD5-CFP
V5-mFZD5-FlAsH436-CFP
V5-mFZD5-FlAsH439-CFP

Figure 13. FZD_5-induced DVL phosphorylation and recruitment.

(A) Non-transfected HEK293 cells or cells stably expressing the receptors V5-mFZD_5-CFP or V5-mFZD_5-FlAsH436-CFP were stimulated with the recombinant protein WNT-3A or WNT-5A. In the case of the receptor with CFP, stimulation with WNTs led to the phosphorylation of DVL, which translated into a reduction of its electrophoretic mobility. In contrast, the sensor V5-mFZD_5-FlAsH436-CFP was not able to induce DVL phosphorylation. Data correspond to a representative experiment that was repeated at least on three independent days. Phosphorylation of DVL was detected with an antibody against endogenous DVL2. **(B)** Representative images of the cellular localization of DVL in the absence of WNTs, when the distinct FZD_5 receptor constructs were overexpressed. While the original construct V5-mFZD_5 and the receptor with CFP were both able to mediate the translocation of DVL1 and DVL2 to the plasma membrane, none of the sensors was capable of inducing that phenotype. When V5-mFZD_5-FlAsH436-CFP or V5-mFZD_5-FlAsH439-CFP were overexpressed, DVL appeared in the cells as punctate or even conformation, similarly to the phenotype observed in the absence of receptor. In the case of GFP-DVL3, no recruitment of the protein to the plasma membrane could be observed in any condition. **(C)** Quantification of GFP-DVL2 distribution in cells. 'n' indicates the number of cells analyzed for each condition. Part of this material has been published in: Wright and Alonso-Cañizal et al., 2018.

4.1.3. FZD_5 receptor undergoes conformational changes upon activation

Many studies involving receptor structures have identify a common feature for GPCR activation. Upon agonist stimulation, the receptor undergoes a structural rearrangement, particularly a relative movement between helix III and VI, which opens the receptor at its cytosolic side, allowing the interaction with G proteins and other intracellular partners (Lohse et al., 2014; Venkatakrishnan et al., 2013; Kobilka, 2007). Crystallization of the SMO receptor (Huang et al., 2018), a distant member of the Frizzled family, confirmed that this movement, and thus the activation process, is also conserved in class F of GPCRs. However, the recent crystal structure of FZD_4 (Yang et al., 2018) showed an unusual architecture of this receptor that might suggest a different activation mechanism for Frizzled.

In order to investigate the conformational changes that the FZD_5 receptor undergoes upon activation, single HEK293 cells stably expressing the sensor V5-mFZD_5-FlAsH436-CFP were stimulated with a saturating concentration of the recombinant protein WNT-5A by using the BioPen microfluidic system (Ainla et al., 2012; Ainla et al., 2010). This device allows ligand perfusion to individual cells with an exchange time between solutions of sub-seconds. CFP and FlAsH fluorescence emissions from single cells were recorded over time, and FRET was measured as a FlAsH/CFP ratio. Upon WNT-5A (2000ng/ml) stimulation, FZD_5 undergoes rapid conformational changes, with a 3-4% decrease in the FRET ratio (**Fig. 14A**). An example of the individual traces of CFP and FlAsH from a single cell is shown in **figure 14B**. This behavior is similar to the ones observed for other class A and B GPCRs using the same technique (Ziegler et al., 2011; Vilardaga et al., 2003), which would indicate that the activation mechanism of FZD_5 resembles the general characteristics of GPCR activation.

It is noticeable that there is a delay from the moment when the ligand is applied to the observed decrease in the FRET signal, which occurred 10-20 seconds after WNT-5A addition, depending on the experiment. In addition, once the WNT protein is removed, the FRET signal does not comes back rapidly to baseline, as seen in other receptors, which might indicate a high binding affinity between FZD_5 and WNT-5A.

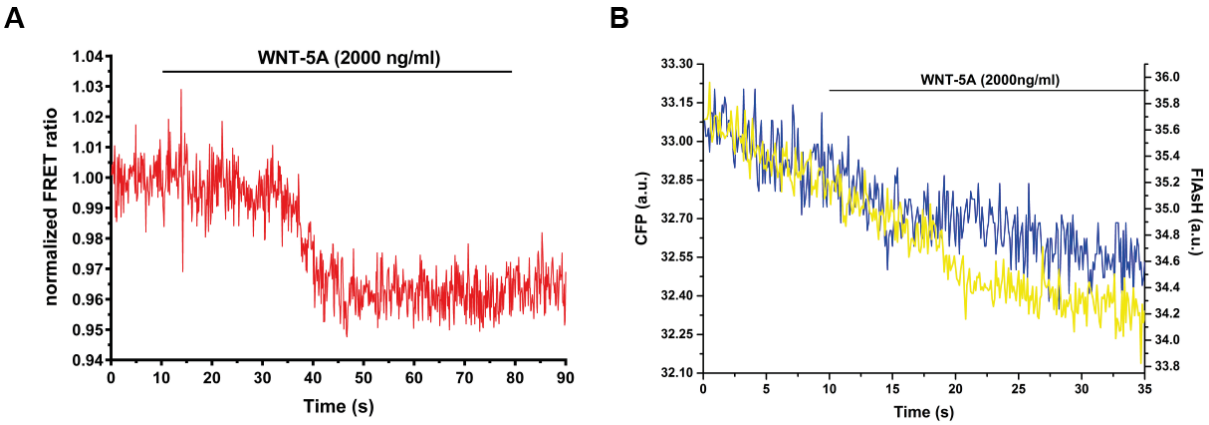

Figure 14. WNT-5A induces FZD_5 receptor activation.

(A) Normalized FRET ratio from a representative experiment, corresponding to a single HEK293 cell stably expressing the sensor V5-mFZD_5-FlAsH436-CFP. Upon stimulation with WNT-5A (2000ng/ml), the receptor underwent a structural rearrangement that translated into a 4% decrease in the FRET signal. **(B)** CFP and FlAsH emission intensities from a different cell. Upon ligand addition, an anti-parallel movement of both fluorescence signals was observed, which led to a change in FRET. This material has been published in: Wright and Alonso-Cañizal et al., 2018.

4.1.4. Measuring FZD_5 activation in a microplate reader

To further analyze the relationship between WNT-5A concentration and the structural rearrangements in the receptor, FRET experiments were performed in a 96-well microplate FRET reader. HEK293 cells stably expressing either the sensor V5-mFZD$_5$-FlAsH436-CFP or V5-mFZD$_5$-FlAsH439-CFP were placed in 96-well plates and stimulated with increasing concentrations of the recombinant ligand WNT-5A. FRET signals were monitored over time, before and after ligand addition, which allowed to observe a similar concentration-dependent FRET change for both sensors. Two representative graphics of these experiments are shown in **figure 15**, for V5-mFZD$_5$-FlAsH436-CFP (**A**) and V5-mFZD$_5$-FlAsH439-CFP (**B**), showing that both receptor sensors undergo a similar conformational change, with a 4% FRET change at saturating concentrations. The effect of different concentrations of ligand on receptor activation can be noted in **figure 15C-D**, where representative FRET signals from individual wells are shown. Concentration-response graphics from experiments repeated on independent days (n=3-6) are displayed in **figure 15E-F**.

The EC_{50} [95% CI] values obtained for receptor activation are comparable for the two FZD_5 sensors: 704.4 [454.3 - 1092.2] ng/ml for V5-mFZD$_5$-FlAsH436-CFP and 699.3 [518.0 - 944.1] ng/ml for V5-mFZD$_5$-FlAsH439-CFP (**Table 1**). Considering a molecular weight of 38KDa for WNT-5A, the calculated EC_{50} values were transformed to molar concentrations. Therefore, WNT-5A ligand activates FZD_5 receptor and the EC_{50} value for this process is found in the low nanomolar range, similarly to what has been observed for other GPCRs. No difference in activation was observed between the two FZD_5 FRET-based sensors (**Fig. 15G**).

Table 1. EC_{50} [95% CI] values for receptor activation determined for both FZD_5 sensors.

Receptor construct	EC_{50} (ng/ml)	Asymmetric CI (95%)	EC_{50} (nM)	Asymmetric CI (95%)
V5-mFZD$_5$-FlAsH436-CFP (n=6)	704.4	454.3 - 1092.2	18.5	12.0 - 28.7
V5-mFZD$_5$-FlAsH439-CFP (n=3)	699.3	518.0 - 944.1	18.4	13.6 - 24.8

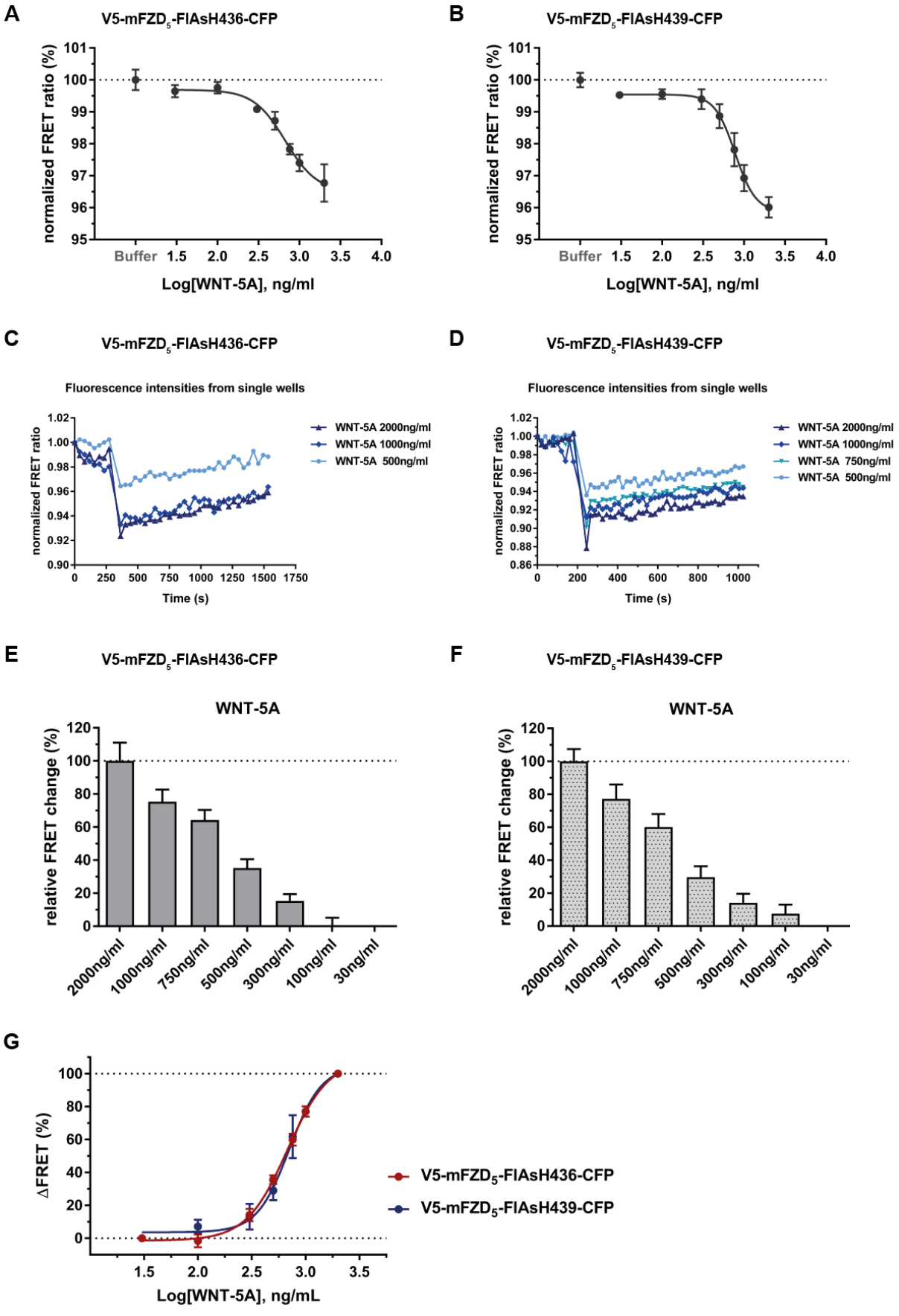
A
V5-mFZD5-FlAsH436-CFP
normalized FRET ratio (%)
Buffer
Log[WNT-5A], ng/ml
B
V5-mFZD5-FlAsH439-CFP
normalized FRET ratio (%)
Buffer
Log[WNT-5A], ng/ml
C
V5-mFZD5-FlAsH436-CFP
Fluorescence intensities from single wells
normalized FRET ratio
Time (s)
WNT-5A 2000ng/ml
WNT-5A 1000ng/ml
WNT-5A 500ng/ml
D
V5-mFZD5-FlAsH439-CFP
Fluorescence intensities from single wells
normalized FRET ratio
Time (s)
WNT-5A 2000ng/ml
WNT-5A 1000ng/ml
WNT-5A 750ng/ml
WNT-5A 500ng/ml
E
V5-mFZD5-FlAsH436-CFP
WNT-5A
relative FRET change (%)
2000ng/ml
1000ng/ml
750ng/ml
500ng/ml
300ng/ml
100ng/ml
30ng/ml
F
V5-mFZD5-FlAsH439-CFP
WNT-5A
relative FRET change (%)
2000ng/ml
1000ng/ml
750ng/ml
500ng/ml
300ng/ml
100ng/ml
30ng/ml
G
ΔFRET (%)
Log[WNT-5A], ng/mL
V5-mFZD5-FlAsH436-CFP
V5-mFZD5-FlAsH439-CFP

Figure 15. Both FZD_5 receptor sensors show comparable activation properties upon WNT-5A stimulation.

(A-G) FRET experiments performed in a 96-well microplate FRET-reader with cells stably expressing the receptor sensors V5-mFZD$_5$-FlAsH436-CFP or V5-mFZD$_5$-FlAsH439-CFP. Both sensors undergo conformational changes upon stimulation with WNT-5A, which are concentration-dependent. **(A-B)** Representative experiments, with an EC_{50} for receptor activation of 556.6ng/ml for V5-mFZD$_5$-FlAsH436-CFP and 777.1ng/ml for V5-mFZD$_5$-FlAsH439-CFP. **(C-D)** Normalized, but non-corrected, FRET signals from individual wells of a 96-well plate. Graphics are representative experiments showing the impact of different concentrations of WNT-5A on FZD_5 receptor activation. **(E-F)** Concentration-response graphics summarizing experiments performed on independent days: six times for V5-mFZD$_5$-FlAsH436-CFP and three times for V5-mFZD$_5$-FlAsH439-CFP. FRET change produced upon stimulation with distinct concentration of ligand has been normalized to the highest concentration. **(G)** No difference in activation was observed between both receptor sensors upon stimulation with WNT-5A. Data were quantify from 3-6 independent experiments performed in quadruplicate, and are represented as mean ± SEM. Part of this material has been published in: Wright and Alonso-Cañizal et al., 2018.

4.1.5. $G\alpha_q$ titration

G proteins are frequently found close to the plasma membrane, sometimes even pre-assembled to receptors in a resting state before ligand stimulation. Therefore, and as a previous step to study the downstream signaling pathways, the possibility of FZD_5 being pre-coupled to G proteins was investigated. FZD_5 was found to be pre-coupled to $G\alpha_q$ protein, but not to $G\alpha_{i1}$, by means of using FRAP microscopy (Wright and Alonso-Cañizal et al., 2018). Thus, the presence or absence of the G proteins in the intracellular side of the receptor might affect the basal conformation of the FZD_5 FRET sensors. To test this possibility, HEK293 cells stably expressing the sensor V5-mFZD_5-FlAsH436-CFP were transfected with constant concentrations of $G\beta_1$ and $G\gamma_2$ subunits, and increasing concentrations of the $G\alpha_q$ subunit. Basal FRET was measured in 96-well plates without ligand stimulation (**Fig. 16**). It was not possible to observe any difference in the basal FRET detected for the different conditions, which might be due to the small size of the FlAsH reagent, whose insertion does not significantly alter the structure of the receptor.

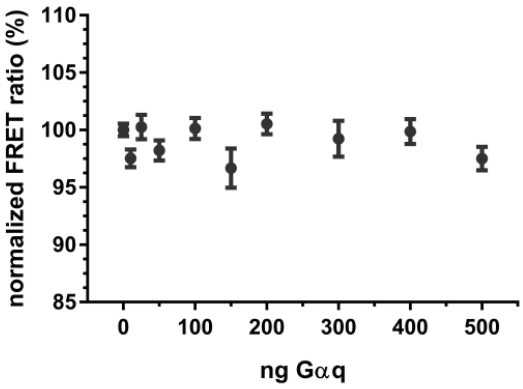

Figure 16. $G\alpha_q$ titration.

Representative experiment showing the effect of $G\alpha_q$ protein concentration on receptor conformation in the absence of ligand. No effect on the basal FRET observed for the sensor V5-mFZD_5-FlAsH436-CFP was detected when cells were transfected with the three subunits of the G protein: $G\beta_1$, $G\gamma_2$ and increasing concentrations of $G\alpha_q$.

4.2. Activation of FZD_5-mediated downstream signaling pathways

4.2.1. FZD_5 mediates $G\alpha_q$ protein activation upon WNT-5A stimulation

One characteristic of many GPCRs is their ability to activate heterotrimeric G proteins. A direct approach to investigate G protein activity is the use of genetically encoded FRET-based sensors. Upon ligand stimulation, the active receptor mediates the dissociation between Gα and Gβγ subunits, which translates into the loss of energy transfer between the fluorophores attached to the Gα and Gγ.

As previously mentioned, FZD_5 was found to be pre-coupled to $G\alpha_q$ proteins in the absence of ligand (Wright and Alonso-Cañizal *et al.*, 2018). In addition, the ligand WNT-5A has been previously shown to induce calcium release and signaling mediated by FZD receptors, particularly in Xenopus and Zebrafish embryos (Seitz et al., 2014; Kohn and Moon, 2005; Slusarski et al., 1997). Many GPCRs are able to induce the activation of the $G\alpha_q$- and PKC-dependent signaling pathway, one of whose outcomes is the release of calcium from the intracellular stores. To investigate the activation of $G\alpha_q$ protein mediated by FZD_5 receptor in real-time, FRET-based sensors for $G\alpha_q$ and the three isoforms of $G\alpha_i$ were used (van Unen et al., 2016; Adjobo-Hermans et al., 2011). These sensors consist of a Gα subunit fused to the fluorophore mTurquoise, a brighter CFP variant that acts as donor, an untagged Gβ subunit, and a Gγ subunit tagged with the fluorophore Venus, which acts as acceptor.

4.2.1.1. Single-cell FRET measurements

HEK293 cells were co-transfected with V5-mFZD_5 receptor and the $G\alpha_q$ sensor, and single cells were used for FRET experiments. Upon stimulation with a saturating concentration of WNT-5A (1000ng/ml), by means of using the BioPen microfluidic system, the dissociation between $G\alpha_q$ and Gβγ subunits led to an antiparallel movement between mTurquoise and Venus emission intensities, which translated into a decrease in the FRET ratio (**Fig. 17A**). Consistent with the previous results obtained for FZD_5 receptor activation, there was a delay of few seconds since the perfusion of the ligand started until the FRET change was detected. No activation of $G\alpha_q$, and thus no change in FRET, was observed when the receptor was not overexpressed in the cells (**Fig. 17B**). Since FZD_5 was not found to be pre-coupled to $G\alpha_{i1}$ proteins, as a control, cells were co-transfected with V5-mFZD_5 receptor and the $G\alpha_{i1}$ sensor (**Fig. 17C**). No response was detected in single-cells upon stimulation with the ligand, which suggests that WNT-5A induces FZD_5-mediated activation of $G\alpha_q$ but not $G\alpha_{i1}$ proteins.

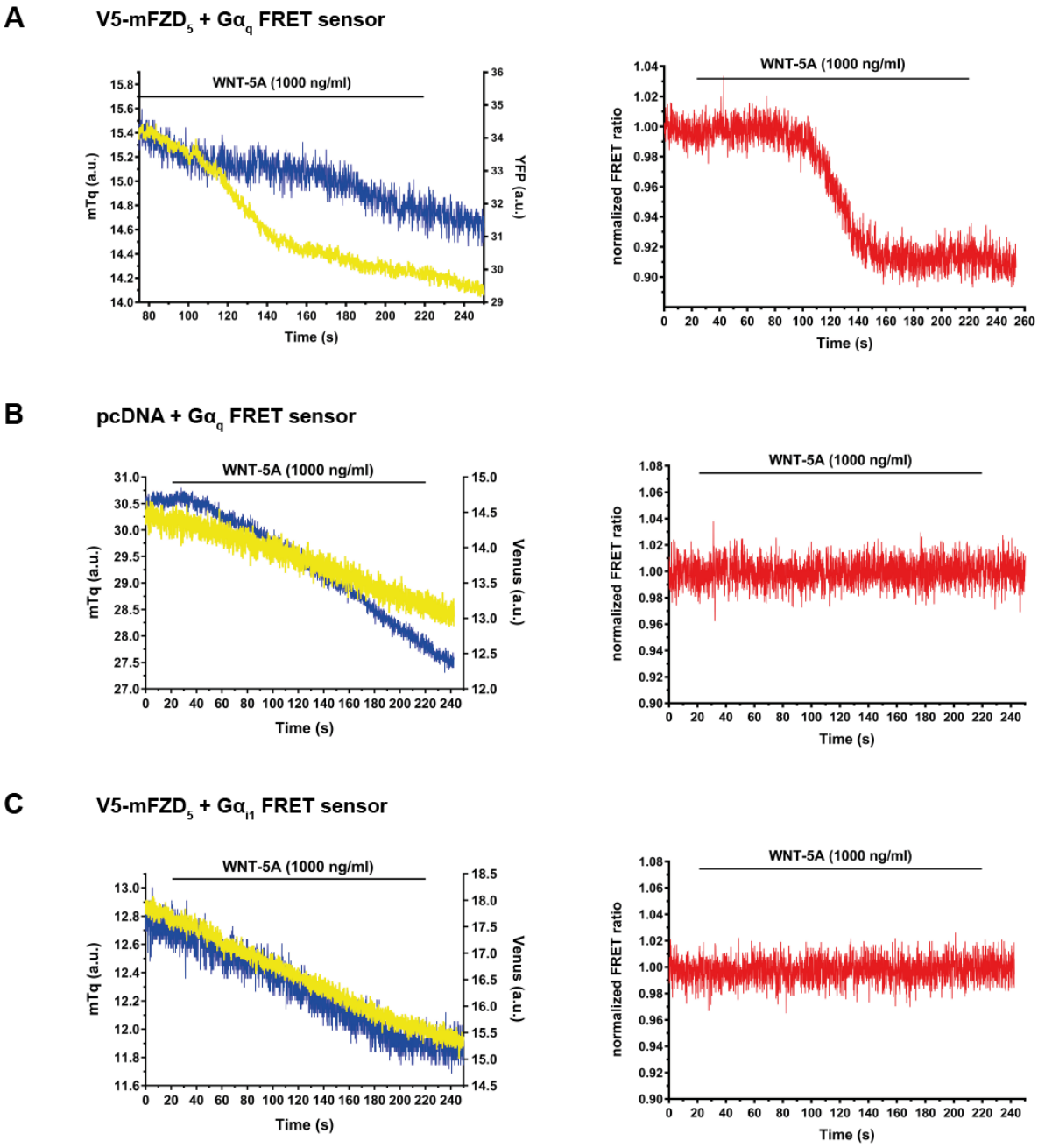

Figure 17. WNT-5A induces Gα$_q$ activation, but not Gα$_{i1}$, mediated by FZD$_5$.

(A-C) Representative graphics showing single-cell FRET experiments. **(A)** Cells co-transfected with the V5-mFZD$_5$ receptor and the Gα$_q$ protein FRET sensor. Upon activation by WNT-5A, the dissociation of the G protein subunits led to a decrease in the FRET ratio. **(B)** No activation of Gα$_q$ and thus no decrease in the FRET ratio was detected in the absence of receptor, when cells co-expressing pcDNA and the Gα$_q$ protein FRET sensor were stimulated with WNT-5A. **(C)** Upon stimulation with the ligand, no activation was observed in cells co-transfected with the V5-mFZD$_5$ receptor and the Gα$_{i1}$ FRET sensor, which indicates no activation of Gα$_{i1}$ protein by WNT-5A. This material has been published in: Wright and Alonso-Cañizal et al., 2018.

4.2.1.2. G protein activation in 96-well plates

To further investigate the G protein activation process, FRET experiments were performed in 96-well plates. HEK293T cells were co-transfected with V5-mFZD$_5$ receptor and the Gα_q sensor, and then stimulated with increasing concentrations of WNT-5A. Similarly to what was observed in single-cell FRET experiments, WNT-5A induced Gα_q activation mediated by FZD$_5$, and the conformational change in the Gα_q protein sensor led to a change in FRET of 2.5%. A representative graphic of these experiments is shown in **figure 18A**.

Since previous experiments revealed that the FZD$_5$ receptor FRET sensors were not able to induce phosphorylation of DVL nor mediate its recruitment to the plasma membrane, the ability of the sensors to activate Gα_q proteins was investigated. HEK293T cells were co-transfected with the Gα_q sensor and the receptor construct containing the FlAsH-binding sequence but not CFP, either V5-mFZD$_5$-FlAsH436 or V5-mFZD$_5$-FlAsH439. Both receptor constructs were still functional and able to mediate Gα_q protein activation (**Fig. 18B-C**). The FRET change detected is comparable to the results obtained for the wild-type receptor (**Fig. 18D**), as well as the EC$_{50}$ [95% CI] values for G protein activation, which are summarized in **table 2**.

Table 2. EC$_{50}$ [95% CI] values for G protein activation mediated by the three FZD$_5$ receptor constructs. A molecular weight of 38KDa for the ligand WNT-5A was considered to transform the data from ng/ml to nanomolar concentrations.

Receptor construct	EC$_{50}$ (ng/ml)	Asymmetric CI (95%)	EC$_{50}$ (nM)	Asymmetric CI (95%)
V5-mFZD$_5$ (n=3)	550.8	327.0 - 927.9	14.5	8.6 - 24.4
V5-mFZD$_5$-FlAsH436 (n=3)	471.0	295.4 - 750.8	12.4	7.8 - 19.8
V5-mFZD$_5$-FlAsH439 (n=2)	653.9	170.9 - 2501.5	17.2	4.5 - 65.8

The fact that the receptor sensors can activate G proteins but not interact with DVL may suggest that, despite being an important component of the downstream signaling pathways, DVL does not contribute to the structural changes that occur in the receptor upon activation. Moreover, even though the wild-type receptor can interact with DVL, FZD_5-mediated G protein activation may be independent of that protein.

To further assess this idea, FRET experiments were performed in 96-well plates by co-expressing both, the $G\alpha_q$ sensor and the V5-mFZD_5 receptor in HEK293 DVL KO cells (**Fig. 18E**) or in HEK293 cells overexpressing the protein DVL2 (**Fig. 18F**). In line with previous results, FZD_5 appears to mediate $G\alpha_q$ activation independently of the intracellular levels of DVL.

Finally, when comparing the results (**Fig. 18G**) obtained for G protein activation mediated by FZD_5 (data normalized from 3 independent experiments) and for FZD_5 receptor activation (curve with normalized data is from figure 15G), it is noticeable that there is a shift between the two curves and that the EC_{50} for G protein activation is lower than for receptor activation. That is consistent with an amplification of the signal that generally occurs throughout a signaling cascade.

No activation of $G\alpha_{i1}$ could be detected in single-cell FRET experiments when cells co-expressed the V5-mFZD_5 receptor and the $G\alpha_{i1}$ protein sensor (**Fig. 17C**). In order to confirm these results, experiments were performed in 96-well plates by employing the three FRET sensors available for $G\alpha_i$ proteins. Therefore, HEK293T cells were co-transfected with V5-mFZD_5 receptor and the corresponding G protein sensor, $G\alpha_{i1}$, $G\alpha_{i2}$ or $G\alpha_{i3}$. Upon stimulation with increasing concentrations of WNT-5A, no significant change in FRET could be observed (**Fig. 19A-C**), which confirms that the axis WNT-5A/FZD_5 does not lead to the activation of $G\alpha_i$ proteins. The FRET change detected is comparable for the three isoforms of $G\alpha_i$ (**Fig. 19D**).

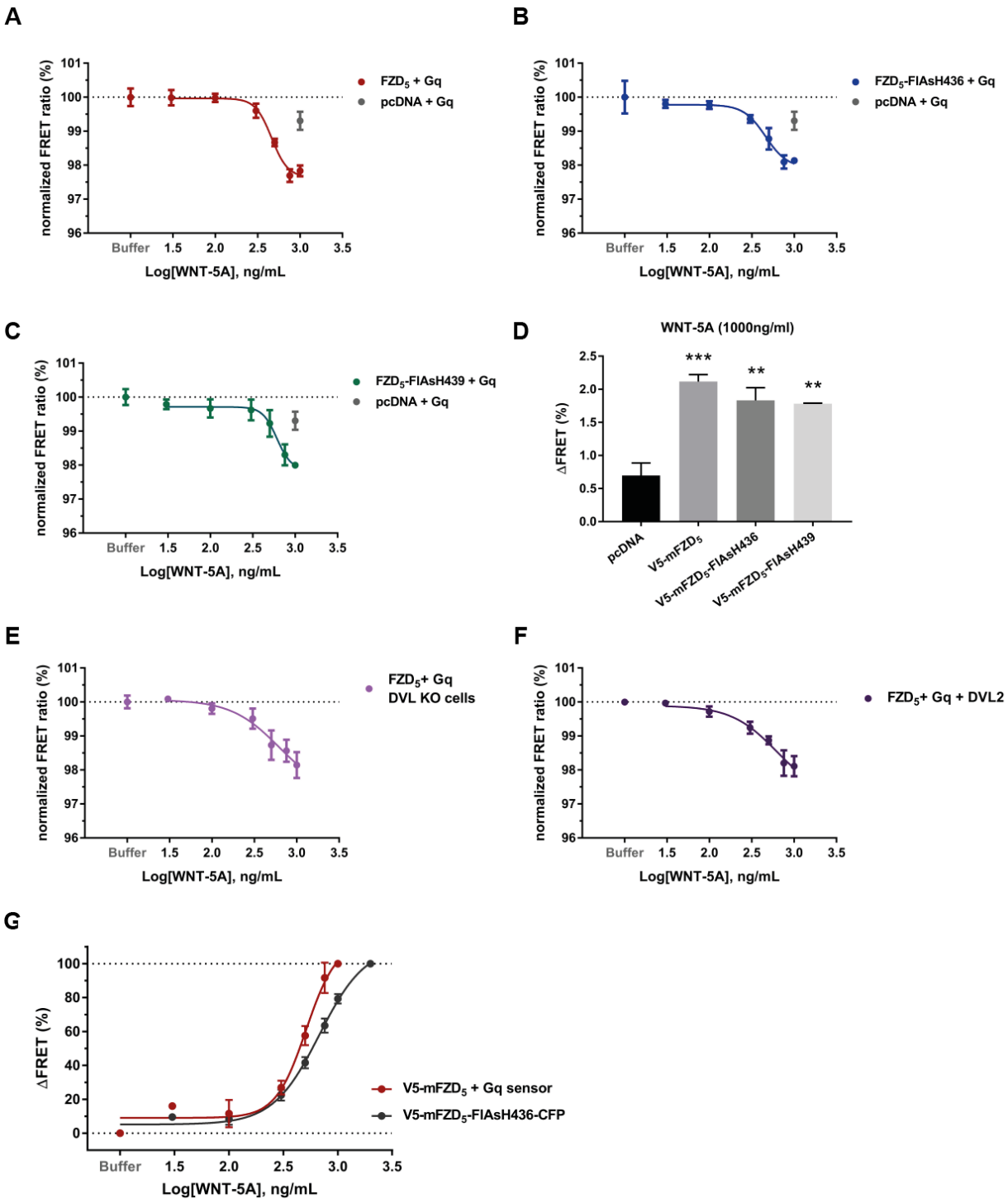
A
normalized FRET ratio (%)
FZD5 + Gq
pcDNA + Gq
Buffer 1.5 2.0 2.5 3.0 3.5
Log[WNT-5A], ng/mL
B
normalized FRET ratio (%)
FZD5-FlAsH436 + Gq
pcDNA + Gq
Log[WNT-5A], ng/mL
C
normalized FRET ratio (%)
FZD5-FlAsH439 + Gq
pcDNA + Gq
Log[WNT-5A], ng/mL
D
WNT-5A (1000ng/ml)
ΔFRET (%)
***
**
**
pcDNA
V5-mFZD5
V5-mFZD5-FlAsH436
V5-mFZD5-FlAsH439
E
normalized FRET ratio (%)
FZD5+ Gq
DVL KO cells
Log[WNT-5A], ng/mL
F
normalized FRET ratio (%)
FZD5+ Gq + DVL2
Log[WNT-5A], ng/mL
G
ΔFRET (%)
V5-mFZD5 + Gq sensor
V5-mFZD5-FlAsH436-CFP
Log[WNT-5A], ng/mL

Figure 18. $G\alpha_q$ protein activation induced by WNT-5A.

(A-C, E-F) Representative graphics showing FRET experiments performed in 96-well plates. In order to investigate the activation of $G\alpha_q$ by FZD_5, cells were transfected with the $G\alpha_q$ sensor and with the receptor construct V5-$mFZD_5$ **(A)**, V5-$mFZD_5$-FlAsH436 **(B)**, or V5-$mFZD_5$-FlAsH439 **(C)**. Upon WNT-5A stimulation, Gα and Gβγ subunits dissociate, producing a change in the FRET signal. The EC_{50} value for $G\alpha_q$ protein activation mediated by FZD_5 in these experiments is 461.6ng/ml for V5-$mFZD_5$, 448.7ng/ml for V5-$mFZD_5$-FlAsH436, and 610.5ng/ml for V5-$mFZD_5$-FlAsH439. **(D)** At saturating concentrations of the ligand WNT-5A (1000ng/ml), the three receptor constructs induced comparable FRET changes in the $G\alpha_q$ protein sensor, which indicates that the receptor sensors are functional and able to activate $G\alpha_q$ despite the insertion of the FlAsH-binding motif in ICL-3. Graphic summarizes the results from experiments performed in quadruplicate, on independent days: n=3 for V5-$mFZD_5$, n=3 for V5-$mFZD_5$-FlAsH436, and n=2 for V5-$mFZD_5$-FlAsH439. Mean ± SEM is shown. *** $P \leq 0.001$; ** $P \leq 0.01$ (one-way ANOVA). In order to evaluate if G protein activation was independent of the intracellular levels of DVL, $G\alpha_q$ activation mediated by V5-$mFZD_5$ was investigated in knock-out cells for the three DVL isoforms **(E)** and in cells overexpressing DVL2 **(F)**. In both cases, the receptor was able to mediate $G\alpha_q$ activation upon WNT-5A stimulation. **(G)** Comparison between FZD_5 receptor activation and $G\alpha_q$ protein activation. Curve of normalized data for receptor activation is the same than in figure 15G and corresponds to six independent experiments performed with the sensor V5-$mFZD_5$-FlAsH436-CFP. Curve of normalized data for $G\alpha_q$ activation mediated by FZD_5 corresponds to three independent experiments performed in quadruplicate. The observed shift in EC_{50} between both curves might be explained by signal amplification. Part of this material has been published in: Wright and Alonso-Cañizal et al., 2018.

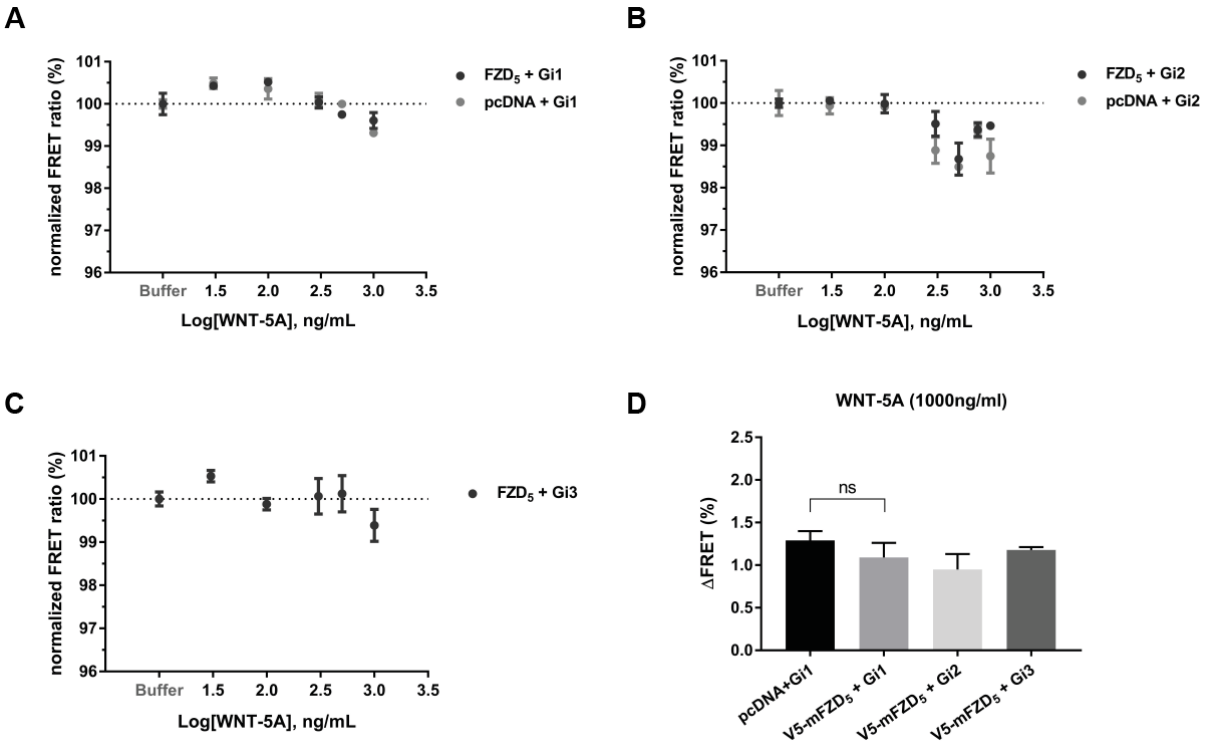

Figure 19. Gα$_i$ protein activation induced by WNT-5A.

(A-C) Representative graphics showing FRET experiments performed in 96-well plates. In order to investigate the activation of Gα$_i$ by FZD$_5$, cells were transfected with the receptor construct V5-mFZD$_5$ and the corresponding Gα$_i$ sensor, either Gα$_{i1}$ **(A)**, Gα$_{i2}$ **(B)**, or Gα$_{i3}$ **(C)**. No activation of Gα$_i$ proteins could be detected upon WNT-5A stimulation. **(D)** Comparison of FRET changes induced in the Gα$_i$ protein sensors at saturating concentrations of the ligand WNT-5A (1000ng/ml). Graphic summarizes the results from experiments performed in quadruplicate on independent days: n=4 for Gα$_{i1}$, n=3 for Gα$_{i2}$, and n=2 for Gα$_{i3}$. Mean ± SEM is shown. ns: non-significant (two-tailed unpaired t test). Part of this material has been published in: Wright and Alonso-Cañizal et al., 2018.

4.2.2. Activation of calcium signaling

The interaction between Frizzled and WNTs can activate many different intracellular routes, both β-catenin-dependent and -independent. Within this last group of non-canonical pathways, calcium signaling is one of the most studied, due to its role during embryogenesis and development (De, 2011). Whereas for many GPCRs, calcium signaling is activated in a $G\alpha_q$-dependent manner, the implication of G proteins in WNT-mediated pathways is still not well stablished.

4.2.2.1. M_3AChR-mediated signaling pathway

To further evaluate the specific activation of the PLC signaling pathway mediated by $G\alpha_q$ activation, a dual DAG/Ca^{2+} sensor was employed (Tewson et al., 2012). This sensor simultaneously detects the generation of DAG and the release of calcium from the intracellular stores: calcium binding to R-GECO induces a conformational change in this protein that leads to an increase in red fluorescence, whereas the DAG sensor consists of the C1 domain of PKC fused to GFP (**Fig. 21A**). In order to validate the potential of this probe, the M_3ACh receptor was employed. The M_3AChR is a so-called classical class A GPCR, which couples to the heterotrimeric $G\alpha_q$ protein and mediates the activation of its downstream signaling pathway (Haga, 2013; Nahorski, 2006). Thus, HEK293 cells stably expressing both the M_3AChR tagged with CFP at the C-terminus and the dual sensor were seeded in 6-well plates, onto crystal coverslips, and analyzed by confocal microscopy (**Fig. 20**). Upon stimulation with saturating concentrations of the ligand Carbachol, a fast increase in red fluorescence intensity was observed upon the rise in calcium levels, together with a decrease in the green fluorescence produced by the translocation of the PKC-GFP to the cellular membrane upon DAG generation. Quantification of these data is shown in **figure 21D**.

As a control, each of the sensors can be individually activated. Addition of ionomycin to cells expressing the dual sensor induced the release of calcium independently of the receptor, without affecting directly the DAG levels (**Fig. 21B**). On the contrary, stimulation of the cells with Phorbol 12,13-dibutyrate (PdBU), an activator of protein kinase C, produced a decrease in the green fluorescence but not an increase in red fluorescence intensity (**Fig. 21C**).

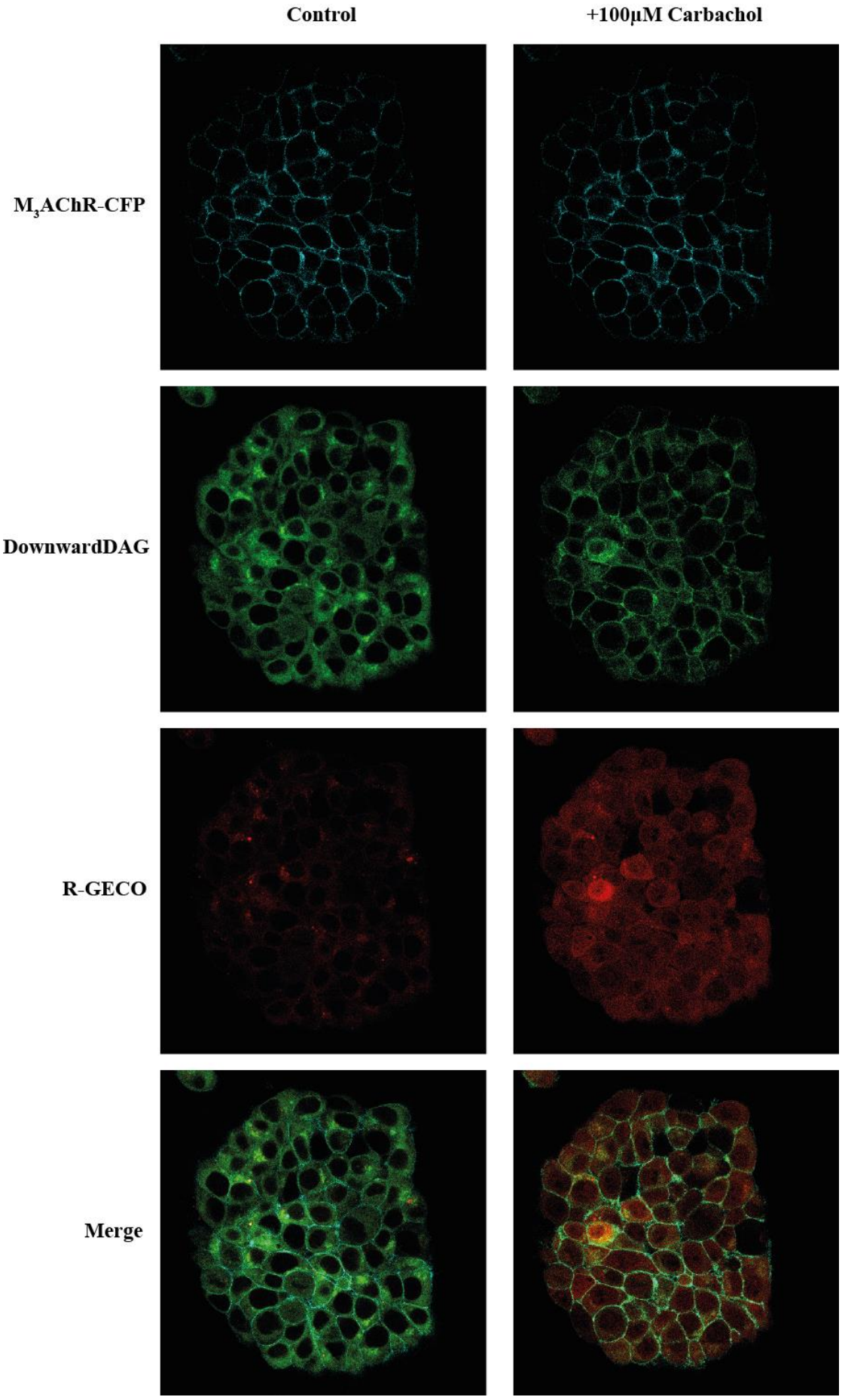
Control
+100μM Carbachol
M3AChR-CFP
DownwardDAG
R-GECO
Merge

Figure 20. Representative images of HEK293 cells stably co-expressing the M_3AChR-CFP and the dual DAG/Ca^{2+} sensor. In the absence of ligand, the green fluorescence emitted by the DAG probe is mostly localized in the cytoplasm, while the red fluorescence intensity is weak. Upon stimulation with Carbachol, the release of calcium leads to an increase in the fluorescence from R-GECO, whereas the DAG probe relocates to the plasma membrane. Description of the sensor and quantification of data are shown in figure 21.

The dual DAG/Ca^{2+} sensor proves to be a useful tool to investigate the specific activation of the M_3ACh receptor and its downstream signaling pathway. In addition, the dual probe has been used with the M_1ACh receptor, another $G\alpha_q$-coupled muscarinic receptor, in order to evaluate its activation by distinct ligands (Agnetta et al., 2017; Meserer et al., 2017).

Nevertheless, due to the biological properties of the recombinant WNT proteins, it would have not been possible to use the same setting with FZD_5 as with the muscarinic receptors. Therefore, µ-Slide 8-well plates were selected as an alternative to perform the experiments, since much less volume of ligand is needed. As a previous step, all the parameters were escalated accordingly and validated using the previously described stable cells for the M_3AChR-CFP and the dual sensor. Similarly to the results obtained before, where cells were placed onto glass coverslips, stimulation with saturating concentrations of Carbachol led to a simultaneous increase in the calcium signal and a decrease in the green fluorescence. The data were comparable when µ-Slide 8-well plates were non-coated (**Fig. 21E**) or pre-coated with poly-D-lysine (**Fig. 21F**).

Altogether, data indicate that the dual DAG/Ca^{2+} sensor is a solid tool to evaluate the activation of the $G\alpha_q$-downstream signaling pathway, which can be used in different settings and with various receptors. Hence, it emerges as a method to investigate FZD_5-mediated PKC/Ca^{2+} signaling pathway.

A

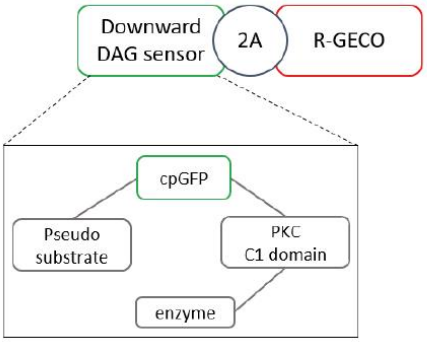
Downward
DAG sensor
2A
R-GECO
cpGFP
Pseudo
substrate
PKC
C1 domain
enzyme

B

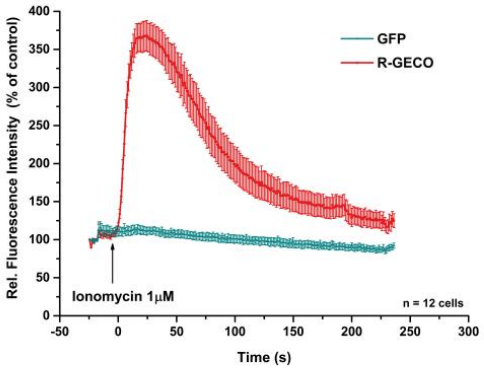
GFP
R-GECO
Rel. Fluorescence Intensity (% of control)
Ionomycin 1μM
n = 12 cells
Time (s)

C

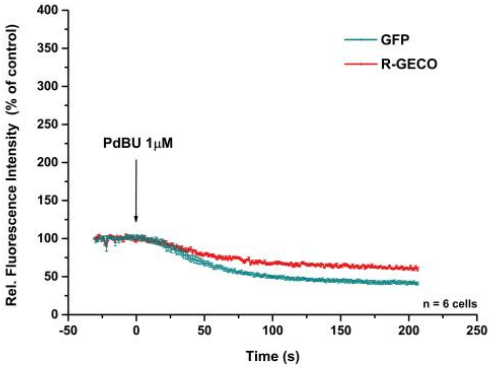
GFP
R-GECO
Rel. Fluorescence Intensity (% of control)
PdBU 1μM
n = 6 cells
Time (s)

D

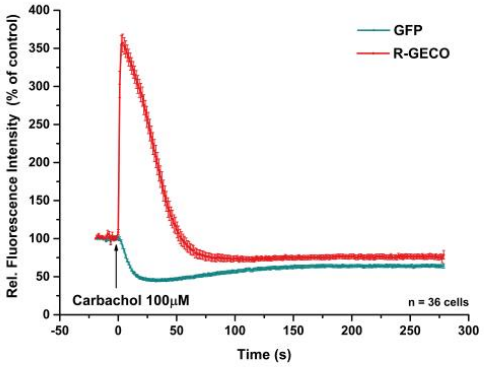
GFP
R-GECO
Rel. Fluorescence Intensity (% of control)
Carbachol 100μM
n = 36 cells
Time (s)

E

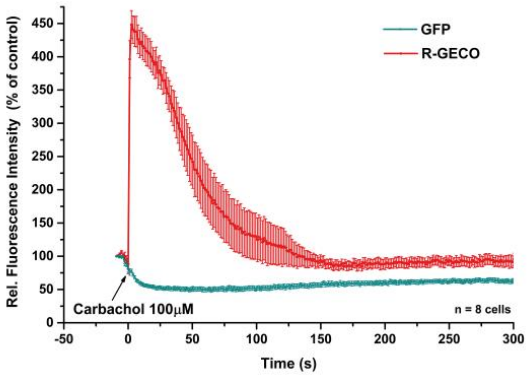
GFP
R-GECO
Rel. Fluorescence Intensity (% of control)
Carbachol 100μM
n = 8 cells
Time (s)

F

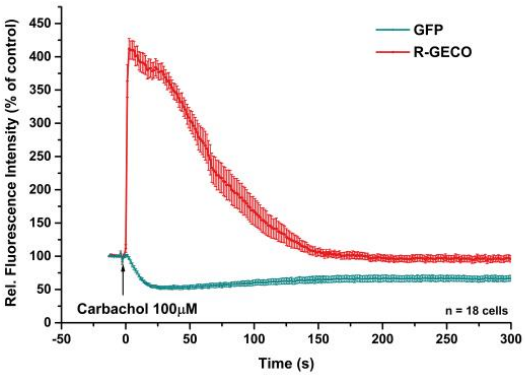
GFP
R-GECO
Rel. Fluorescence Intensity (% of control)
Carbachol 100μM
n = 18 cells
Time (s)

Figure 21. (A) Sketch depicting the dual DAG/Ca^{2+} sensor, developed by Montana Molecular (Tewson et al., 2012). It consists of two independent probes cloned in phase with a self-cleaved 2A peptide in between, thus there is a balance production of both sensors in the cells. The calcium sensor is R-GECO, a protein which undergoes a conformational change upon calcium binding that leads to an increase in red fluorescence. The DAG probe comprises a GFP fused to the C1 domain of a PKC. When activated, translocation of PKC to the membrane to bind DAG produces a decrease of the green fluorescence. **(B)** Cells overexpressing the dual sensor were stimulated with ionomycin, which led to a rise in the intracellular levels of calcium that translated into an increase in red fluorescence. No response from the DAG probe was detected. **(C)** Cells overexpressing the dual sensor were stimulated with PdBU, which led to PKC activation and produced a decrease in the green fluorescence. No response from the calcium probe was detected. **(D)** Cells overexpressing the dual sensor and M_3AChR-CFP were stimulated with saturating concentrations of the ligand Carbachol. There was a rapid and simultaneous response, with a decrease in the green and an increase in the red fluorescence. **(E-F)** Experiments were escalated to a smaller setting. Cells stably co-expressing the dual sensor and M_3AChR-CFP were placed in µ-Slide 8-well plates non-coated **(E)** or pre-coated with poly-D-lysine **(F)**, and stimulated with saturating concentrations of Carbachol. Results were comparable to what was previously observed **(D)**. Data are represented as Mean ± SEM of several cells. 'n' is indicated in the graphics.

4.2.2.2. FZD_5 mediates the activation of PKC-dependent signaling pathway.

In order to investigate the activation of the PLC pathway mediated by FZD_5, a HEK293 stable cell line was generated that co-expressed the DAG/Ca^{2+} sensor and the V5-mFZD_5 receptor tagged with CFP. In view of the difficulty of using recombinant WNT proteins, experiments were performed by using control- or WNT-5A-conditioned medium provided by Dr. Vítězslav Bryja (Masaryk University, Brno).

Stable cells expressing both the dual sensor and the V5-mFZD_5-CFP receptor were seeded onto glass coverslips placed in 6-well plates, and analyzed by confocal microscopy. Several minutes after stimulation with WNT-5A-conditioned medium, a robust increase in the red fluorescence produced by the release of calcium could be observed, accompanied by a decrease in the green fluorescence (**Fig. 22C**). The signals were detected around 15-25 minutes after ligand addition, depending on the experiment. No response was observed when the stable cells were stimulated with control medium (**Fig. 22A**). As a control, HEK293 cells expressing only the DAG/Ca^{2+} sensor, without receptor overexpression, were stimulated with WNT-5A conditioned medium (**Fig. 22B**). No response could be detected. Quantification of calcium release from several cells measured in the different conditions is shown in **figure 22D**.

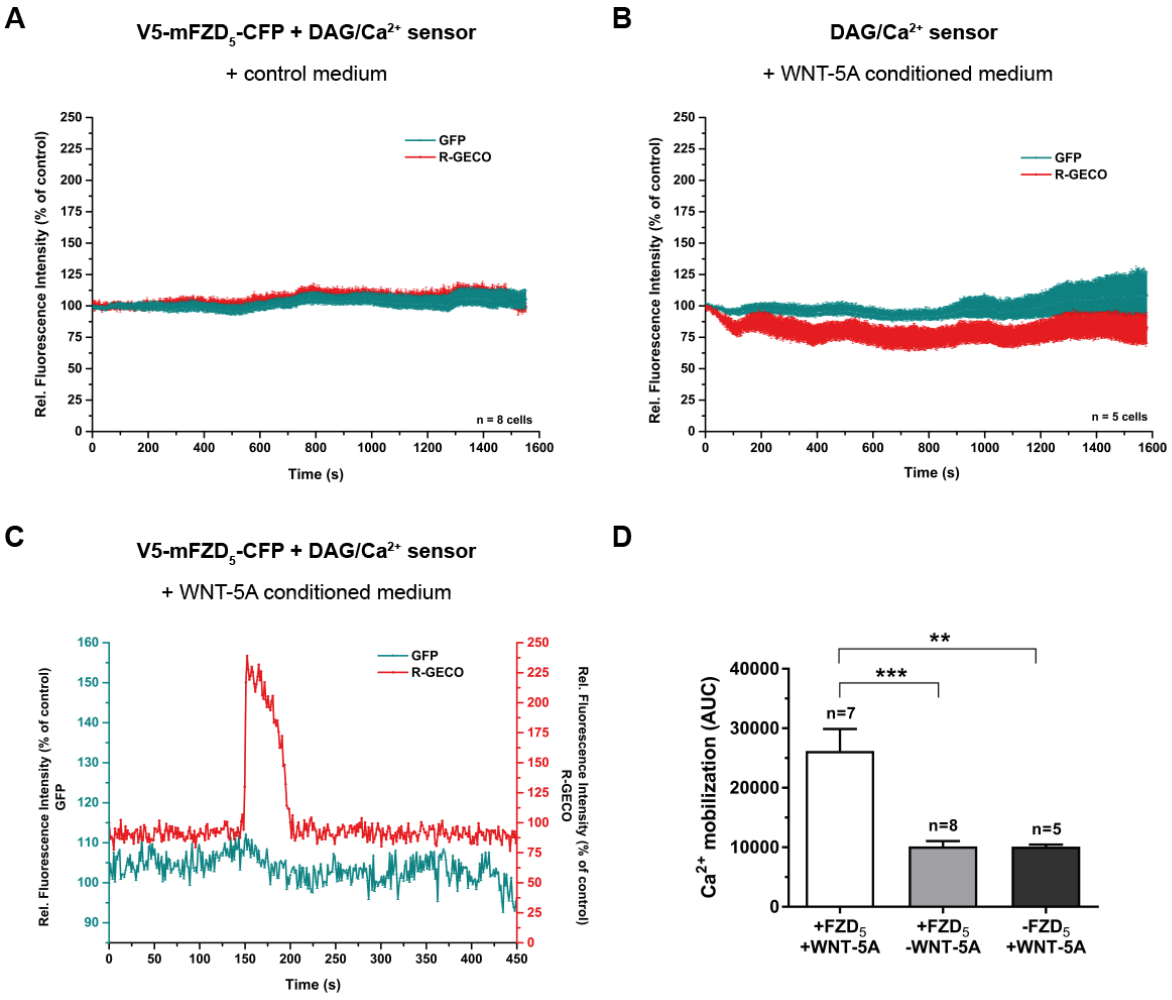

Figure 22. FZD_5 activates $G\alpha_q$-downstream effectors DAG and calcium flux

(A) Cells stably co-expressing the V5-mFZD_5-CFP receptor and the DAG/Ca^{2+} sensor were stimulated with control medium. No activation of the sensor was detected when the ligand was not present. **(B)** Cells stably expressing the DAG/Ca^{2+} sensor were stimulated with WNT-5A conditioned medium. No activation of the sensor was detected when the receptor was not present. **(C)** Representative experiment of cells stably co-expressing the V5-mFZD_5-CFP receptor and the DAG/Ca^{2+} sensor. Upon stimulation with WNT-5A-conditioned medium, a simultaneous DAG-dependent signal and an increase in intracellular calcium were detected. The cellular responses were observed 15-25 minutes after ligand stimulation, depending on the analyzed cell. **(D)** Data for calcium release in several cells were quantified. A significant difference was observed in comparison to the control conditions. *** $P \leq 0.001$; ** $P \leq 0.01$ (unpaired t test).

4.3. Characterization of FZD_5 activation and signaling by WNT proteins.

4.3.1. FZD_5 receptor activation

The previous results obtained with the endogenous agonist WNT-5A suggest that the FZD_5 receptor FRET sensors could be used as a readout to test the effect of other ligands on receptor activation. To further investigate this possibility, several recombinant WNT proteins were employed. As it was previously described in section 4.1.4, similar results were obtained regarding receptor activation when HEK293 cells stably expressing either the sensor V5-mFZD_5-FlAsH436-CFP or V5-mFZD_5-FlAsH439-CFP were stimulated with WNT-5A. While the cells expressing the second sensor belong to a heterogeneous cell line, the cells expressing the first sensor correspond to a homogenous clone. Therefore, stable cells for the receptor V5-mFZD_5-FlAsH436-CFP were selected to perform further experiments.

Cells were placed in a microplate FRET reader, and the FRET emission was detected before and after stimulation with increasing concentrations of WNTs. Representative graphics of receptor activation induced by each of the tested ligands are displayed in **figure 23**. Upon activation by various WNTs, the receptor sensor undergoes structural rearrangements that translate into distinct FRET changes. Interestingly, co-stimulation of the corresponding WNT with the WNT-inhibitory factor 1 (WIF-1) partially reduces the FRET change detected, which underlines the idea that the activation of the sensor is specifically induced by each of the proteins.

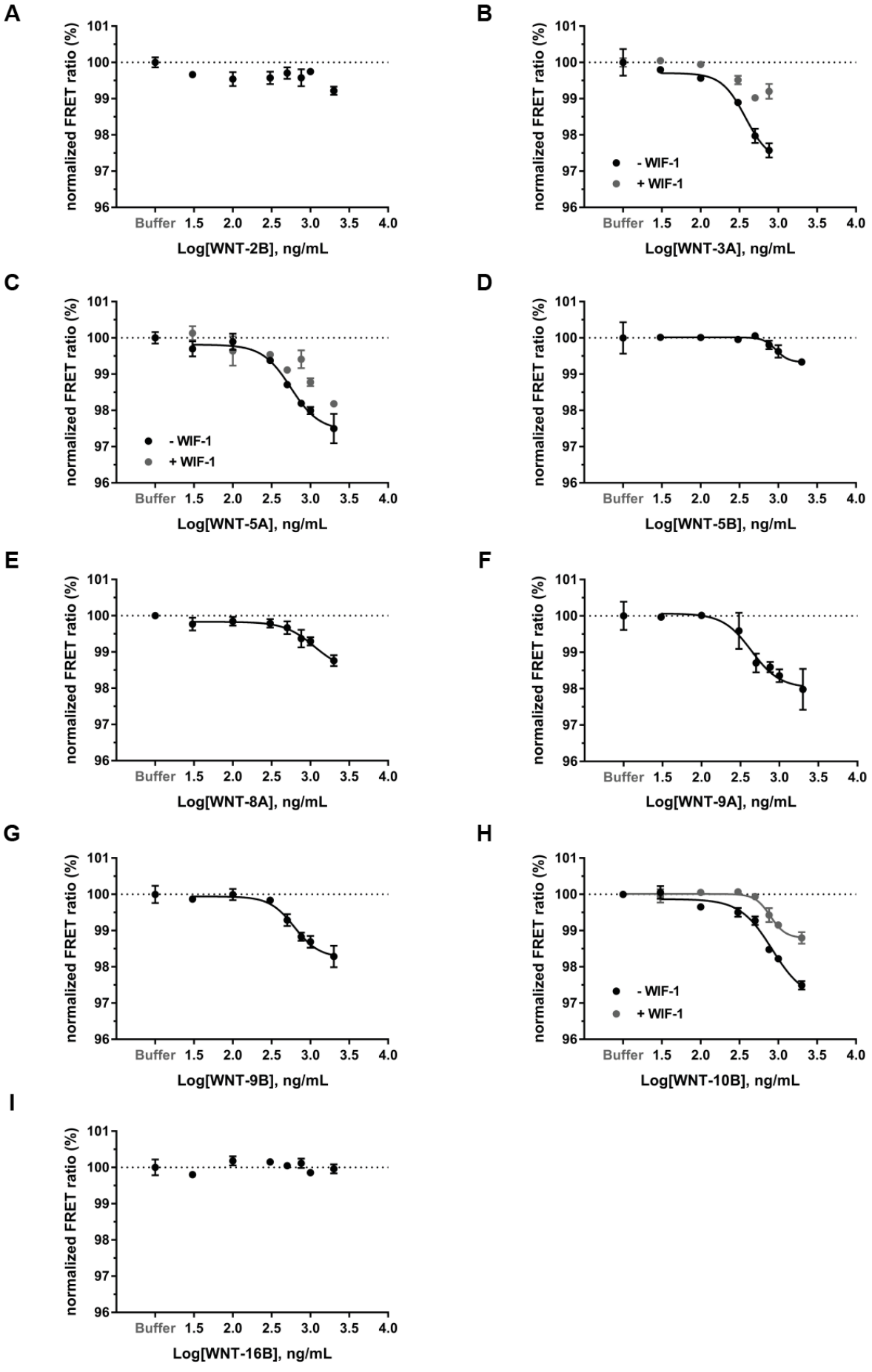
A
normalized FRET ratio (%)
101
100
99
98
97
96
Buffer 1.5 2.0 2.5 3.0 3.5 4.0
Log[WNT-2B], ng/mL
B
normalized FRET ratio (%)
- WIF-1
+ WIF-1
Buffer 1.5 2.0 2.5 3.0 3.5 4.0
Log[WNT-3A], ng/mL
C
normalized FRET ratio (%)
- WIF-1
+ WIF-1
Buffer 1.5 2.0 2.5 3.0 3.5 4.0
Log[WNT-5A], ng/mL
D
normalized FRET ratio (%)
Buffer 1.5 2.0 2.5 3.0 3.5 4.0
Log[WNT-5B], ng/mL
E
normalized FRET ratio (%)
Buffer 1.5 2.0 2.5 3.0 3.5 4.0
Log[WNT-8A], ng/mL
F
normalized FRET ratio (%)
Buffer 1.5 2.0 2.5 3.0 3.5 4.0
Log[WNT-9A], ng/mL
G
normalized FRET ratio (%)
Buffer 1.5 2.0 2.5 3.0 3.5 4.0
Log[WNT-9B], ng/mL
H
normalized FRET ratio (%)
- WIF-1
+ WIF-1
Buffer 1.5 2.0 2.5 3.0 3.5 4.0
Log[WNT-10B], ng/mL
I
normalized FRET ratio (%)
Buffer 1.5 2.0 2.5 3.0 3.5 4.0
Log[WNT-16B], ng/mL

Figure 23. WNTs selectively activate the FZD_5 receptor.

(A-I) Representative graphics of FZD_5 receptor activation induced by several WNTs. Cells stably expressing the sensor V5-mFZD_5-FlAsH436-CFP were used to perform FRET experiments in a 96-well microplate reader. When co-stimulation with 5X WIF-1, the FRET signals are partially reduced. Graphic of stimulation with WNT-5A **(C)** is from figure 15A, but data of co-stimulation with WIF-1 have been added. Quantification of data is shown in figure 24. The EC_{50} for receptor activation calculated in these particular experiments are the following: 377.4ng/ml WNT-3A **(B)**, 556.6ng/ml WNT5A **(C)**, 932.8ng/ml WNT-5B **(D)**, 1112ng/ml (estimated) WNT-8A **(E)**, 436.2ng/ml WNT-9A **(F)**, 620.1ng/ml WNT-9B **(G)** and 829.5ng/ml WNT-10B **(H)**.

WNT-3A and WNT-5A are the most well-known endogenous ligands for FZD_5. Assuming that WNT-5A would act as a full agonist of FZD_5 receptor, the response induced by this protein has been normalized to 100% in **figure 24**. Consequently, the FRET changes induced in the receptor upon activation by saturating concentrations of the different WNT proteins have been normalized to the maximal response induced by WNT-5A (**Fig. 24A**). It is noticeable that both WNT-3A and WNT-5A produce a similar FRET change at saturating concentrations, while the amplitude of the signal is slightly reduced when WNT-9A, WNT-9B or WNT-10B are used. These three ligands induced 60-70% FRET change, while WNT-5B and WNT-8A only led to a 40-50% change. In contrast, the signal is drastically reduced in the case of WNT-2B, and no FRET change could be measured when cells were stimulated with WNT-16B, suggesting that this ligand does not activate the FZD_5 receptor under these experimental conditions.

Differences are also observed when comparing concentration-response curves of several ligands (**Fig. 24B**). Although the EC_{50} for receptor activation is similar for the ligands WNT-5A, WNT-5B and WNT-9B, the responses produced by the different agonists widely vary. In addition, when comparing normalized concentration-response curves of WNT-5A and WNT-3A, the EC_{50} of the latter for FZD_5 activation is shifted to the left (**Fig. 24B**), which suggests that this ligand is more potent than WNT-5A at the level of receptor activation.

Regarding the potency of the agonists analyzed, **table 3** summarizes the EC_{50} for FZD_5 receptor activation. As can be noted from table 3, variability also exits regarding the activity of each ligand. Data are compiled in **figure 24C-D**, where the activity of the different WNTs is represented in relation to the structural changes that they induce in the FZD_5 receptor sensor upon activation. WNT-3A is a more potent agonist than WNT-5A, although both have comparable efficacy. WNT-9B and WNT-10B present similar potency to WNT-5A, whereas their maximal response is lower. Interestingly, WNT-9A induces a FRET change in the FZD_5 sensor comparable to these two agonists, WNT-9B and WNT-10B, whereas the EC_{50} for this process is more similar to WNT-3A. Otherwise, WNT-5B and WNT-8A appear to have a slightly higher EC_{50} for FZD_5 receptor activation.

Table 3. EC_{50} [95% CI] values for receptor activation induced by various WNTs. For each protein, the indicated molecular weight was used to transform ng/ml into nanomolar concentrations. Data were calculated from at least 3 independent experiments, for each of the ligands. Data for WNT-5A are from table 1. n.d.: not determined.

Ligand	EC_{50} (ng/ml)	Asymmetric CI (95%)	Predicted Mw (KDa)	EC_{50} (nM)	Asymmetric CI (95%)
WNT-2B (n=4)	n.d.		38.0	n.d.	
WNT-3A (n=3)	322.1	192.9 - 537.9	37.0	8.7	5.2 - 14.5
WNT-5A (n=6)	704.4	454.3 - 1092.2	38.0	18.5	12.0 - 28.7
WNT-5B (n=4)	805.0	423.8 - 1529.1	38.6	20.9	11.0 - 39.6
WNT-8A (n=4)	967.2	206.1 - 4538.2	37.0	26.1	5.6 - 122.7
WNT-9A (n=4)	484.9	181.5 - 1295.6	37.0	13.1	4.9 - 35.0
WNT-9B (n=3)	593.8	413.6 - 852.7	36.8	16.1	11.2 - 23.2
WNT-10B (n=3)	674.0	534.9 - 849.3	40.1	16.8	13.0 - 21.2
WNT-16B (n=3)	n.d.		38.0	n.d.	

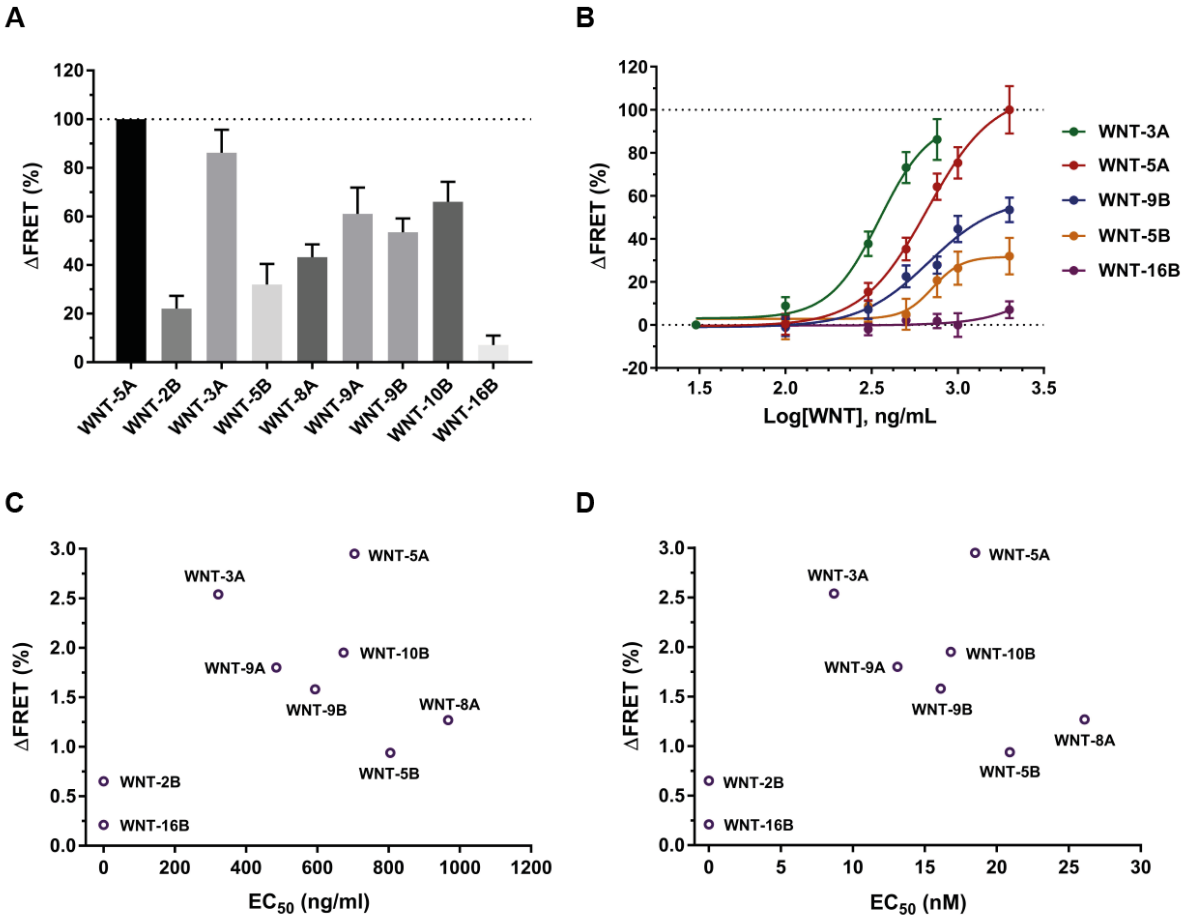

Figure 24. WNT proteins activate the FZD_5 receptor with different efficacy and potency.

(A-D) FRET measurements were performed in a 96-well microplate reader by using cells stably expressing the sensor V5-mFZD_5-FlAsH436-CFP. Data were quantified from experiments performed in quadruplicate, at least 3 times for each of the ligands. **(A)** FRET change induced in the FZD_5 receptor sensor by the different WNTs at saturating concentrations. Data have been normalized to the response induced by WNT-5A. **(B)** Concentration-response curves of several WNTs. Data normalized to the FRET signal induced by the highest concentration of WNT-5A. Comparison between the concentration-response curves of WNT-5A and WNT-3A reveals a shift in receptor activation. **(C-D)** Activity of the tested WNTs in relation to the structural changes that they induce in FZD_5 receptor upon activation. No activation of FZD_5 by WNT-16 could be detected.

4.3.2. G protein activation mediated by FZD_5 receptor

Upon stimulation with the recombinant ligand WNT-5A, FZD_5 receptor mediates the activation of $G\alpha_q$, but not $G\alpha_i$ heterotrimeric proteins, as mentioned in section 4.2.1. Considering the previous results, where WNTs induced distinct responses in the FZD_5 receptor sensor, the possibility that the same agonists could selectively activate $G\alpha_q$ was investigated.

HEK293T cells were co-transfected with the $G\alpha_q$ FRET sensor and either the V5-mFZD_5 receptor or pcDNA, and FRET experiments were performed in a microplate FRET reader. Thus, mTurquoise and Venus emission and the FRET ratio were detected before and after stimulation with increasing concentrations of recombinant WNT proteins. Representative graphics of $G\alpha_q$ protein activation induced by each of the tested ligands are presented in **figure 25**. If the specified ligand induces $G\alpha_q$ protein activation, upon stimulation with WNTs, the dissociation between Gα and Gβγ subunits would produce a change in the FRET signal. This outcome could only be observed for WNT-9B (**Fig. 25F**) and WNT-10B (**Fig. 25G**), which suggests that only these two ligands activate $G\alpha_q$ mediated by FZD_5 receptor.

Figure 25. $G\alpha_q$ protein activation induced by WNT proteins and mediated by FZD_5.

(A-H) Representative graphics of $G\alpha_q$ protein activation induced by WNTs and mediated by FZD_5. FRET experiments were performed in a 96-well microplate reader. Black dots indicate cells co-transfected with the V5-mFZD_5 receptor and the $G\alpha_q$ protein FRET sensor, while grey dots refer to co-expression of pcDNA and the $G\alpha_q$ sensor (no overexpression of the receptor). Activation of $G\alpha_q$ could only be observed for WNT-9B **(F)** and WNT-10B **(G)**. The EC_{50} for $G\alpha_q$ protein activation mediated by FZD_5 in these particular experiments are: 512.2ng/ml WNT-9B and 659.5ng/ml WNT-10B.

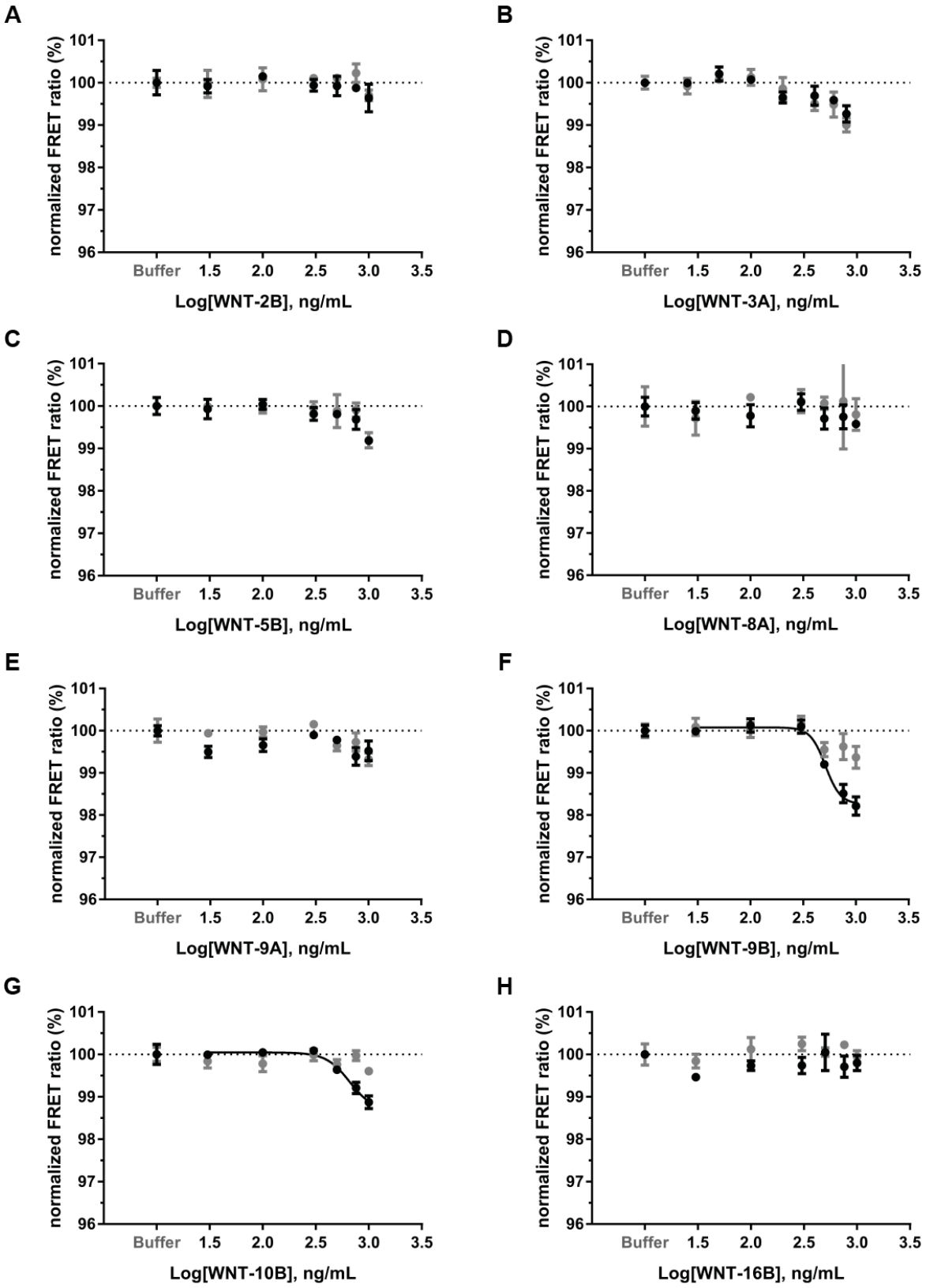
A
B
C
D
E
F
G
H
normalized FRET ratio (%)
101
100
99
98
97
96
Buffer
1.5
2.0
2.5
3.0
3.5
Log[WNT-2B], ng/mL
Log[WNT-3A], ng/mL
Log[WNT-5B], ng/mL
Log[WNT-8A], ng/mL
Log[WNT-9A], ng/mL
Log[WNT-9B], ng/mL
Log[WNT-10B], ng/mL
Log[WNT-16B], ng/mL

Even though no activation of $G\alpha_i$ could be observed upon WNT-5A stimulation (section 4.2.1), WNT-3A might be able to induce the activation of these protein subtypes mediated by FZD_5. Several studies have detected a FZD-dependent $G\alpha_{i/o}$ activation upon stimulation with WNT-3A, and the observed responses were PTX-sensitive (Halleskog and Schulte, 2013; Koval and Katanaev, 2011; Nalesso et al., 2011).

Therefore, HEK293T cells were co-transfected with V5-mFZD_5 receptor or pcDNA, and the $G\alpha_{i2}$ FRET sensor. Upon stimulation with WNT-3A, a strong activation of $G\alpha_{i2}$ could be observed, although it was not dependent on FZD_5 (**Fig. 26**).

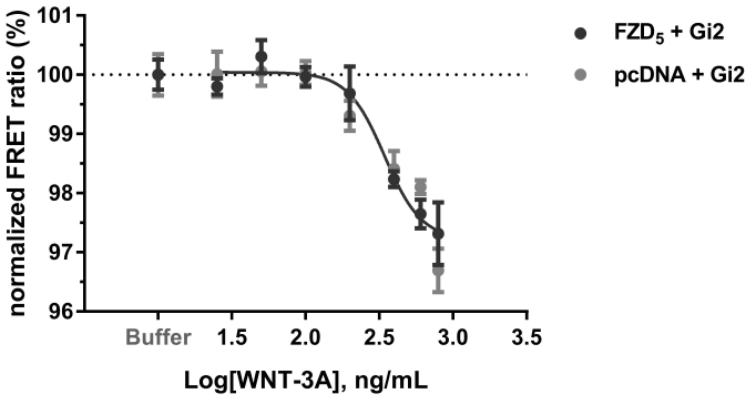

Figure 26. WNT-3A induces $G\alpha_{i2}$ protein activation independently on FZD_5.

Representative graphic of $G\alpha_{i2}$ protein activation induced by WNT-3A. The EC_{50} for $G\alpha_{i2}$ protein activation in this particular experiment is 342.5ng/ml.

These results are in agreement with previous studies indicating that the ligand WNT-3A, besides being involved in the traditional β-catenin-dependent pathway, is also able to induce G protein-dependent signaling. Endogenous levels of FZD in the cells appear to be sufficient to induce the activation of $G\alpha_{i2}$, and overexpression of FZD_5 does not influence the amplitude of the observed response.

Quantification of data for $G\alpha_q$ protein activation induced by WNTs showed that stimulation with the ligands WNT-2B, WNT-8A or WNT-9A only led to a 10-20% FRET change at the highest concentration, in comparison to WNT-5A, while WNT-16B did not produce a significant response (**Fig. 27A**). None of these four ligands seemed to induce activation of $G\alpha_q$. In contrast, WNT-3A and WNT-5B were able to induce a bigger change in FRET, of around 30-40% in comparison to WNT-5A. Nevertheless, the responses produced by the previous six ligands were independent of FZD_5 overexpression, which suggests that they are mediated by endogenous levels of FZD receptors present in HEK293T cells (**Fig. 27A-B**).

On the contrary, WNT-9B and WNT-10B were both able to induce $G\alpha_q$ activation, with 60% of FRET change in comparison to WNT-5A. In both cases, the amplitude of the signals were considerably higher when FZD_5 was overexpressed (**Fig. 27A-B**), which suggests that this receptor is mediating the cellular response. The EC_{50} values for $G\alpha_q$ protein activation are shown in **table 4**.

Table 4. EC_{50} [95% CI] values for $G\alpha_q$ protein activation mediated by FZD_5 and induced by various WNTs. For each protein, the indicated molecular weight was used to transform ng/ml into nanomolar concentrations. Data for WNT-5A are from table 2.

Ligand	EC_{50} (ng/ml)	Asymmetric CI (95%)	Predicted Mw (KDa)	EC_{50} (nM)	Asymmetric CI (95%)
WNT-5A (n=3)	550.8	327.0 - 927.9	38.0	14.5	8.6 - 24.4
WNT-9B (n=4)	623.0	190.7 – 2035.1	36.8	16.9	5.2 – 55.3
WNT-10B (n=2)	627.3	284.0 – 1385.8	40.1	15.6	7.1 – 34.6

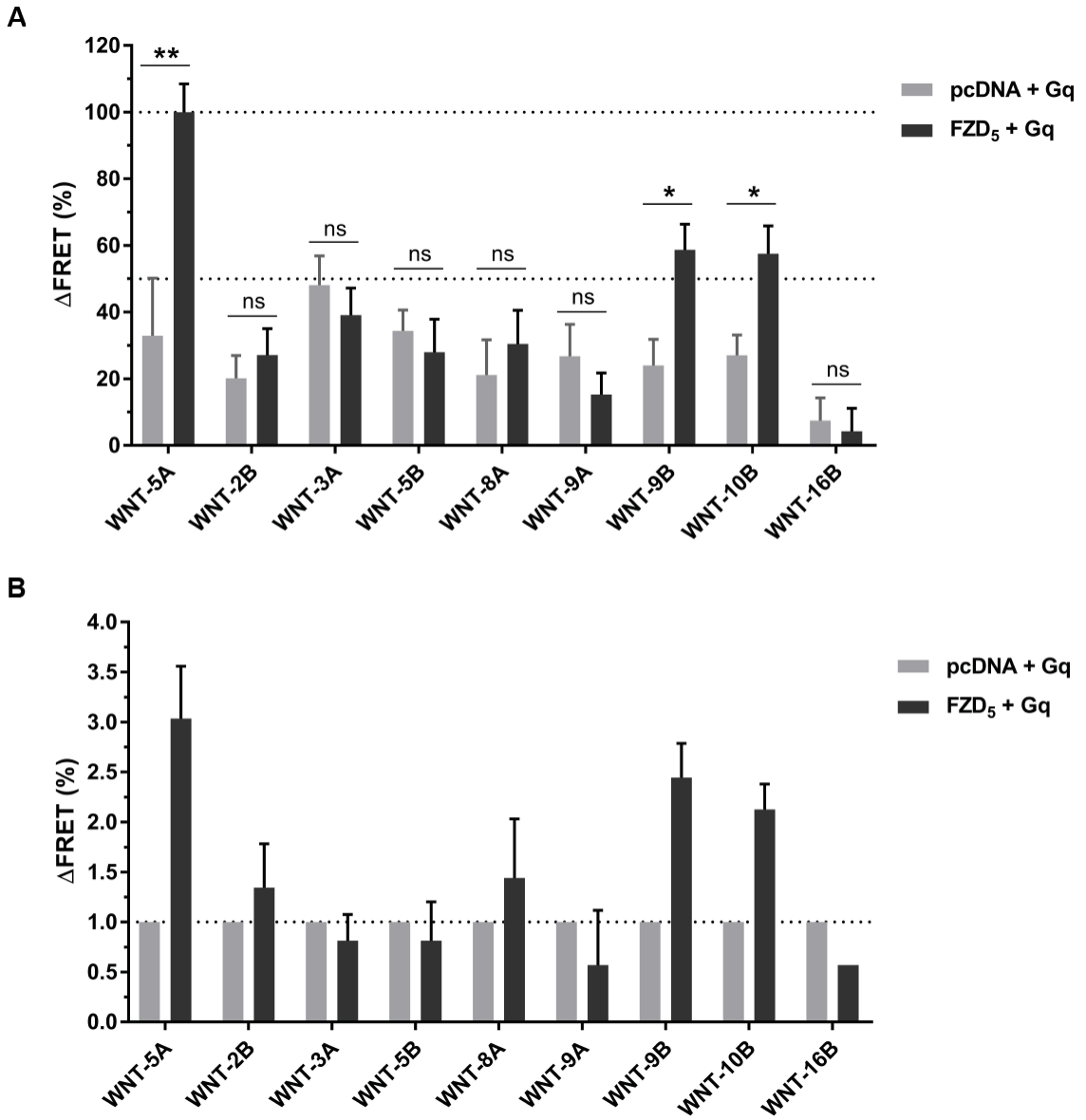

Figure 27. Quantification of Gα_q protein activation induced by WNT proteins.

Comparison between the FRET changes induced by WNTs at their maximal concentration, with and without overexpression of FZD_5. Experiments were performed in quadruplicate, at least 3 times for each of the ligands. **(A)** Data normalized to the response induced by WNT-5A (1000ng/ml), represented as mean ± SEM. Data for WNT-5A from figure 18D were normalized and shown here. Statistical analysis was done by using the raw data, not the normalized data. ** $P \leq 0.01$; * $P \leq 0.05$; ns: non-significant (two-tailed unpaired t test). **(B)** Data are the same as in (A) but the FRET change induced when FZD_5 was overexpressed has been normalized to the response measured in the absence of receptor, for each of the ligands.

5. Discussion

FZD are highly conserved receptors involved in many different pathologies, which makes them valuable pharmacological targets. However, the complexity of the pathways, the limited information regarding, for instance, ligand-receptor selectivity or signal initiation, and the few number of readouts available, especially with respect to non-canonical signaling, have limited the progress in the research field. In this project, FRET-based techniques have been employed in order to elucidate the mechanisms of FZD_5 receptor activation. Particularly, FZD_5 FRET-based biosensors have been developed and characterized in order to address essential questions regarding receptor activation. Furthermore, the activation of G proteins and the $G\alpha_q$-dependent signaling pathway mediated by FZD_5 have been investigated. The results of this study show that FZD_5 exhibits a similar behavior to other well-known GPCRs, not only regarding the activation mechanism of the receptor but also the activation of G protein-mediated signaling pathways.

5.1. FZD_5 receptor activation resembles the general GPCR activation mechanism

Four FZD_5 FRET-based biosensors were created in order to monitor the structural rearrangements that the receptor undergoes upon activation. Therefore, CFP was fused to the C-terminus of the receptor constructs, whereas the FlAsH-binding motif was inserted in different positions within the intracellular loops. The combination CFP-FlAsH has been commonly used as a FRET donor-acceptor pair to report ligand-induced conformational changes in several GPCRs. Since FRET is a distance-dependent technique, the positions of the two fluorophores have been optimized in these receptors. Traditionally, best results have been achieved when the donor and acceptor fluorophores where placed in the C-terminus and ICL-3, respectively. In general, insertion of the fluorophores did not affect receptor functionality or interaction with G proteins. However, FZD receptors have additional intracellular partners, such as DVL, which has been described to interact with the receptor at three different motifs, two of them located in ICL-3. Therefore, other positions within ICL-2 were considered to place the FlAsH-binding sequence in FZD_5.

Characterization of the four sensors revealed that, while insertion of the FlAsH-binding motif within ICL-2 altered the overall structure of the receptor sensors, restricting their cellular expression to the intracellular membranes, the two sensors with the FlAsH-binding motif

inserted within ICL-3 localized to the plasma membrane (**Fig**. **10**). It therefore follows that insertion of the two fluorophores, CFP and FlAsH, did not interfere with the folding of the proteins, their transport to the plasma membrane or their ability to bind ligands, since the sensor V5-mFZD$_5$-FlAsH436-CFP showed comparable binding properties to the wild-type receptor (**Fig. 11**).

In addition, both receptor sensors, V5-mFZD$_5$-FlAsH436-CFP and V5-mFZD$_5$-FlAsH439-CFP, exhibited basal intramolecular FRET, with FRET efficiencies of 6.42% and 6.16%, respectively (**Fig. 12**). Since the only difference between both receptor sensors is the localization of the FlAsH-binding sequence, which is placed 3 amino acids further in the construct V5-mFZD$_5$-FlAsH439-CFP, it appears that this difference in the primary sequence of the receptors did not have a significant impact in the relative distance or orientation between the fluorophores in the 3D structure. More importantly, no basal energy transfer was detected when receptors individually tagged with CFP and FlAsH were co-expressed in the cells. Considering that some FZDs have been shown to form dimers and higher order complexes, these results excluded the possibility that the FRET signal could be influenced by neighboring receptors. Altogether, the characterization of the sensors indicate that they are suitable to investigate the ligand-induced activation of FZD$_5$.

Considering the previous validation, the sensor V5-mFZD$_5$-FlAsH436-CFP was employed to investigate receptor activation by means of single-cell FRET experiments. WNT-5A was selected as a reference agonist in this project, since it is one of the best-studied endogenous ligands for FZD$_5$. In order to reach a maximal activation of all the receptors in the cell surface, a saturating concentration of the recombinant protein WNT-5A was employed.

The results of these experiments revealed an anti-parallel movement of CFP and FlAsH emissions upon ligand stimulation, which translated into a 4% decrease in the FRET ratio (**Fig. 14**). These data suggest that, upon binding to WNT-5A, FZD$_5$ undergoes rapid structural rearrangements that involve a relative movement of the domains where CFP and FlAsH are attached. These conformational changes are similar to those observed in other GPCRs using similar FRET sensors, which have been linked to receptor activation. These results would support the hypothesis that the general activation mechanism described for GPCRs (section 1.3.1.1) is also conserved in class F. This is in line with recent evidence, regarding the crystal structure of active SMO receptor (Huang P et al., 2018).

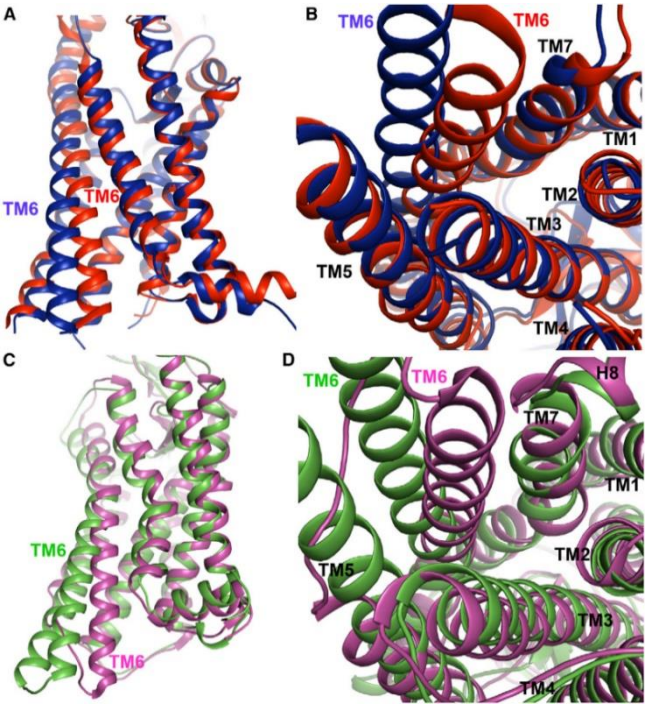

Figure 28. Superimposed ribbon models comparing active and inactive conformations of GPCRs. **(A-B)** Inactive (red) and active (blue) SMO receptor. **(C-D)** Inactive (pink) and active (green) rhodopsin receptor. B and D show a view from the cytoplasmic side (Huang et al., 2018; Fig. 3).

To date, ten structures of active-state GPCRs forming complexes with heterotrimeric G proteins have been published, corresponding to class A and B receptors in complex with $G\alpha_i$ or $G\alpha_s$. All of these structures showed conserved movements upon receptor activation, especially in TM6 and TM7. Interestingly, it appears that the shift in TM6 partially depends on the G protein subunit, and might also be influenced by the length of TM6 and ICL-3 (Glukhova et al., 2018). While the inactive, ligand-free structure of FZD_4 showed a receptor in a close conformation with a packed helix VI that might not be involved in receptor activation, the comparison between the active and inactive conformations of SMO showed rearrangements in the transmembrane domains of the receptor, with a noticeable shift of TM6 (**Fig. 28A-B**). This movement appears to be more similar to what was observed in Rhodopsin (**Fig. 28C-D**), and not as drastic as for other GPCRs (**Fig. 29A-C**), but it definitely resembles the conserved conformational change that would result in the opening of the receptor at its cytosolic side.

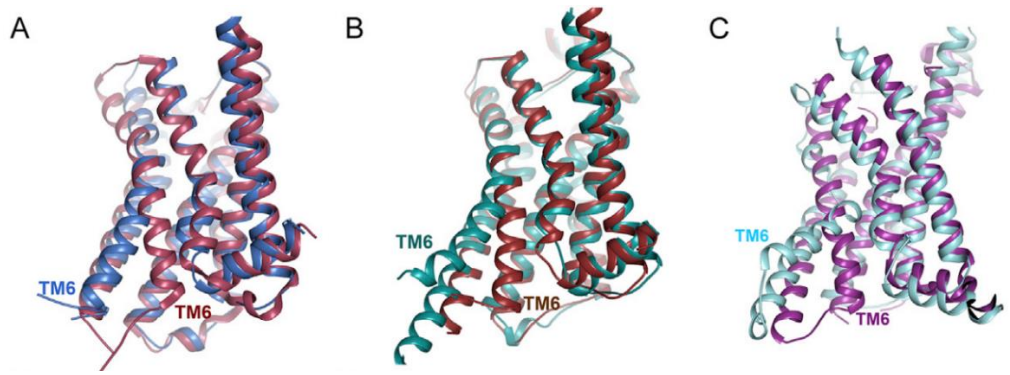

Figure 29. Ribbon models comparing active and inactive conformations of class A and B GPCRs. **(A)** Inactive (raspberry) and active (blue) M_2AChR. **(B)** Inactive (red) and active (teal) β2-AR. **(C)** Inactive glucagon receptor (purple) and active (cyan) glucagon-like peptide-1 receptor (Huang et al., 2018; Fig. S4).

In summary, in this project, CFP and the FlAsH-binding motif were attached to the C-terminus and the ICL-3 of FZD_5, respectively, which are domains sensitive to conformational changes in the receptor. The results obtained are in agreement with a classical activation mechanism that involved the TM6 and the C-terminus. While the main activation mechanism appears to be conserved, there are few appreciable points that have been observed in FZD_5 receptor activation (**Fig. 14**), as well as in G protein activation mediated by FZD_5 (**Fig. 17**).

First, there appear to be a delay in the response, since the ligand starts to be perfused to the moment when the FRET signal decreases. This might be due to the mechanism by which a WNT protein binds and activates a FZD receptor. Although prior studies showed that WNT interacts with the CRD of FZD at two distinct motifs (Janda et al., 2012), it is still unclear if more interactions are established, for instance, between WNT and the extracellular loops of the FZD receptor. Moreover, the N-terminus of FZD could undergo conformational changes upon WNT binding that allowed those interactions. Nevertheless, there are other factors that may have an influence, for instance, the presence of Glypicans in the extracellular surface of the cell, as well as other components of the ECM. WNTs have been shown to have affinity and bind to these molecules, which would limit or increase the amount of ligand available for FZD receptors. It is then possible that certain concentrations of WNT around the receptors have to be reached before activation occurs.

Second, the kinetics of FZD_5 activation appear to be slower than those determined for other class A or B GPCRs using FRET-based sensors, such as rhodopsin (1ms; Makino et al., 2003), α_{2A}-adrenergic receptor (50ms; Vilardaga et al., 2003), muscarinic receptors (60-70ms; Ziegler

et al., 2011) or the class B PTHR (1 second; Vilardaga et al., 2003). While these results could be also influenced by the binding mechanism between WNT and FZD, it has been previously suggested that FZD receptors might behave like classical GPCRs but with altered or slower kinetics (Nichols et al., 2013). Considering that the Biopen microfluidic system was employed to deliver the WNT proteins in single-cell FRET experiments, and that this perfusion system had not been used in the research group until recently, a previous validation was performed in order to assure comparable results to the traditional perfusion system. For this reason, the α_{2A}-adrenergic receptor was used as a control, since it is a well-studied receptor in the group. The signal amplitude and kinetics of receptor activation measured upon agonist stimulation were comparable for both perfusion systems, and therefore helped to exclude the possibility that the different setting might affect the results obtained with the FZD_5 receptor sensor. FRET experiments were performed by other member of the group and thus they are not part of this thesis.

A third observation is that, upon wash-out of the ligand with buffer, the FRET signal did not return immediately to baseline, at least not during the time frame of the experiment. This would be compatible with a high binding affinity between WNT-5A and FZD_5. Moreover, it might also suggest a long ligand residence time.

5.2. FZD_5 induces $G\alpha_q$ activation and signaling in response to WNT-5A

In addition to the conserved receptor movement detected with the FZD_5 FRET-based sensor, which suggests an activation mechanism for FZD_5 similar to classical GPCRs, the direct activation of G proteins mediated by FZD_5 has also been addressed in this thesis. In order to do so, FRET-based sensors for $G\alpha_q$ and $G\alpha_i$ proteins have been employed.

Single-cell FRET experiments reported activation of $G\alpha_q$ in cells overexpressing the FZD_5 receptor upon stimulation with a saturating concentration of WNT-5A (**Fig. 17**). The activation mechanism of $G\alpha_q$ mediated by FZD_5 showed similar characteristics to those for receptor activation, which have been previously mentioned (section 5.1), such as the delay in the response or the apparent slower kinetics. Interestingly, WNT-5A did not induce activation of any of the tested $G\alpha_i$ isoforms mediated by FZD_5 in the same conditions. To further investigate the axis WNT-5A/FZD_5, a dual DAG/Ca^{2+} sensor was employed. FZD_5 mediated the specific activation of the PLC pathway (**Fig. 22**), which involved PKC activation and calcium release, similarly to the M_3AChR. This provides further evidence of FZD_5 as a GPCR.

Altogether, WNT-5A has been found to induce $G\alpha_q$ activation mediated by FZD_5 by employing a FRET sensor for the $G\alpha_q$ protein, as well as calcium release and PKC activation, which was determined by means of using a dual sensor for both second messengers, with endogenous levels of $G\alpha_q$ in the cells (**Fig. 30**). These experiments were performed in a cellular system where the FZD_5 receptor was overexpressed. However, the involvement of WNT-5A in other signaling pathways mediated by FZD_5, such as PCP signaling, might occur in certain cellular contexts, where the endogenous presence of other FZD receptors, co-receptors or intracellular proteins could influence the signaling outcome.

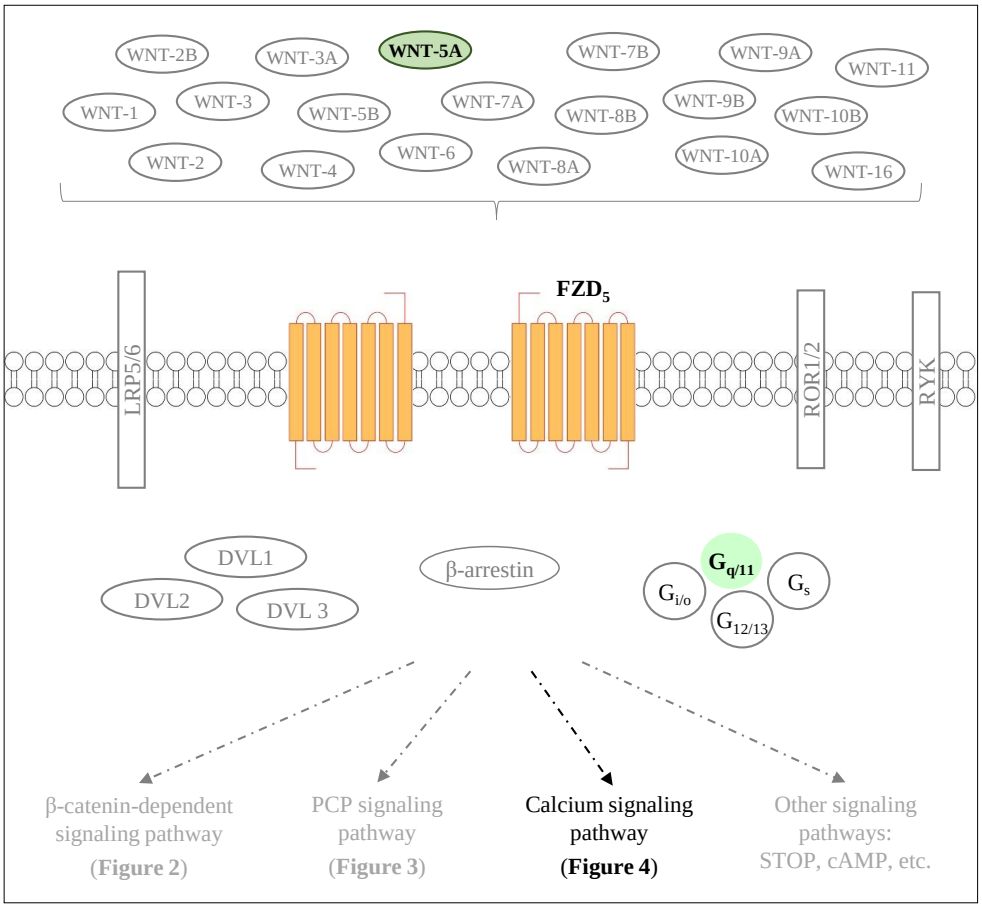

Figure 30. WNT-5A induces $G\alpha_q$ activation and signaling (modified from figure 1).

Regarding the intracellular partners of FZD_5, DVL has been shown to interact with this receptor in the β-catenin-dependent signaling pathway. Therefore, it could be also involved in the conformational changes measured in the FZD_5 receptor or in the activation of G proteins. Previous studies have found that FZD_6 is able to interact with both DVL and G proteins

(Kilander et al., 2014). In addition, the ability of this receptor to bind and activate G proteins depends on the intracellular levels of DVL. On the contrary, FZD_{10} and FZD_4 coupling to G proteins are independent of DVL (Hot et al., 2017; Arthofer et al., 2016).

Within this project, the construct V5-mFZD_5 was found able to mediate DVL recruitment and phosphorylation (**Fig. 13**). In addition, this receptor also mediated the activation of $G\alpha_q$ upon WNT-5A stimulation (**Fig. 17A** and **18A**), which suggests that FZD_5 can also interact with both downstream effectors, DVL and G proteins. However, the inability of the FZD_5 receptor FRET sensors to induce DVL recruitment to the plasma membrane, added to the fact that the two constructs V5-mFZD_5-FlAsH436 and V5-mFZD_5-FlAsH439 were able to mediate $G\alpha_q$ activation (**Fig. 18B-D**), might indicate that the cytoplasmic levels of DVL do not influence the activation of $G\alpha_q$ by WNT-5A mediated by FZD_5. In addition, the direct interaction between FZD_5 and DVL might not be necessary for the activation of the receptor and the associated conformational movements upon WNT stimulation.

5.3. WNT proteins selectively induce FZD_5 activation and signaling

In order to perform a fast screening of ligands, FZD_5 receptor activation was further investigated in a 96-well microplate FRET reader, which involved escalating and further optimization of FRET experiments from single cells to a microplate reader format. This technology has allowed to examine the WNT-FZD selectivity by employing various recombinant WNT proteins and a full-length FZD_5, which directly reports receptor activation.

In general, the tested WNTs selectively activated the FZD_5 receptor sensor with different efficacy and potency (**Fig. 24 and 31**). WNT-3A and WNT-5A induced a similar response in the receptor, with comparable signal amplitudes at saturating concentrations. Therefore, both can be considered full agonists for FZD_5. This is consistent with which is known in the literature about FZD_5 receptor. However, despite exhibiting the same activity at the level of receptor activation, WNT-3A and WNT-5A have varying potencies, being the former a more potent agonist than the latter. Considering that FZD_5 activation mediated by WNT-3A leads to the β-catenin-dependent signaling pathway (**Fig. 2**), which involves the participation of LRP5/6 co-receptors, DVL and other proteins that may form complexes with FZD, the difference in activity between WNT-3A and WNT-5A might be influenced by the presence of other proteins.

Regarding the other tested WNT proteins, most of them induced concentration-dependent conformational changes in the FZD_5 sensor. Two groups of partial agonists could be identified. On one hand, WNT-9A, WNT-9B and WNT-10B induce 60-70% of FRET change at saturating concentrations; on the other hand, WNT-5B and WNT-8A produce only a 40% FRET change in the FZD_5 sensor. WNT-16B did not induce FZD_5 receptor activation, while WNT-2B might cause a slight activation of the sensor at high concentrations. These differences in signal amplitude might be due to distinct conformational changes that each ligand induces in the receptor. These results are in agreement with previous data showing that WNT-3A and WNT-5A exhibited strong binding to the CRD of FZD_5, while WNT-5B exhibited intermediate binding (Dijksterhuis et al., 2015; section 1.2.3). With regard to the potency of the analyzed proteins, WNT-9A showed similar potency to WNT-3A, whereas the EC_{50} values determined for the other four ligands are more similar to WNT-5A (**Table 3**).

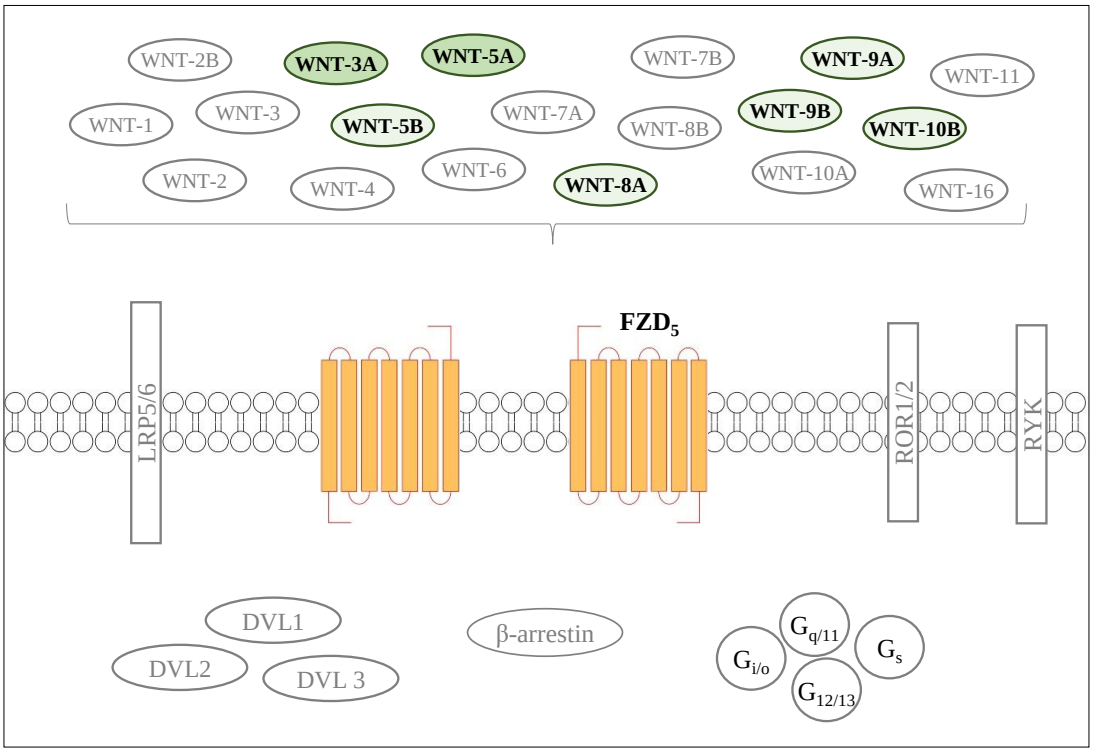

Figure 31. FZD_5 receptor activation induced by full (dark green) and partial (clear green) agonists.

Interestingly, a prior study showed that WNT-9A did not signal via FZD_5 receptor (Voloshanenko et al., 2017). By means of using CRISPR/Cas9 technology, the mapping of certain WNT-FZD interactions was done by evaluating which combinations of ligand-receptor rescued the activation of β-catenin-dependent signaling. Therefore, while WNT-9A was not found to induce β-catenin activation mediated by FZD_5 in that study, this ligand could induce a different cellular response via FZD_5.

It has been proposed that various agonists can stabilize distinct receptor conformations, which can selectively activate the downstream signaling cascade (Galandrin et al., 2007). This argument arises the question whether the behavior of certain WNTs with respect to FZD_5 receptor activation could indeed be related to the signaling pathway that they induce. To further assess this question, $G\alpha_q$ activation induced by various recombinant WNT proteins was also investigated in the microplate FRET reader (**Fig. 25 and 27**). Surprisingly, only two of the tested ligands, besides WNT-5A, induced $G\alpha_q$ activation mediated by FZD_5: WNT-9B and WNT-10B (**Fig. 32**).

Notably, these two proteins behave as partial agonists for FZD_5 regarding receptor activation, and they also induce lower signal amplitudes than WNT-5A in the $G\alpha_q$–FRET sensor. The EC_{50} for $G\alpha_q$ activation were comparable for the three WNT proteins (**Table 4**). Regarding the other tested ligands, some of them slightly induced $G\alpha_q$ activation, but this process was not mediated by FZD_5.

Evidence exists of β-catenin-dependent activation induced by WNT-9B and mediated by FZD_5 (Voloshanenko et al., 2017), whereas $G\alpha_q$ activation induced by WNT-9B and mediated by FZD_5 has been observed in this study. The fact that the same combination of ligand and receptor could lead to the activation of different downstream cascades underlines the importance of the cellular context and the presence of other proteins in discerning the signaling outcome.

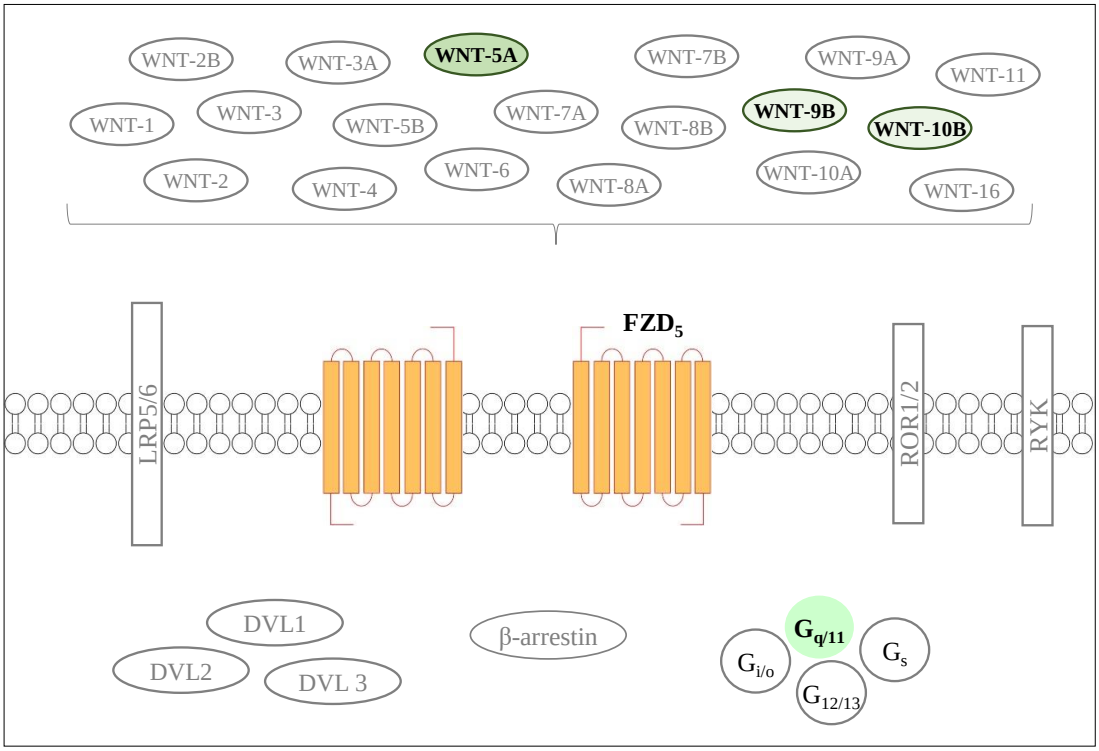

Figure 32. $G\alpha_q$ protein activation mediated by FZD_5 receptor and induced by full (dark green) and partial (clear green) agonists.

5.4. Final remarks and future directions

The development of FZD_5 FRET-based biosensors have allowed to monitor the activation of the receptor upon stimulation with various WNT proteins, which revealed that FZD_5 undergoes conformational movements upon activation that are reminiscent of other GPCRs. In addition, the use of G protein FRET-based sensors additionally showed that FZD_5 mediates the activation of $G\alpha_q$ upon stimulation with certain WNTs.

The selectivity between FZD_5 and several WNT proteins has been addressed by employing FRET sensors in a microplate reader, and concentration-response curves have been obtained for receptor activation and $G\alpha_q$ protein activation. The use of a HEK293 cell line stably expressing the receptor sensor V5-mFZD_5-FlAsH436-CFP allowed to maintain similar expression levels of the receptor in different experiments. Moreover, due to the characteristics of the recombinant WNT proteins, as well as their ability to bind to the extracellular surface of the cell, receptor activation experiments were performed several times in order to assure reproducibility of the results.

While the differences in signal amplitudes allowed to determine full and partial agonists at the level of receptor activation, the calculated EC_{50} values provided information about the different potencies of the WNT proteins with respect to FZD_5. In addition, the data obtained were in agreement with previous studies (section 1.2.3) that showed a strong binding between WNT and FZD, as well as EC_{50} values in the low nanomolar range for the activation of the downstream signaling cascade.

The setting employed to measure FZD_5 receptor activation in the microplate FRET reader proved to be a useful and valuable tool to characterize the pharmacological effect of several ligands on receptor activation. Considering the limited number of read-outs available to investigate FZD-WNT selectivity, this technique opens the possibility to look directly at the level of ligand-induced receptor activation. This technology would help to identify molecules targeting FZD_5, as well as to characterize potential pharmacological compounds. Furthermore, G protein-dependent signaling is required in several FZD-mediated processes. Hence, it is relevant to understand which combinations of WNTs and FZDs drive the activation of the different signaling cascades.

The knowledge and results of this project could be applied to other FZD receptors in the future. The development of FRET-based biosensors for other members of the family would allow to compare their activation mechanism to the conformational changes observed for FZD_5. Furthermore, ligand selectivity could be addressed by means of using the optimized setting in the microplate reader. Resonance-energy transfer techniques might be also employed to further investigate the kinetics of ligand binding and receptor activation. In addition, and with focus on FZD_5, it would be interesting to further investigate other aspects of FZD_5-dependent signaling by employing other technologies, such as BRET. In particular, determining the selective activation of other G protein isoforms or β-arrestins induced by various WNT proteins would provide a more complete view of the signaling cascades mediated by this receptor.

6. Annexes

6.1. Abbreviations

7TM	Seven Transmembrane
AC	Adenylyl Cyclase
APC	Adenomatous Polyposis Coli
BRET	Bioluminescence Resonance Energy Transfer
BSA	Bovine Serum Albumin
Ca^{2+}	Calcium
CaMKII	Calcium/Calmodulin-Dependent Protein Kinase II
CFP	Cyan Fluorescent Protein
CK1α/ε	Casein Kinase 1 α or ε
CNS	Central Neural System
CRD	Cysteine Rich Domain
DAAM1	Dishevelled-Associated Activator of Morphogenesis 1
DAG	Diacylglycerol
DEP	Dishevelled, Egl-10, Pleckstrin
DMEM	Dulbecco's Modified Eagle Medium
DVL	Dishevelled
ECL	Extracellular Loop
ECM	Extracellular Membrane
EDT	1,2-Ethanedithiol
FBS	Fetal Bovine Serum
FCS	Fluorescence Correlation Spectroscopy
FlAsH	Fluorescein Arsenical Hairpin
FRAP	Fluorescence Recovery After Photobleaching
FRET	Förster Resonance Energy Transfer
FZD	Frizzled
G-418	Geneticin
GFP	Green Fluorescent Protein

GPCR	G Protein-Coupled Receptor
GRK	G protein-coupled Receptor Kinases
GSK3	Glycogen Synthase Kinase 3
ICL	Intracellular Loop
IUPHAR	International Union of Pharmacology
IP_3	Inositol Trisphosphate
JNK	c-JUN-N-terminal kinase
LEF/TCF	Lymphoid Enhancer-binding Factor/T cell-specific
LRP5/6	Low Density Lipoprotein Receptor-Related Protein 5 or 6
M_1AChR	Muscarinic Acetylcholine Receptor 1
M_3AChR	Muscarinic Acetylcholine Receptor 3
MMTV	Mouse Mammary Tumor Virus
PBS	Phosphate-Buffered Saline
PCP	Planar Cell Polarity
PCR	Polymerase Chain Reaction
PDZ	Atypical Postsynaptic Density 95/disc-large/zona Occludens-1
PIP_2	Phosphatidylinositol 4,5-Bisphosphate
PKA	Protein Kinase A
PKC (a)	(atypical) Protein Kinase C
PLC	Phospholipase C
PTHR	Parathyroid Hormone Receptor
PTX	Pertussis Toxin
QCM	Quartz Crystal Microbalance
ReAsH	Resorufin Arsenical Hairpin
ROCK	Rho-associated Kinase
ROR1/2	Tyrosine-protein Kinase Transmembrane Receptor ROR1 and ROR2
RSPO	R-spondin Secreted Protein
RT	Room Temperature
sFRP	Soluble Frizzled-related Proteins
SMO	Smoothened Receptor

TMD	Transmembrane Domains
Vangl1/2	Van Gogh-like 1 and 2
VFT	Venus Flytrap
WIF-1	WNT Inhibitory Factor 1
WNT	**W**ingless-Related I**nt**egration Site
wt	Wild-type
YFP	Yellow Fluorescent Protein

6.2. DNA sequences

- Legend: V5 tag
  Signal peptide
  AAGCTT HindIII site
  TCTAGA XbaI site
  ATG / TAA Start / Stop codon V5-mFZD$_5$
  GTG / TAA First / Stop codon CFP
  ATG / ATG / GTG First codon of mCherry / GFP / YFP
  TGTTGCCCGGGCTGCTGT FlAsH-binding sequence

V5-mFZD$_5$ in pcDNA3.4

AAGCTTGCCACCATGGTCCCGTGCACGCTGCTCCTGCTGTTGGCAGCCGCCCTGGCTCCGACTCAG
ACCCGGGCCGGTACCGGCAAACCGATTCCGAACCCGCTGCTGGGCCTGGATAGCACTGCCTCCAA
GGCCCCGGTGTGCCAGGAAATCACGGTGCCCATGTGCCGAGGCATCGGCTACAACCTGACGCACA
TGCCCAACCAGTTCAACCATGACACGCAGGACGAAGCAGGCCTGGAGGTGCACCAATTCTGGCCG
CTTGTGGAGATCCACTGCTCACCGGACCTGCGCTTCTTCCTGTGCTCTATGTACACGCCCATCTGTT
TGCCTGACTACCACAAGCCGCTACCACCGTGCCGTTCCGTGTGCGAGCGCGCCAAGGCCGGCTGCT
CGCCGCTCATGCGCCAGTACGGCTTCGCCTGGCCCGAGCGCATGAGCTGCGACCGCCTCCCTGTGC
TGGGCGGCGACGCCGAGGTTCTGTGTATGGATTATAACCGAAGCGAAGCCACCACCGCGTCCCCT
AAGTCCTTCCCGGCCAAACCTACACTCCCAGGACCACCAGGGGCGCCATCTTCCGGGGGCGAGTG
CCCCTCGGGAGGCCCATCCGTGTGCACGTGCCGCGAGCCCTTCGTGCCCATCCTGAAGGAGTCACA
CCCACTCTACAACAAGGTGCGCACCGGCCAAGTGCCCAACTGCGCGGTGCCCTGCTACCAGCCGT
CCTTCAGCCCGGACGAGCGCACATTCGCCACCTTCTGGATTGGCCTGTGGTCTGTGCTGTGCTTCAT
CTCCACGTCCACCACCGTTGCCACCTTCCTCATTGACATGGAACGATTCCGCTACCCTGAGCGCCC
CATCATCTTCTTGTCTGCGTGCTACCTGTGTGTGTCACTGGGATTCTTGGTGCGCCTGGTAGTGGGC
CATGCCAGCGTCGCTTGCAGCCGTGAGCACAGCCACATTCACTATGAGACTACCGGCCCTGCGCTG
TGCACGGTTGTCTTCCTCTTAGTCTATTTCTTTGGCATGGCCAGCTCCATCTGGTGGGTCATCCTGT
CGCTCACCTGGTTCTTGGCGGCTGGCATGAAGTGGGGCAATGAAGCCATCGCAGGTTATGCACAG
TACTTCCACCTTGCTGCCTGGCTCATCCCCAGTGTCAAGTCCATTACGGCGCTGGCACTGAGCTCG
GTGGACGGGGACCCAGTGGCTGGCATCTGCTATGTGGGCAACCAAAACCTGAACTCACTACGAGG
CTTTGTCTTGGGCCCACTGGTGCTGTACCTGTTGGTGGGCACGCTCTTCCTTCTGGCAGGCTTCGTG
TCACTCTTCCGCATCCGGAGCGTCATCAAGCAGGGTGGCACTAAGACGGACAAGCTAGAGAAGCT
CATGATCCGCATCGGCATCTTCACCCTGCTCTACACGGTGCCAGCCAGCATCGTGGTGGCCTGCTA
CCTGTATGAGCAGCACTACCGGGAGAGCTGGGAGGCAGCCCTCACCTGCGCGTGTCCGGGACCGG
ACGCTGGCCAGCCACGCGCCAAACCCGAGTACTGGGTGCTCATGCTCAAGTACTTCATGTGCCTGG
TGGTGGGCATCACGTCGGGAGTCTGGATCTGGTCCGGCAAGACTCTGGAGTCTTGGCGGCGGTTCA
CCAGCCGCTGCTGCTGCAGCTCTCGGCGGGGCCACAAGAGCGGTGGCGCTATGGCCGCAGGAGAC
TATGCGGAGGCCAGCGCCGCGCTCACCGGCAGGACCGGGCCGCCTGGCCCCACCGCCGCATACCA
CAAGCAAGTGTCCCTGTCGCACGTATAATCTAGA

V5-mFZD$_5$–CFP in pcDNA3

AAGCTTGCCACCATGGTCCCGTGCACGCTGCTCCTGCTGTTGGCAGCCGCCCTGGCTCCGACTCAG
ACCCGGGCCGGTACCGGCAAACCGATTCCGAACCCGCTGCTGGGCCTGGATAGCACTGCCTCCAA
GGCCCCGGTGTGCCAGGAAATCACGGTGCCCATGTGCCGAGGCATCGGCTACAACCTGACGCACA
TGCCCAACCAGTTCAACCATGACACGCAGGACGAAGCAGGCCTGGAGGTGCACCAATTCTGGCCG
CTTGTGGAGATCCACTGCTCACCGGACCTGCGCTTCTTCCTGTGCTCTATGTACACGCCCATCTGTT
TGCCTGACTACCACAAGCCGCTACCACCGTGCCGTTCCGTGTGCGAGCGCGCCAAGGCCGGCTGCT
CGCCGCTCATGCGCCAGTACGGCTTCGCCTGGCCCGAGCGCATGAGCTGCGACCGCCTCCCTGTGC
TGGGCGGCGACGCCGAGGTTCTGTGTATGGATTATAACCGAAGCGAAGCCACCACCGCGTCCCCT
AAGTCCTTCCCGGCCAAACCTACACTCCCAGGACCACCAGGGGCGCCATCTTCCGGGGGCGAGTG
CCCCTCGGGAGGCCCATCCGTGTGCACGTGCCGCGAGCCCTTCGTGCCCATCCTGAAGGAGTCACA

CCCACTCTACAACAAGGTGCGCACCGGCCAAGTGCCCAACTGCGCGGTGCCCTGCTACCAGCCGT
CCTTCAGCCCGGACGAGCGCACATTCGCCACCTTCTGGATTGGCCTGTGGTCTGTGCTGTGCTTCAT
CTCCACGTCCACCACCGTTGCCACCTTCCTCATTGACATGGAACGATTCCGCTACCCTGAGCGCCC
CATCATCTTCTTGTCTGCGTGCTACCTGTGTGTGTCACTGGGATTCTTGGTGCGCCTGGTAGTGGGC
CATGCCAGCGTCGCTTGCAGCCGTGAGCACAGCCACATTCACTATGAGACTACCGGCCCTGCGCTG
TGCACGGTTGTCTTCCTCTTAGTCTATTTCTTTGGCATGGCCAGCTCCATCTGGTGGGTCATCCTGT
CGCTCACCTGGTTCTTGGCGGCTGGCATGAAGTGGGGCAATGAAGCCATCGCAGGTTATGCACAG
TACTTCCACCTTGCTGCCTGGCTCATCCCCAGTGTCAAGTCCATTACGGCGCTGGCACTGAGCTCG
GTGGACGGGGACCCAGTGGCTGGCATCTGCTATGTGGGCAACCAAAACCTGAACTCACTACGAGG
CTTTGTCTTGGGCCCACTGGTGCTGTACCTGTTGGTGGGCACGCTCTTCCTTCTGGCAGGCTTCGTG
TCACTCTTCCGCATCCGGAGCGTCATCAAGCAGGGTGGCACTAAGACGGACAAGCTAGAGAAGCT
CATGATCCGCATCGGCATCTTCACCCTGCTCTACACGGTGCCAGCCAGCATCGTGGTGGCCTGCTA
CCTGTATGAGCAGCACTACCGGGAGAGCTGGGAGGCAGCCCTCACCTGCGCGTGTCCGGGACCGG
ACGCTGGCCAGCCACGCGCCAAACCCGAGTACTGGGTGCTCATGCTCAAGTACTTCATGTGCCTGG
TGGTGGGCATCACGTCGGGAGTCTGGATCTGGTCCGGCAAGACTCTGGAGTCTTGGCGGCGGTTCA
CCAGCCGCTGCTGCTGCAGCTCTCGGCGGGGCCACAAGAGCGGTGGCGCTATGGCCGCAGGAGAC
TATGCGGAGGCCAGCGCCGCGCTCACCGGCAGGACCGGGCCGCCTGGCCCCACCGCCGCATACCA
CAAGCAAGTGTCCCTGTCGCACGTATCTAGAGTGAGCAAGGGCGAGGAGCTGTTCACCGGGGTGG
TGCCCATCCTGGTCGAGCTGGACGGCGACGTAAACGGCCACAGGTTCAGCGTGTCCGGCGAGGGC
GAGGGCGATGCCACCTACGGCAAGCTGACCCTGAAGTTCATCTGCACCACCGGCAAGCTGCCCGT
GCCCTGGCCCACCCTCGTGACCACCCTGACCTGGGGCGTGCAGTGCTTCAGCCGCTACCCCGACCA
CATGAAGCAGCACGACTTCTTCAAGTCCGCCATGCCCGAAGGCTACGTCCAGGAGCGTACCATCTT
CTTCAAGGACGACGGCAACTACAAGACCCGCGCCGAGGTGAAGTTCGAGGGCGACACCCTGGTGA
ACCGCATCGAGCTGAAGGGCATCGACTTCAAGGAGGACGGCAACATCCTGGGGCACAAGCTGGA
GTACAACTACATCAGCCACAACGTCTATATCACCGCCGACAAGCAGAAGAACGGCATCAAGGCCC
ACTTCAAGATCCGCCACAACATCGAGGACGGCAGCGTGCAGCTCGCCGACCACTACCAGCAGAAC
ACCCCCATCGGCGACGGCCCCGTGCTGCTGCCCGACAACCACTACCTGAGCACCCAGTCCGCCCTG
AGCAAAGACCCCAACGAGAAGCGCGATCACATGGTCCTGCTGGAGTTCGTGACCGCCGCCGGGAT
CACTCTCGGCATGGACGAGCTGTACAAGTAA

V5-mFZD$_5$–FlAsH436-CFP in pcDNA3

AAGCTTGCCACCATGGTCCCGTGCACGCTGCTCCTGCTGTTGGCAGCCGCCCTGGCTCCGACTCAG
ACCCGGGCCGGTACCGGCAAACCGATTCCGAACCCGCTGCTGGGCCTGGATAGCACTGCCTCCAA
GGCCCCGGTGTGCCAGGAAATCACGGTGCCCATGTGCCGAGGCATCGGCTACAACCTGACGCACA
TGCCCAACCAGTTCAACCATGACACGCAGGACGAAGCAGGCCTGGAGGTGCACCAATTCTGGCCG
CTTGTGGAGATCCACTGCTCACCGGACCTGCGCTTCTTCCTGTGCTCTATGTACACGCCCATCTGTT
TGCCTGACTACCACAAGCCGCTACCACCGTGCCGTTCCGTGTGCGAGCGCGCCAAGGCCGGCTGCT
CGCCGCTCATGCGCCAGTACGGCTTCGCCTGGCCCGAGCGCATGAGCTGCGACCGCCTCCCTGTGC
TGGGCGGCGACGCCGAGGTTCTGTGTATGGATTATAACCGAAGCGAAGCCACCACCGCGTCCCCT
AAGTCCTTCCCGGCCAAACCTACACTCCCAGGACCACCAGGGGCGCCATCTTCCGGGGGCGAGTG
CCCCTCGGGAGGCCCATCCGTGTGCACGTGCCGCGAGCCCTTCGTGCCCATCCTGAAGGAGTCACA
CCCACTCTACAACAAGGTGCGCACCGGCCAAGTGCCCAACTGCGCGGTGCCCTGCTACCAGCCGT
CCTTCAGCCCGGACGAGCGCACATTCGCCACCTTCTGGATTGGCCTGTGGTCTGTGCTGTGCTTCAT
CTCCACGTCCACCACCGTTGCCACCTTCCTCATTGACATGGAACGATTCCGCTACCCTGAGCGCCC
CATCATCTTCTTGTCTGCGTGCTACCTGTGTGTGTCACTGGGATTCTTGGTGCGCCTGGTAGTGGGC
CATGCCAGCGTCGCTTGCAGCCGTGAGCACAGCCACATTCACTATGAGACTACCGGCCCTGCGCTG
TGCACGGTTGTCTTCCTCTTAGTCTATTTCTTTGGCATGGCCAGCTCCATCTGGTGGGTCATCCTGT
CGCTCACCTGGTTCTTGGCGGCTGGCATGAAGTGGGGCAATGAAGCCATCGCAGGTTATGCACAG
TACTTCCACCTTGCTGCCTGGCTCATCCCCAGTGTCAAGTCCATTACGGCGCTGGCACTGAGCTCG
GTGGACGGGGACCCAGTGGCTGGCATCTGCTATGTGGGCAACCAAAACCTGAACTCACTACGAGG
CTTTGTCTTGGGCCCACTGGTGCTGTACCTGTTGGTGGGCACGCTCTTCCTTCTGGCAGGCTTCGTG
TCACTCTTCCGCATCCGGAGCGTCATCAAGCAGGGTTGTTGCCCGGGCTGCTGTGGCACTAAGACG
GACAAGCTAGAGAAGCTCATGATCCGCATCGGCATCTTCACCCTGCTCTACACGGTGCCAGCCAGC
ATCGTGGTGGCCTGCTACCTGTATGAGCAGCACTACCGGGAGAGCTGGGAGGCAGCCCTCACCTG
CGCGTGTCCGGGACCGGACGCTGGCCAGCCACGCGCCAAACCCGAGTACTGGGTGCTCATGCTCA
AGTACTTCATGTGCCTGGTGGTGGGCATCACGTCGGGAGTCTGGATCTGGTCCGGCAAGACTCTGG

AGTCTTGGCGGCGGTTCACCAGCCGCTGCTGCTGCAGCTCTCGGCGGGGCCACAAGAGCGGTGGC
GCTATGGCCGCAGGAGACTATGCGGAGGCCAGCGCCGCGCTCACCGGCAGGACCGGGCCGCCTGG
CCCCACCGCCGCATACCACAAGCAAGTGTCCCTGTCGCACGTATCTAGAGTGAGCAAGGGCGAGG
AGCTGTTCACCGGGGTGGTGCCCATCCTGGTCGAGCTGGACGGCGACGTAAACGGCCACAGGTTC
AGCGTGTCCGGCGAGGGCGAGGGCGATGCCACCTACGGCAAGCTGACCCTGAAGTTCATCTGCAC
CACCGGCAAGCTGCCCGTGCCCTGGCCCACCCTCGTGACCACCCTGACCTGGGGCGTGCAGTGCTT
CAGCCGCTACCCCGACCACATGAAGCAGCACGACTTCTTCAAGTCCGCCATGCCCGAAGGCTACG
TCCAGGAGCGTACCATCTTCTTCAAGGACGACGGCAACTACAAGACCCGCGCCGAGGTGAAGTTC
GAGGGCGACACCCTGGTGAACCGCATCGAGCTGAAGGGCATCGACTTCAAGGAGGACGGCAACA
TCCTGGGGCACAAGCTGGAGTACAACTACATCAGCCACAACGTCTATATCACCGCCGACAAGCAG
AAGAACGGCATCAAGGCCCACTTCAAGATCCGCCACAACATCGAGGACGGCAGCGTGCAGCTCGC
CGACCACTACCAGCAGAACACCCCCATCGGCGACGGCCCCGTGCTGCTGCCCGACAACCACTACC
TGAGCACCCAGTCCGCCCTGAGCAAAGACCCCAACGAGAAGCGCGATCACATGGTCCTGCTGGAG
TTCGTGACCGCCGCCGGGATCACTCTCGGCATGGACGAGCTGTACAAGTAA

V5-mFZD$_5$–FlAsH439-CFP in pcDNA3

AAGCTTGCCACCATGGTCCCGTGCACGCTGCTCCTGCTGTTGGCAGCCGCCCTGGCTCCGACTCAG
ACCCGGGCCGGTACCGGCAAACCGATTCCGAACCCGCTGCTGGGCCTGGATAGCACTGCCTCCAAG
GCCCCGGTGTGCCAGGAAATCACGGTGCCCATGTGCCGAGGCATCGGCTACAACCTGACGCACATG
CCCAACCAGTTCAACCATGACACGCAGGACGAAGCAGGCCTGGAGGTGCACCAATTCTGGCCGCTT
GTGGAGATCCACTGCTCACCGGACCTGCGCTTCTTCCTGTGCTCTATGTACACGCCCATCTGTTTGC
CTGACTACCACAAGCCGCTACCACCGTGCCGTTCCGTGTGCGAGCGCGCCAAGGCCGGCTGCTCGC
CGCTCATGCGCCAGTACGGCTTCGCCTGGCCCGAGCGCATGAGCTGCGACCGCCTCCCTGTGCTGG
GCGGCGACGCCGAGGTTCTGTGTATGGATTATAACCGAAGCGAAGCCACCACCGCGTCCCCTAAGT
CCTTCCCGGCCAAACCTACACTCCCAGGACCACCAGGGGCGCCATCTTCCGGGGGCGAGTGCCCCT
CGGGAGGCCCATCCGTGTGCACGTGCCGCGAGCCCTTCGTGCCCATCCTGAAGGAGTCACACCCAC
TCTACAACAAGGTGCGCACCGGCCAAGTGCCCAACTGCGCGGTGCCCTGCTACCAGCCGTCCTTCA
GCCCGGACGAGCGCACATTCGCCACCTTCTGGATTGGCCTGTGGTCTGTGCTGTGCTTCATCTCCAC
GTCCACCACCGTTGCCACCTTCCTCATTGACATGGAACGATTCCGCTACCCTGAGCGCCCCATCATC
TTCTTGTCTGCGTGCTACCTGTGTGTGTCACTGGGATTCTTGGTGCGCCTGGTAGTGGGCCATGCCA
GCGTCGCTTGCAGCCGTGAGCACAGCCACATTCACTATGAGACTACCGGCCCTGCGCTGTGCACGG
TTGTCTTCCTCTTAGTCTATTTCTTTGGCATGGCCAGCTCCATCTGGTGGGTCATCCTGTCGCTCACC
TGGTTCTTGGCGGCTGGCATGAAGTGGGGCAATGAAGCCATCGCAGGTTATGCACAGTACTTCCAC
CTTGCTGCCTGGCTCATCCCCAGTGTCAAGTCCATTACGGCGCTGGCACTGAGCTCGGTGGACGGG
GACCCAGTGGCTGGCATCTGCTATGTGGGCAACCAAAACCTGAACTCACTACGAGGCTTTGTCTTG
GGCCCACTGGTGCTGTACCTGTTGGTGGGCACGCTCTTCCTTCTGGCAGGCTTCGTGTCACTCTTCC
GCATCCGGAGCGTCATCAAGCAGGGTGGCACTAAGTGTTGCCCGGGCTGCTGTACGGACAAGCTA
GAGAAGCTCATGATCCGCATCGGCATCTTCACCCTGCTCTACACGGTGCCAGCCAGCATCGTGGTG
GCCTGCTACCTGTATGAGCAGCACTACCGGGAGAGCTGGGAGGCAGCCCTCACCTGCGCGTGTCCG
GGACCGGACGCTGGCCAGCCACGCGCCAAACCCGAGTACTGGGTGCTCATGCTCAAGTACTTCATG
TGCCTGGTGGTGGGCATCACGTCGGGAGTCTGGATCTGGTCCGGCAAGACTCTGGAGTCTTGGCGG
CGGTTCACCAGCCGCTGCTGCTGCAGCTCTCGGCGGGGCCACAAGAGCGGTGGCGCTATGGCCGCA
GGAGACTATGCGGAGGCCAGCGCCGCGCTCACCGGCAGGACCGGGCCGCCTGGCCCCACCGCCGC
ATACCACAAGCAAGTGTCCCTGTCGCACGTATCTAGAGTGAGCAAGGGCGAGGAGCTGTTCACCG
GGGTGGTGCCCATCCTGGTCGAGCTGGACGGCGACGTAAACGGCCACAGGTTCAGCGTGTCCGGC
GAGGGCGAGGGCGATGCCACCTACGGCAAGCTGACCCTGAAGTTCATCTGCACCACCGGCAAGCT
GCCCGTGCCCTGGCCCACCCTCGTGACCACCCTGACCTGGGGCGTGCAGTGCTTCAGCCGCTACCC
CGACCACATGAAGCAGCACGACTTCTTCAAGTCCGCCATGCCCGAAGGCTACGTCCAGGAGCGTAC
CATCTTCTTCAAGGACGACGGCAACTACAAGACCCGCGCCGAGGTGAAGTTCGAGGGCGACACCC
TGGTGAACCGCATCGAGCTGAAGGGCATCGACTTCAAGGAGGACGGCAACATCCTGGGGCACAAG
CTGGAGTACAACTACATCAGCCACAACGTCTATATCACCGCCGACAAGCAGAAGAACGGCATCAA
GGCCCACTTCAAGATCCGCCACAACATCGAGGACGGCAGCGTGCAGCTCGCCGACCACTACCAGC
AGAACACCCCCATCGGCGACGGCCCCGTGCTGCTGCCCGACAACCACTACCTGAGCACCCAGTCCG
CCCTGAGCAAAGACCCCAACGAGAAGCGCGATCACATGGTCCTGCTGGAGTTCGTGACCGCCGCC
GGGATCACTCTCGGCATGGACGAGCTGTACAAGTAA

- **V5-mFZD$_5$–FlAsH436 in pcDNA3.4**

AAGCTTGCCACCATGGTCCCGTGCACGCTGCTCCTGCTGTTGGCAGCCGCCCTGGCTCCGACTCAG
ACCCGGGCCGGTACCGGCAAACCGATTCCGAACCCGCTGCTGGGCCTGGATAGCACTGCCTCCAAG
GCCCCGGTGTGCCAGGAAATCACGGTGCCCATGTGCCGAGGCATCGGCTACAACCTGACGCACATG
CCCAACCAGTTCAACCATGACACGCAGGACGAAGCAGGCCTGGAGGTGCACCAATTCTGGCCGCTT
GTGGAGATCCACTGCTCACCGGACCTGCGCTTCTTCCTGTGCTCTATGTACACGCCCATCTGTTTGC
CTGACTACCACAAGCCGCTACCACCGTGCCGTTCCGTGTGCGAGCGCGCCAAGGCCGGCTGCTCGC
CGCTCATGCGCCAGTACGGCTTCGCCTGGCCCGAGCGCATGAGCTGCGACCGCCTCCCTGTGCTGG
GCGGCGACGCCGAGGTTCTGTGTATGGATTATAACCGAAGCGAAGCCACCACCGCGTCCCCTAAGT
CCTTCCCGGCCAAACCTACACTCCCAGGACCACCAGGGGCGCCATCTTCCGGGGGCGAGTGCCCCT
CGGGAGGCCCATCCGTGTGCACGTGCCGCGAGCCCTTCGTGCCCATCCTGAAGGAGTCACACCCAC
TCTACAACAAGGTGCGCACCGGCCAAGTGCCCAACTGCGCGGTGCCCTGCTACCAGCCGTCCTTCA
GCCCGGACGAGCGCACATTCGCCACCTTCTGGATTGGCCTGTGGTCTGTGCTGTGCTTCATCTCCAC
GTCCACCACCGTTGCCACCTTCCTCATTGACATGGAACGATTCCGCTACCCTGAGCGCCCCATCATC
TTCTTGTCTGCGTGCTACCTGTGTGTGTCACTGGGATTCTTGGTGCGCCTGGTAGTGGGCCATGCCA
GCGTCGCTTGCAGCCGTGAGCACAGCCACATTCACTATGAGACTACCGGCCCTGCGCTGTGCACGG
TTGTCTTCCTCTTAGTCTATTTCTTTGGCATGGCCAGCTCCATCTGGTGGGTCATCCTGTCGCTCACC
TGGTTCTTGGCGGCTGGCATGAAGTGGGGCAATGAAGCCATCGCAGGTTATGCACAGTACTTCCAC
CTTGCTGCCTGGCTCATCCCCAGTGTCAAGTCCATTACGGCGCTGGCACTGAGCTCGGTGGACGGG
GACCCAGTGGCTGGCATCTGCTATGTGGGCAACCAAAACCTGAACTCACTACGAGGCTTTGTCTTG
GGCCCACTGGTGCTGTACCTGTTGGTGGGCACGCTCTTCCTTCTGGCAGGCTTCGTGTCACTCTTCC
GCATCCGGAGCGTCATCAAGCAGGGTTGTTGCCCGGGCTGCTGTGGCACTAAGACGGACAAGCTA
GAGAAGCTCATGATCCGCATCGGCATCTTCACCCTGCTCTACACGGTGCCAGCCAGCATCGTGGTG
GCCTGCTACCTGTATGAGCAGCACTACCGGGAGAGCTGGGAGGCAGCCCTCACCTGCGCGTGTCCG
GGACCGGACGCTGGCCAGCCACGCGCCAAACCCGAGTACTGGGTGCTCATGCTCAAGTACTTCATG
TGCCTGGTGGTGGGCATCACGTCGGGAGTCTGGATCTGGTCCGGCAAGACTCTGGAGTCTTGGCGG
CGGTTCACCAGCCGCTGCTGCTGCAGCTCTCGGCGGGGCCACAAGAGCGGTGGCGCTATGGCCGCA
GGAGACTATGCGGAGGCCAGCGCCGCGCTCACCGGCAGGACCGGGCCGCCTGGCCCCACCGCCGC
ATACCACAAGCAAGTGTCCCTGTCGCACGTATAATCTAGA

- **V5-mFZD$_5$–FlAsH439 in pcDNA3.4**

AAGCTTGCCACCATGGTCCCGTGCACGCTGCTCCTGCTGTTGGCAGCCGCCCTGGCTCCGACTCAG
ACCCGGGCCGGTACCGGCAAACCGATTCCGAACCCGCTGCTGGGCCTGGATAGCACTGCCTCCAAG
GCCCCGGTGTGCCAGGAAATCACGGTGCCCATGTGCCGAGGCATCGGCTACAACCTGACGCACATG
CCCAACCAGTTCAACCATGACACGCAGGACGAAGCAGGCCTGGAGGTGCACCAATTCTGGCCGCTT
GTGGAGATCCACTGCTCACCGGACCTGCGCTTCTTCCTGTGCTCTATGTACACGCCCATCTGTTTGC
CTGACTACCACAAGCCGCTACCACCGTGCCGTTCCGTGTGCGAGCGCGCCAAGGCCGGCTGCTCGC
CGCTCATGCGCCAGTACGGCTTCGCCTGGCCCGAGCGCATGAGCTGCGACCGCCTCCCTGTGCTGG
GCGGCGACGCCGAGGTTCTGTGTATGGATTATAACCGAAGCGAAGCCACCACCGCGTCCCCTAAGT
CCTTCCCGGCCAAACCTACACTCCCAGGACCACCAGGGGCGCCATCTTCCGGGGGCGAGTGCCCCT
CGGGAGGCCCATCCGTGTGCACGTGCCGCGAGCCCTTCGTGCCCATCCTGAAGGAGTCACACCCAC
TCTACAACAAGGTGCGCACCGGCCAAGTGCCCAACTGCGCGGTGCCCTGCTACCAGCCGTCCTTCA
GCCCGGACGAGCGCACATTCGCCACCTTCTGGATTGGCCTGTGGTCTGTGCTGTGCTTCATCTCCAC
GTCCACCACCGTTGCCACCTTCCTCATTGACATGGAACGATTCCGCTACCCTGAGCGCCCCATCATC
TTCTTGTCTGCGTGCTACCTGTGTGTGTCACTGGGATTCTTGGTGCGCCTGGTAGTGGGCCATGCCA
GCGTCGCTTGCAGCCGTGAGCACAGCCACATTCACTATGAGACTACCGGCCCTGCGCTGTGCACGG
TTGTCTTCCTCTTAGTCTATTTCTTTGGCATGGCCAGCTCCATCTGGTGGGTCATCCTGTCGCTCACC
TGGTTCTTGGCGGCTGGCATGAAGTGGGGCAATGAAGCCATCGCAGGTTATGCACAGTACTTCCAC
CTTGCTGCCTGGCTCATCCCCAGTGTCAAGTCCATTACGGCGCTGGCACTGAGCTCGGTGGACGGG
GACCCAGTGGCTGGCATCTGCTATGTGGGCAACCAAAACCTGAACTCACTACGAGGCTTTGTCTTG
GGCCCACTGGTGCTGTACCTGTTGGTGGGCACGCTCTTCCTTCTGGCAGGCTTCGTGTCACTCTTCC
GCATCCGGAGCGTCATCAAGCAGGGTGGCACTAAGTGTTGCCCGGGCTGCTGTACGGACAAGCTA
GAGAAGCTCATGATCCGCATCGGCATCTTCACCCTGCTCTACACGGTGCCAGCCAGCATCGTGGTG
GCCTGCTACCTGTATGAGCAGCACTACCGGGAGAGCTGGGAGGCAGCCCTCACCTGCGCGTGTCCG
GGACCGGACGCTGGCCAGCCACGCGCCAAACCCGAGTACTGGGTGCTCATGCTCAAGTACTTCATG

TGCCTGGTGGTGGGCATCACGTCGGGAGTCTGGATCTGGTCCGGCAAGACTCTGGAGTCTTGGCGG
CGGTTCACCAGCCGCTGCTGCTGCAGCTCTCGGCGGGGCCACAAGAGCGGTGGCGCTATGGCCGCA
GGAGACTATGCGGAGGCCAGCGCCGCGCTCACCGGCAGGACCGGGCCGCCTGGCCCCACCGCCGC
ATACCACAAGCAAGTGTCCCTGTCGCACGTATAATCTAGA

- **V5-mFZD$_5$ in pmCherry-N1**

AGATCTACCATGGTCCCGTGCACGCTGCTCCTGCTGTTGGCAGCCGCCCTGGCTCCGACTCAGACCC
GGGCCGGTACCGGCAAACCGATTCCGAACCCGCTGCTGGGCCTGGATAGCACTGCCTCCAAGGCCC
CGGTGTGCCAGGAAATCACGGTGCCCATGTGCCGAGGCATCGGCTACAACCTGACGCACATGCCCA
ACCAGTTCAACCATGACACGCAGGACGAAGCAGGCCTGGAGGTGCACCAATTCTGGCCGCTTGTG
GAGATCCACTGCTCACCGGACCTGCGCTTCTTCCTGTGCTCTATGTACACGCCCATCTGTTTGCCTG
ACTACCACAAGCCGCTACCACCGTGCCGTTCCGTGTGCGAGCGCGCCAAGGCCGGCTGCTCGCCGC
TCATGCGCCAGTACGGCTTCGCCTGGCCCGAGCGCATGAGCTGCGACCGCCTCCCTGTGCTGGGCG
GCGACGCCGAGGTTCTGTGTATGGATTATAACCGAAGCGAAGCCACCACCGCGTCCCCTAAGTCCT
TCCCGGCCAAACCTACACTCCCAGGACCACCAGGGGCGCCATCTTCCGGGGGCGAGTGCCCCTCGG
GAGGCCCATCCGTGTGCACGTGCCGCGAGCCCTTCGTGCCCATCCTGAAGGAGTCACACCCACTCT
ACAACAAGGTGCGCACCGGCCAAGTGCCCAACTGCGCGGTGCCCTGCTACCAGCCGTCCTTCAGCC
CGGACGAGCGCACATTCGCCACCTTCTGGATTGGCCTGTGGTCTGTGCTGTGCTTCATCTCCACGTC
CACCACCGTTGCCACCTTCCTCATTGACATGGAACGATTCCGCTACCCTGAGCGCCCCATCATCTTC
TTGTCTGCGTGCTACCTGTGTGTGTCACTGGGATTCTTGGTGCGCCTGGTAGTGGGCCATGCCAGCG
TCGCTTGCAGCCGTGAGCACAGCCACATTCACTATGAGACTACCGGCCCTGCGCTGTGCACGGTTG
TCTTCCTCTTAGTCTATTTCTTTGGCATGGCCAGCTCCATCTGGTGGGTCATCCTGTCGCTCACCTGG
TTCTTGGCGGCTGGCATGAAGTGGGGCAATGAAGCCATCGCAGGTTATGCACAGTACTTCCACCTT
GCTGCCTGGCTCATCCCCAGTGTCAAGTCCATTACGGCGCTGGCACTGAGCTCGGTGGACGGGGAC
CCAGTGGCTGGCATCTGCTATGTGGGCAACCAAAACCTGAACTCACTACGAGGCTTTGTCTTGGGC
CCACTGGTGCTGTACCTGTTGGTGGGCACGCTCTTCCTTCTGGCAGGCTTCGTGTCACTCTTCCGCA
TCCGGAGCGTCATCAAGCAGGGTGGCACTAAGACGGACAAGCTAGAGAAGCTCATGATCCGCATC
GGCATCTTCACCCTGCTCTACACGGTGCCAGCCAGCATCGTGGTGGCCTGCTACCTGTATGAGCAG
CACTACCGGGAGAGCTGGGAGGCAGCCCTCACCTGCGCGTGTCCGGGACCGGACGCTGGCCAGCC
ACGCGCCAAACCCGAGTACTGGGTGCTCATGCTCAAGTACTTCATGTGCCTGGTGGTGGGCATCAC
GTCGGGAGTCTGGATCTGGTCCGGCAAGACTCTGGAGTCTTGGCGGCGGTTCACCAGCCGCTGCTG
CTGCAGCTCTCGGCGGGGCCACAAGAGCGGTGGCGCTATGGCCGCAGGAGACTATGCGGAGGCCA
GCGCCGCGCTCACCGGCAGGACCGGGCCGCCTGGCCCCACCGCCGCATACCACAAGCAAGTGTCC
CTGTCGCACGTACAACCGGTCGCCACCATGGTGAGCAAGGGCGAGGAGGATAACATGGCCATCAT
CAAGGAGTTCATGCGCTTCAAGGTGCACATGGAGGGCTCCGTGAACGGCCACGAGTTCGAGATCG

- **V5-mFZD$_5$–GFP in pcDNA3**

AAGCTTGCCACCATGGTCCCGTGCACGCTGCTCCTGCTGTTGGCAGCCGCCCTGGCTCCGACTCAG
ACCCGGGCCGGTACCGGCAAACCGATTCCGAACCCGCTGCTGGGCCTGGATAGCACTGCCTCCAAG
GCCCCGGTGTGCCAGGAAATCACGGTGCCCATGTGCCGAGGCATCGGCTACAACCTGACGCACATG
CCCAACCAGTTCAACCATGACACGCAGGACGAAGCAGGCCTGGAGGTGCACCAATTCTGGCCGCTT
GTGGAGATCCACTGCTCACCGGACCTGCGCTTCTTCCTGTGCTCTATGTACACGCCCATCTGTTTGC
CTGACTACCACAAGCCGCTACCACCGTGCCGTTCCGTGTGCGAGCGCGCCAAGGCCGGCTGCTCGC
CGCTCATGCGCCAGTACGGCTTCGCCTGGCCCGAGCGCATGAGCTGCGACCGCCTCCCTGTGCTGG
GCGGCGACGCCGAGGTTCTGTGTATGGATTATAACCGAAGCGAAGCCACCACCGCGTCCCCTAAGT
CCTTCCCGGCCAAACCTACACTCCCAGGACCACCAGGGGCGCCATCTTCCGGGGGCGAGTGCCCCT
CGGGAGGCCCATCCGTGTGCACGTGCCGCGAGCCCTTCGTGCCCATCCTGAAGGAGTCACACCCAC
TCTACAACAAGGTGCGCACCGGCCAAGTGCCCAACTGCGCGGTGCCCTGCTACCAGCCGTCCTTCA
GCCCGGACGAGCGCACATTCGCCACCTTCTGGATTGGCCTGTGGTCTGTGCTGTGCTTCATCTCCAC
GTCCACCACCGTTGCCACCTTCCTCATTGACATGGAACGATTCCGCTACCCTGAGCGCCCCATCATC
TTCTTGTCTGCGTGCTACCTGTGTGTGTCACTGGGATTCTTGGTGCGCCTGGTAGTGGGCCATGCCA
GCGTCGCTTGCAGCCGTGAGCACAGCCACATTCACTATGAGACTACCGGCCCTGCGCTGTGCACGG

TTGTCTTCCTCTTAGTCTATTTCTTTGGCATGGCCAGCTCCATCTGGTGGGTCATCCTGTCGCTCACC
TGGTTCTTGGCGGCTGGCATGAAGTGGGGCAATGAAGCCATCGCAGGTTATGCACAGTACTTCCAC
CTTGCTGCCTGGCTCATCCCCAGTGTCAAGTCCATTACGGCGCTGGCACTGAGCTCGGTGGACGGG
GACCCAGTGGCTGGCATCTGCTATGTGGGCAACCAAAACCTGAACTCACTACGAGGCTTTGTCTTG
GGCCCACTGGTGCTGTACCTGTTGGTGGGCACGCTCTTCCTTCTGGCAGGCTTCGTGTCACTCTTCC
GCATCCGGAGCGTCATCAAGCAGGGTGGCACTAAGACGGACAAGCTAGAGAAGCTCATGATCCGC
ATCGGCATCTTCACCCTGCTCTACACGGTGCCAGCCAGCATCGTGGTGGCCTGCTACCTGTATGAGC
AGCACTACCGGGAGAGCTGGGAGGCAGCCCTCACCTGCGCGTGTCCGGGACCGGACGCTGGCCAG
CCACGCGCCAAACCCGAGTACTGGGTGCTCATGCTCAAGTACTTCATGTGCCTGGTGGTGGGCATC
ACGTCGGGAGTCTGGATCTGGTCCGGCAAGACTCTGGAGTCTTGGCGGCGGTTCACCAGCCGCTGC
TGCTGCAGCTCTCGGCGGGGCCACAAGAGCGGTGGCGCTATGGCCGCAGGAGACTATGCGGAGGC
CAGCGCCGCGCTCACCGGCAGGACCGGGCCGCCTGGCCCCACCGCCGCATACCACAAGCAAGTGT
CCCTGTCGCACGTATCTAGAATGAGCAAGGGCGAGGAACTGTTCACTGGCGTGGTCCCAATTCTCG
TGGAACTGGATGGCGATGTGAATGGGCACAAATTTTCTGTCAGCGGAGAGGGTGAAGGTGATGCC
ACATACGGAAAGCTCACCCTGAAATTCATCTGCACCACTGGAAAGCTCCCTGTGCCATGGCCAACA
CTGGTCACTACCTTCACCTATGGCGTGCAGTGCTTTTCCAGATACCCAGACCATATGAAGCAGCAT
GACTTTTTCAAGAGCGCCATGCCCGAGGGCTATGTGCAGGAGAGAACCATCTTTTTCAAAGATGAC
GGGAACTACAAGACCCGCGCTGAAGTCAAGTTCGAAGGTGACACCCTGGTGAATAGAATCGAGCT
GAAGGGCATTGACTTTAAGGAGGATGGAAACATTCTCGGCCACAAGCTGGAATACAACTATAACT
CCCACAATGTGTACATCATGGCCGACAAGCAAAAGAATGGCATCAAGGTCAACTTCAAGATCAGA
CACAACATTGAGGATGGATCCGTGCAGCTGGCCGACCATTATCAACAGAACACTCCAATCGGCGAC
GGCCCTGTGCTCCTCCC

V5-mFZD$_5$–YFP in pcDNA3

AAGCTTGCCACCATGGTCCCGTGCACGCTGCTCCTGCTGTTGGCAGCCGCCCTGGCTCCGACTCAG
ACCCGGGCCGGTACCGGCAAACCGATTCCGAACCCGCTGCTGGGCCTGGATAGCACTGCCTCCAAG
GCCCCGGTGTGCCAGGAAATCACGGTGCCCATGTGCCGAGGCATCGGCTACAACCTGACGCACATG
CCCAACCAGTTCAACCATGACACGCAGGACGAAGCAGGCCTGGAGGTGCACCAATTCTGGCCGCTT
GTGGAGATCCACTGCTCACCGGACCTGCGCTTCTTCCTGTGCTCTATGTACACGCCCATCTGTTTGC
CTGACTACCACAAGCCGCTACCACCGTGCCGTTCCGTGTGCGAGCGCGCCAAGGCCGGCTGCTCGC
CGCTCATGCGCCAGTACGGCTTCGCCTGGCCCGAGCGCATGAGCTGCGACCGCCTCCCTGTGCTGG
GCGGCGACGCCGAGGTTCTGTGTATGGATTATAACCGAAGCGAAGCCACCACCGCGTCCCCTAAGT
CCTTCCCGGCCAAACCTACACTCCCAGGACCACCAGGGGCGCCATCTTCCGGGGGCGAGTGCCCCT
CGGGAGGCCCATCCGTGTGCACGTGCCGCGAGCCCTTCGTGCCCATCCTGAAGGAGTCACACCCAC
TCTACAACAAGGTGCGCACCGGCCAAGTGCCCAACTGCGCGGTGCCCTGCTACCAGCCGTCCTTCA
GCCCGGACGAGCGCACATTCGCCACCTTCTGGATTGGCCTGTGGTCTGTGCTGTGCTTCATCTCCAC
GTCCACCACCGTTGCCACCTTCCTCATTGACATGGAACGATTCCGCTACCCTGAGCGCCCCATCATC
TTCTTGTCTGCGTGCTACCTGTGTGTGTCACTGGGATTCTTGGTGCGCCTGGTAGTGGGCCATGCCA
GCGTCGCTTGCAGCCGTGAGCACAGCCACATTCACTATGAGACTACCGGCCCTGCGCTGTGCACGG
TTGTCTTCCTCTTAGTCTATTTCTTTGGCATGGCCAGCTCCATCTGGTGGGTCATCCTGTCGCTCACC
TGGTTCTTGGCGGCTGGCATGAAGTGGGGCAATGAAGCCATCGCAGGTTATGCACAGTACTTCCAC
CTTGCTGCCTGGCTCATCCCCAGTGTCAAGTCCATTACGGCGCTGGCACTGAGCTCGGTGGACGGG
GACCCAGTGGCTGGCATCTGCTATGTGGGCAACCAAAACCTGAACTCACTACGAGGCTTTGTCTTG
GGCCCACTGGTGCTGTACCTGTTGGTGGGCACGCTCTTCCTTCTGGCAGGCTTCGTGTCACTCTTCC
GCATCCGGAGCGTCATCAAGCAGGGTGGCACTAAGACGGACAAGCTAGAGAAGCTCATGATCCGC
ATCGGCATCTTCACCCTGCTCTACACGGTGCCAGCCAGCATCGTGGTGGCCTGCTACCTGTATGAGC
AGCACTACCGGGAGAGCTGGGAGGCAGCCCTCACCTGCGCGTGTCCGGGACCGGACGCTGGCCAG
CCACGCGCCAAACCCGAGTACTGGGTGCTCATGCTCAAGTACTTCATGTGCCTGGTGGTGGGCATC
ACGTCGGGAGTCTGGATCTGGTCCGGCAAGACTCTGGAGTCTTGGCGGCGGTTCACCAGCCGCTGC
TGCTGCAGCTCTCGGCGGGGCCACAAGAGCGGTGGCGCTATGGCCGCAGGAGACTATGCGGAGGC
CAGCGCCGCGCTCACCGGCAGGACCGGGCCGCCTGGCCCCACCGCCGCATACCACAAGCAAGTGT
CCCTGTCGCACGTATCTAGAGTGAGCAAGGGCGAGGAGCTGTTCACCGGGGTGGTGCCCATCCTGG
TCGAGCTGGACGGCGACGTAAACGGCCACAAGTTCAGCGTGTCCGGCGAGGGCGAGGGCGATGCC
ACCTACGGCAAGCTGACCCTGAAGTTCATCTGCACCACCGGCAAGCTGCCCGTGCCCTGGCCCACC
CTCGTGACCACCTTCGGCTACGGCCTGCAGTGCTTCGCCCGCTACCCCGACCACATGAAGCAGCAC
GACTTCTTCAAGTCCGCCATGCCCGAAGGCTACGTCCAGGAGCGCACCATCTTCTTCAAGGACGAC
GGCAACTACAAGACCCGCGCCGAGGTGAAGTTCGAGGGCGACACCCTGGTGAACCGCATCGAGCT

7. References

- Ainla, A., Jansson, E.T., Stepanyants, N., Orwar, O., and Jesorka, A. (2010). A Microfluidic Pipette for Single-Cell Pharmacology. *Analytical Chemistry, 82*(11), 4529-4536.
- Ainla, A., Jeffries, G.D.M., Brune, R., Orwar, O., and Jesorka, A. (2012). A multifunctional pipette. *Lab Chip, 12*(7), 1255-1261.
- Aastrup, T., Wright, S., Proverbio, D., Valnohova, J., and Schulte, G. (2014). Label-free cell-based assay for the characterisation of peptide receptor interactions. *Clinical & Medical Research, International Pharmaceutical Industry, 6*(2), 54-57.
- Adjobo-Hermans, M.J.W., Goedhart, J., van Weeren, L., Nijmeijer, S., Manders, E.M. M., Offermanns, S., and Gadella (jr.), T.W.J. (2011). Real-time visualization of heterotrimeric G protein Gq activation in living cells. *BMC Biology, 9*, 32.
- Agnetta, L.*, Kauk, M.*, Canizal, M.C.A., Messerer, R., Holzgrabe, U., Hoffmann, C., and Decker, M. (2017). A Photoswitchable Dualsteric Ligand Controlling Receptor Efficacy. *Angewandte Chemie International Edition, 56*(25), 7282 – 7287.
- Angers, S., and Moon, R.T. (2009). Proximal events in Wnt signal transduction. *Nature Reviews Molecular Cell Biology, 10*(7), 468–477.
- Arthofer, E.*, Hot, B.*, Petersen, J., Strakova, K., Jäger, S., Grundmann, M., Kostenis, E., Gutkind, J.S., and Schulte, G. (2016). WNT Stimulation Dissociates a Frizzled 4 Inactive-State Complex with $G\alpha_{12/13}$. *Molecular Pharmacology, 90*(4), 447-459.
- Bernatík, O.*, Šedová, K.*, Schille, C., Ganji, R.S., Červenka, I., Trantírek, L., Schambony, A., Zdráhal, Z., and Bryja, V. (2014). Functional analysis of dishevelled-3 phosphorylation identifies distinct mechanisms driven by casein kinase 1ϵ and frizzled5. *The Journal of biological chemistry, 289*(34), 23520-23533.
- Bhanot, P., Brink, M., Samos, C. H., Hsieh, J. C., Wang, Y., Macke, J. P., Andrew, D., Nathans, J., and Nusse, R. (1996). A new member of the frizzled family from Drosophila functions as a Wingless receptor. *Nature, 382*(6588), 225-30.
- Blumenthal, A., Ehlers, S., Lauber, J., Buer, J., Lange, C., Goldmann, T., Heine, H., Brandt, E., and Reiling, N. (2006). The Wingless homolog WNT5A and its receptor Frizzled-5 regulate inflammatory responses of human mononuclear cells induced by microbial stimulation. *Blood, 108*(3), 965-973.
- Bünemann, M., Frank, M., and Lohse, M.J. (2003). Gi protein activation in intact cells involves subunit rearrangement rather than dissociation. *Proc. Natl. Acad. Sci. USA, 100*(26), 16077-16082.
- Briddon, S.J., Kilpatrick, L.E., and Hill, S.J. (2018). Studying GPCR pharmacology in membrane microdomains: fluorescence correlation spectroscopy comes of age. *Trends in Pharmacological Sciences, 39*(2), 158–174.

- Bridges, C.B., Brehme, K.S. (1944). The mutants of Drosophila melanogaster. *Publications Carnegie Institution, 552*, 1-257.
- Bryja, V.*, Schulte, G.*, Rawal, N., Grahn, A., and Arenas, E. (2007). Wnt-5a induces Dishevelled phosphorylation and dopaminergic differentiation via a CK1-dependent mechanism. *Journal of Cell Science, 120*, 586-595.
- Byrne, E.F.X.*, Sircar, R.*, Miller, P.S., Hedger, G., Luchetti, G., Nachtergaele, S., Tully, M.D., Mydock-McGrane, L., Covey, D.F., Rambo, R.P., Sansom, M.S.P., Newstead, S., Rohatgi, R., and Siebold, C. (2016). Structural basis of Smoothened regulation by its extracellular domains. *Nature, 535*(7613), 517-522.
- Cabrera, C.V., Alonso, M.C., Johnston, P., Phillips, R.G., and Lawrence, P.A. (1987). Phenocopies induced with antisense RNA identify the wingless gene. *Cell, 50*(4), 659-663.
- Capurro, M., Martin, T., Shi, W., and Filmus, J. (2014). Glypican-3 binds to Frizzled and plays a direct role in the stimulation of canonical Wnt signaling. *Journal of Cell Science, 127*, 1565-1575.
- Carmon, K.S., and Loose, D.S. (2010). Development of a bioassay for detection of Wnt-binding affinities for individual frizzled receptors. *Analytical Biochemistry, 401*(2), 288-94.
- Carpenter, B., Nehmé, R., Warne, T., Leslie, A. G., & Tate, C. G. (2016). Structure of the adenosine A(2A) receptor bound to an engineered G protein. *Nature, 536*(7614), 104-107.
- Castro, M., Nikolaev, V.O., Palm, D., Lohse, M.J., and Vilardaga, J.P. (2005). Turn-on switch in parathyroid hormone receptor by a two-step parathyroid hormone binding mechanism. *Proc. Natl. Acad. Sci. USA, 102*(44), 16084-9.
- Chen, M., Zhong, W., Hu, Y., Liu, J., and Cai, X. (2015). Wnt5a/FZD5/CaMKII signaling pathway mediates the effect of BML-111 on inflammatory reactions in sepsis. *International Journal of Clinical and Experimental Medicine, 8*(10), 17824-17829.
- Chun, L., Zhang, W. H., and Liu, J. F. (2012). Structure and ligand recognition of class C GPCRs. *Acta pharmacologica Sinica, 33*(3), 312-323.
- Clausen, T.M., Pereira, M.A., Oo, H.Z., Resende, M., Gustavson, T., Mao, Y., Sugiura, N., Liew, J., Fazli, L., Theander, T. G., Daugaard, M. and Salanti, A. (2016). Real-time and label free determination of ligand binding-kinetics to primary cancer tissue specimens; a novel tool for the assessment of biomarker targeting. *Sensing and Bio-Sensing Research, 9*, 23-30.
- De, A. (2011). Wnt/Ca2+ signaling pathway: a brief overview. *Acta biochimica et biophysica Sinica, 43*, 745–756.
- de Graaf, C.*, Song, G.*, Cao, C.*, Zhao, Q., Wang, M.W., Wu, B., and Stevens, R.C. (2017). Extending the Structural View of Class B GPCRs. *Trends in Biochemical Sciences 42*(12), 946-960.

- DeBruine, Z.J.*, Ke, J.*, Harikumar, K.G.*, Gu, X., Borowsky, P., Williams, B.O., Xu, W., Miller, L.J., Xu, H.E., and Melcher, K. (2017). Wnt5a promotes Frizzled-4 signalosome assembly by stabilizing cysteine-rich domain dimerization. *Genes & development, 31*(9), 916-926.
- Dijksterhuis, J.P.*, Petersen, J.*, and Schulte, G. (2014). WNT/Frizzled signalling: receptor-ligand selectivity with focus on FZD-G protein signaling and its physiological relevance: IUPHAR Review 3. *British Journal of Pharmacology, 171*, 1195-1209.
- Dijksterhuis, J.P., Baljinnyam, B., Stanger, K., Sercan, H.O., Ji, Y., Andres, O., Rubin, J.S., Hannoush, R.N., and Schulte, G. (2015). Systematic mapping of WNT-FZD protein interactions reveals functional selectivity by distinct WNT-FZD pairs. *Journal of Biological Chemistry, 290*(11), 6789-6798.
- Ferré, S. (2015). The GPCR heterotetramer: challenging classical pharmacology. *Trends in pharmacological sciences, 36*(3), 145-52.
- Filmus, J., Capurro, M., & Rast, J. (2008). Glypicans. *Genome biology, 9*(5), 224.
- Foord, S.M., Bonner, T.I., Neubig, R.R., Rosser, E.M., Pin, J.P., Davenport, A.P., Spedding, M., and Harmar, A.J. (2005). International Union of Pharmacology. XLVI. G protein-coupled receptor list. *Pharmacological Reviews, 57*(2), 279-288.
- Foulquier S., Daskalopoulos E.P., Lluri G., Hermans K.C.M., Deb A., and Blankesteijn W.M. (2018) WNT Signaling in Cardiac and Vascular Disease. *Pharmacological Reviews, 70*(1), 68-141.
- Fredriksson, R., Lagerström, M.C., Lundin, L.G., and Schiöth, H.B. (2003). The G-protein-coupled receptors in the human genome form five main families. Phylogenetic analysis, paralogon groups, and fingerprints. *Molecular Pharmacology, 63*(6), 1256-1272.
- Galandrin, S.*, Oligny-Longpré, G.*, and Bouvier, M. (2007). The evasive nature of drug efficacy: implications for drug discovery. *Trends in Pharmacological Sciences, 28*(8), 423-430.
- Gammons, M.V., Renko, M., Johnson, C.M., Rutherford, T.J., and Bienz, M. (2016). Wnt Signalosome Assembly by DEP Domain Swapping of Dishevelled. *Molecular cell, 64*(1), 92-104.
- Gammons, M., and Bienz, M. (2018). Multiprotein complexes governing Wnt signal transduction. *Current Opinion in Cell Biology, 51*, 42-49.
- Gentzel, M.*, Schille, C.*, Rauschenberger, V., and Schambony, A. (2015). Distinct functionality of dishevelled isoforms on Ca2+/calmodulin-dependent protein kinase 2 (CamKII) in Xenopus gastrulation. *Molecular biology of the cell, 26*(5), 966-77.
- Glukhova, A., Draper-Joyce, C.J., Sunahara, R.K., Christopoulos, A., Wootten, D., and Sexton, P.M. (2018). Rules of Engagement: GPCRs and G Proteins. *ACS Pharmacology & Translational Science, 1*(2), 73–83.

- González-Sancho, J.M., Brennan, K.R., Castelo-Soccio, L.A., and Brown, A.M. (2004). Wnt proteins induce Dishevelled phosphorylation via an LRP5/6-independent mechanism, irrespective of their ability to stabilize β-catenin. *Molecular and Cellular Biology, 24*(11), 4757–4768.
- Grainger, S., and Willert, K. (2018). Mechanisms of Wnt signaling and control. *Wiley Interdisciplinary Reviews: Systems Biology and Medicine,* e1422.
- Green, J., Nusse, R., and van Amerongen, R. (2014). The role of Ryk and Ror receptor tyrosine kinases in Wnt signal transduction. *Cold Spring Harbor perspectives in biology, 6*(2), a009175.
- Haga, T. (2013). Molecular properties of muscarinic acetylcholine receptors. *Proc. Japan Acad. Ser. B, Phys. Biol. Sci., 89(*6), 226-256.
- Halleskog, G., and Schulte, G. (2013). Pertussis toxin-sensitive heterotrimeric $G\alpha_{i/o}$ proteins mediate WNT/β-catenin and WNT/ERK1/2 signaling in mouse primary microglia stimulated with purified WNT-3A. *Cellular Signalling, 25*(4), 822-828.
- Hamann, J., Aust, G., Araç, D., Engel, F.B., Formstone, C., Fredriksson, R., […] and Schiöth, H.B. (2015). International Union of Basic and Clinical Pharmacology. XCIV. Adhesion G protein-coupled receptors. *Pharmacological reviews, 67*(2), 338-367.
- Hauser, A.S., Attwood, M.M., Rask-Andersen, M., Schiöth, H.B., and Gloriam, D.E. (2017). Trends in GPCR drug discovery: new agents, targets and indications. *Nature Reviews Drug Discovery, 16*(12), 829-842.
- He, X., Saint-Jeannet, J.P., Wang, Y., Nathans, J., Dawid, I., and Varmus, H. (1997). A member of the Frizzled protein family mediating axis induction by Wnt-5A. *Science 275*(5306), 1652-1654.
- Hilger, D.*, Masureel, M.*, and Kobilka, B.K. (2018). Structure and dynamics of GPCR signaling complexes. *Nature Structural and Molecular Biology, 25*(1), 4-12.
- Hoffmann, C., Gaietta, G., Bünemann, M., Adams, S.R., Oberdorff-Maass, S., Behr, B., Vilardaga, J.P., Tsien, R.Y., Ellisman, M.H., and Lohse, M.J. (2005). A FlAsH-based FRET approach to determine G protein-coupled receptor activation in living cells. *Nature Methods, 2*(3), 171-176.
- Hoffmann, C., Gaietta, G., Zürn, A., Adams, S. R., Terrillon, S., Ellisman, M. H., Tsien, R. Y., and Lohse, M. J. (2010). Fluorescent labeling of tetracysteine-tagged proteins in intact cells. *Nature Protocols, 5*(10), 1666-1677.
- Hoffmann, C., Nuber, S., Zabel, U., Ziegler, N., Winkler, C., Hein, P., Berlot, C.H., Bünemann, M., and Lohse, M.J. (2012). Comparison of the Activation Kinetics of the M3 Acetylcholine Receptor and a Constitutively Active Mutant Receptor in Living Cells. *Molecular Pharmacology, 82*(2), 236-245.
- Holstein, T.W. (2012). The evolution of the Wnt pathway. *Cold Spring Harbor perspectives in biology,* 4(7), a007922.

- Hot, B., Valnohova, J., Arthofer, E., Simon, K., Shin, J., Uhlén, M., Kostenis, E., Mulder, J., and Schulte, G. (2017). FZD_{10}-$G\alpha_{13}$ signaling axis points to a role of FZD_{10} in CNS angiogenesis. *Cellular Signalling, 32*, 93-103.
- Huang, P., Zheng, S., Wierbowski, B.M., Kim, Y., Nedelcu, D., Aravena, L., Liu, J., Kruse, A.C., and Salic, A. (2018). Structural Basis of Smoothened Activation in Hedgehog Signaling. *Cell, 175*(1), 295-297.
- Humphries, A.C., and Mlodzik, M. (2018). From instruction to output: Wnt/PCP signaling in development and cancer. *Current Opinion in Cell Biology, 51*, 110-116.
- Ishikawa, T.*, Tamai, Y.*, Zorn, A.M., Yoshida, H., Seldin, M.F., Nishikawa, S., and Taketo, M.M. (2001). Mouse Wnt receptor gene Fzd5 is essential for yolk sac and placental angiogenesis. *Development*, 128(1), 25-33.
- IUPHAR/BPS Guide to Pharmacology: http://www.guidetopharmacology.org/
- Janda, C.Y., Waghray, D., Levin, A.M., Thomas, C., and Garcia, K.C. (2012). Structural basis of Wnt recognition by Frizzled. *Science, 337*(6090), 59-64.
- Jares-Erijman, E.A., and Jovin, T.M. (2003). FRET imaging. *Nature Biotechnology, 21*(11), 1387-1395.
- Jost, C.A., Reither, G., Hoffmann, C., and Schultz, C. (2008). Contribution of fluorophores to protein kinase C FRET probe performance. *Chembiochem, 9*, 1379-1384.
- Kang, Y.*, Zhou, X.E.*, Gao, X*., He, Y.*, Liu, W., Ishchenko, A., […] and Xu, H.E. (2015). Crystal structure of rhodopsin bound to arrestin by femtosecond X-ray laser. *Nature, 523*(7562), 561-567.
- Katoh, M. (2005). WNT/PCP signaling pathway and human cancer. *Oncology Reports, 14*(6), 1583-1588.
- Kauk, M., and Hoffmann, C. (2018). Intramolecular and Intermolecular FRET Sensors for GPCRs – Monitoring Conformational Changes and Beyond. *Trends in Pharmacological Sciences, 39*(2), 123-135.
- Kilander, M.B.C.*, Petersen, J.*, Andressen, K.W., Ganji, R.S. Levy, F.O., Schuster, J., Dahl N., Bryja, V., and Schulte, G. (2014). Disheveled regulates precoupling of heterotrimeric G proteins to Frizzled 6. *FASEB Journal, 28*(5), 2293-2305.
- Kobilka, B.K. (2007). G protein coupled receptor structure and activation. *Biochimica et Biophysica Acta, 1768*(4), 794-807.
- Kohn, A.D., and Moon, R.T. (2005). Wnt and calcium signaling: beta-catenin-independent pathways. *Cell Calcium, 38*(3-4), 439-446.
- Komiya, Y., and Habas, R. (2008). Wnt signal transduction pathways. *Organogenesis, 4*(2), 68-75
- Koval, A., and Katanaev, V.L. (2011). Wnt3a stimulation elicits G-protein-coupled receptor properties of mammalian Frizzled proteins. *Biochemical Journal, 433*(3), 435-440.

- Krasnow, R.E., and Adler P.N., (1994). A single *frizzled* protein has a dual function in tissue polarity. *Development, 120*(7), 1883-1893.
- Krasnow, R.E., Wong, L.L., and Adler, P.N. (1995). Dishevelled is a component of the frizzled signaling pathway in Drosophila. *Development, 121*(12), 4095-4102.
- Kremers, G.J., Piston, D.W., and Davidson, M.W. (2018). Basics of FRET Microscopy. Fundamental Principles of Förster Resonance Energy Transfer (FRET) Microscopy with Fluorescent Proteins. Retrieved from

  https://www.microscopyu.com/applications/fret/basics-of-fret-microscopy.
- Kühl, M., Sheldahl, L.C., Malbon, C.C., and Moon, R.T. (2000a). Ca2+/calmodulin-dependent protein kinase II is stimulated by Wnt and Frizzled homologs and promotes ventral cell fates in Xenopus. *Journal of Biological Chemistry, 275*(17), 12701-12711.
- Kühl, M., Sheldahl, L.C., Park, M., Miller, J.R., and Moon, R.T. (2000b). The Wnt/Ca2+ pathway: a new vertebrate Wnt signaling pathway takes shape. *Trends in Genetics, 16*(7), 279-283.
- Lagerström, M.C., and Schiöth, H.B. (2008). Structural diversity of G protein-coupled receptors and significance for drug discovery. *Nature Reviews Drug Discovery, 7*(4), 339-357.
- Langenhan, T.*, Aust, G.*, and Hamann, J.* (2013). Sticky signaling--adhesion class G protein-coupled receptors take the stage. *Science Signaling, 6*(276), re3.
- Lohse, M.J., Nuber, S., and Hoffmann, C. (2012). Fluorescence/bioluminescence resonance energy transfer techniques to study G-protein-coupled receptor activation and signaling. *Pharmacological Reviews, 64*(2), 299-336.
- Lohse, M.J., Maiellaro, I., and Calebiro, D. (2014). Kinetics and mechanism of G protein-coupled receptor activation. *Current Opinion in Cell Biology, 27*, 87-93.
- Mahoney, J.P., and Sunahara R.K. (2016). Mechanistic insights into GPCR-G protein interactions. *Current Opinion in Structural Biology, 41*, 247-254.
- Makino, C.L., Wen, X.H., and Lem, J. (2003). Piecing together the timetable for visual transduction with transgenic animals. *Current Opinion in Neurobiology, 13*(4), 404-412.
- Malbon, C.C. (2004). Frizzleds: new members of the superfamily of G-protein-coupled receptors. *Frontiers in Bioscience, 9*, 1048-1058.
- McMahon, A.P., and Moon, R.T. (1989). Ectopic expression of the proto-oncogene int-1 in Xenopus embryos leads to duplication of the embryonic axis. *Cell, 58*(6), 1075-1084.
- Messerer, R.*, Kauk, M.*, Volpato, D., Alonso Canizal, M.C., Klöckner, J., Zabel, U., Nuber, S., Hoffmann, C., and Holzgrabe, U. (2017). FRET studies of quinolone-based bitopic ligands and their structural analogues at the muscarinic M_1 receptor. *ACS Chemical Biology, 12*(3), 833-843.
- Milligan, G., and Kostenis, E. (2006). Heterotrimeric G-proteins: a short history. *British journal of pharmacology, 147*, S46-S55.

- Nahorski, S.R. (2006). Pharmacology of intracellular signaling pathways. *British journal of pharmacology, 147*, S38-S45.
- Nalesso, G., Sherwood, J., Bertrand, J., Pap, T., Ramachandran, M., De Bari, C., Pitzalis C and Dell'accio, F. (2011). WNT-3A modulates articular chondrocyte phenotype by activating both canonical and noncanonical pathways. *Journal of Cell Biology, 193*(3), 551-564.
- Nichols, A.S., Floyd, D.H., Bruinsma, S.P., Narzinski, K., and Baranski, T.J. (2013). Frizzled receptors signal through G proteins. *Cellular Signalling, 25*(6), 1468-1475.
- Niehrs, C. (2012). The complex world of WNT receptor signaling. *Nature Reviews Molecular Cell Biology, 13*(12), 767-779.
- Nikolaev, V.O., Bünemann, M., Hein, L., Hannawacker, A., and Lohse, M.J. (2004). Novel single chain cAMP sensors for receptor-induced signal propagation. *Journal of Biological Chemistry, 279*(36), 37215-37218.
- Nile, A.H., Mukund, S., Stanger, K., Wang, W., and Hannoush, R.N. (2017). Unsaturated fatty acyl recognition by Frizzled receptors mediates dimerization upon Wnt ligand binding. *Proc. Natl. Acad. Sci. USA, 114*(16), 4147-4152.
- Nuber, S., Zabel, U., Lorenz, K., Nuber, A., Milligan, G., Tobin, A.B., Lohse, M.J., and Hoffmann, C. (2016). β-Arrestin biosensors reveal a rapid, receptor-dependent activation/deactivation cycle. *Nature, 531*(7596), 661-664.
- Nusse, R., and Varnus, H. (1982). Many tumors induced by the mouse mammary tumor virus contain a provirus integrated in the same region of the host genome. *Cell, 31*(1), 99-109.
- Nusse, R., Brown, A., Papkoff, J., Scambler, P., Shackleford, G., McMahon, A., Moon, R., and Varmus, H. (1991). A new nomenclature for int-1 and related genes: the Wnt gene family. *Cell, 64*(2), 231.
- Nusse, R., and Varnus, H. (2012). Three decades of Wnts: a personal perspective on how a scientific field developed. *EMBO Journal, 31*(12), 2670-2684.
- Nusse, R., and Clevers, H. (2017). Wnt/β-catenin signaling, disease, and emerging therapeutic modalities. *Cell, 169*(6), 985-999.
- Oldham, W.M., and Hamm, H.E. (2008). Heterotrimeric G protein activation by G-protein-coupled receptors. *Nature Reviews Molecular Cell Biology, 9*(1), 60-71.
- Palczewski, K., Kumasaka, T., Hori, T., Behnke, C.A., Motoshima, H., Fox, B.A., Le Trong, I., Teller, D.C., Okada, T., Stenkamp, R.E., Yamamoto, M., and Miyano, M. (2000). Crystal structure of rhodopsin: A G protein-coupled receptor. *Science, 289*(5480), 739-745.
- Perrimon, N., and Mahowald, A.P. (1987). Multiple Functions of Segment Polarity Genes in Drosophila. *Developmental Biology, 119*(2), 587-600.

- Petersen, J.*, Wright, S.C.*, Rodríguez, D., Matricon, P., Lahav, N., Vromen, A., Friedler, A., Strömqvist, J., Wennmalm, S., Carlsson, J., and Schulte, G. (2017). Agonist-induced dimer dissociation as a macromolecular step in G protein-coupled receptor signaling. *Nature Communications, 8*(1), 226.
- Pin, J.P., Kniazeff, J., Goudet, C., Bessis, A.S., Liu, J., Galvez, T., Acher, F., Rondard, P., and Prézeau, L. (2004). The activation mechanism of class-C G-protein coupled receptors. *Biology of the Cell, 96*(5), 335-342.
- Rijsewijk, F., Schuermann, M., Wagenaar, E., Parren, P., Weigel, D., and Nusse, R. (1987). The Drosophila homolog of the mouse mammary oncogene int-1 is identical to the segment polarity gene wingless. *Cell, 50*(4), 649-657.
- Roed, S.N., Orgaard, A., Jorgensen, R., and De Meyts, P. (2012). Receptor oligomerization in family B1 of G-protein-coupled receptors: focus on BRET investigations and the link between GPCR oligomerization and binding cooperativity. *Frontiers in endocrinology, 3*, 62.
- Romero, G., Sneddon, W.B., Yang, Y., Wheeler, D., Blair, H.C., and Friedman, P.A. (2010). Parathyroid hormone receptor directly interacts with Dishevelled to regulate β-catenin signaling and osteoclastogenesis. *The Journal of Biological Chemistry, 285*(19), 14756–14763.
- Sahores, M., Gibb, A., and Salinas, P. C. (2010). Frizzled-5, a receptor for the synaptic organizer Wnt7a, regulates activity-mediated synaptogenesis. *Development, 137*(13), 2215-2225.
- Schulte, G.*, Bryja, V.*, Rawal, N., Castelo-Branco, G., Sousa, K.M., and Arenas, E. (2005). Purified Wnt-5a increases differentiation of midbrain dopaminergic cells and dishevelled phosphorylation. *Journal of Neurochemistry, 92*(6), 1550-1553.
- Schulte, G., and Bryja, V. (2007). The Frizzled family of unconventional G-protein-coupled receptors. *Trends in Pharmacological Sciences, 28*(10), 518-525.
- Schulte, G. (2010). International Union of Basic and Clinical Pharmacology. LXXX. The class Frizzled receptors. *Pharmacological Reviews, 62*(4), 632-667.
- Seifert, J.R.K., and Mlodzik, M. (2007). Frizzled/PCP signaling: a conserved mechanism regulating cell polarity and directed motility. *Nature Reviews Genetics, 8*(2), 126-138.
- Seitz, K.*, Dürsch, V.*, Harnoš, J., Bryja, V., Gentzel, M., and Schambony, A. (2014). β-Arrestin interacts with the beta/gamma subunits of trimeric G-proteins and dishevelled in the Wnt/Ca2+ pathway in xenopus gastrulation. *PLoS One, 9*(1), e87132.
- Sharma, M., Castro-Piedras, I., Simmons, G.E., and Pruitt, K. (2018). Dishevelled: A masterful conductor of complex Wnt signals. *Cellular Signalling, 47*, 52-64.
- Sheldahl, L.C., Park, M., Malbon, C.C., and Moon, R.T. (1999). Protein kinase C is differentially stimulated by Wnt and Frizzled homologs in a G-protein-dependent manner. *Current Biology, 9*(13), 695-698.

- Sheldahl, L.C., Slusarski, D.C., Pandur, P., Miller, J.R., Kühl, M., and Moon, R.T. (2003). Dishevelled activates Ca2+ flux, PKC, and CamKII in vertebrate embryos. *The Journal of cell biology, 161*(4), 769-77.
- Slater, P.G., Ramirez, V.T., Gonzalez-Billault, C., Varela-Nallar, L., and Inestrosa, N.C. (2013). Frizzled-5 receptor is involved in neuronal polarity and morphogenesis of hippocampal neurons. *PLoS One, 8*(10), e78892.
- Slusarski, D.C., Yang-Snyder, J., Busa, W.B., and Moon, R.T. (1997a). Modulation of embryonic intracellular Ca2+ signaling by Wnt-5A. *Developmental Biology, 182*(1), 114-120.
- Slusarski, D.C., Corces, V.G., and Moon, R.T. (1997b). Interaction of Wnt and a Frizzled homologue triggers G-protein-linked phosphatidylinositol signaling. *Nature, 390*(6658), 410-413.
- Sriram, K., and Insel, P.A. (2018). G Protein-Coupled Receptors as Targets for Approved Drugs: How Many Targets and How Many Drugs?. *Molecular Pharmacology, 93*(4):251-258.
- Steinhart, Z., Pavlovic, Z., Chandrashekhar, M., Hart, T., Wang, X., Zhang, X., Robitaille, M., Brown, K.R., Jaksani, S., Overmeer, R., Boj, S.F., Adams, J., Pan, J., Clevers, H., Sidhu, S., Moffat, J., and Angers, S. (2017). Genome-wide CRISPR screens reveal a Wnt-FZD_5 signaling circuit as a druggable vulnerability of RNF43-mutant pancreatic tumors. *Nature Medicine, 23*(1), 60-68.
- Steinhart, Z., and Angers, S. (2018). Wnt signaling in development and tissue homeostasis. *Development, 145*(11), dev146589.
- Stoddart, L.A.*, Kilpatrick, L.E.*, and Hill, S.J. (2018). NanoBRET approaches to study ligand binding to GPCRs and RTKs. *Trends in Pharmacological Sciences, 39*(2), 136-147.
- Stumpf, A.D., and Hoffmann, C. (2015). Optical probes based on G protein-coupled receptors - added work or added value?. *British Journal of Pharmacology, 173*(2), 255-266.
- Swarup, S., and Verheyen, E.M. (2012). Wnt/Wingless signaling in Drosophila. *Cold Spring Harbor perspectives in biology, 4*(6), a007930.
- Tauriello, D.V.*, Jordens, I.*, Kirchner, K., Slootstra, J.W., Kruitwagen, T., Bouwman, B.A., Noutsou, M., Rüdiger, S.G., Schwamborn, K., Schambony, A., and Maurice, M.M. (2012). Wnt/β-catenin signaling requires interaction of the Dishevelled DEP domain and C terminus with a discontinuous motif in Frizzled. *Proc. Natl. Acad. Sci. USA, 109*(14), E812-820.
- Tewson, P., Westenberg, M., Zhao, Y., Campbell, R.E., Quinn, A.M., and Hughes, T.E. (2012). Simultaneous detection of Ca2+ and diacylglycerol signaling in living cells. *PLoS One, 7*(8), e42791.

- Thiele, S., Zimmer, A., Göbel, A., Rachner, T.D., Rother, S., Fuessel, S., Froehner, M., Wirth, M.P., Muders, M.H., Baretton, G.B., Jakob, F., Rauner, M., and Hofbauer, L.C. (2018). Role of WNT5A receptors FZD_5 and RYK in prostate cancer cells. *Oncotarget, 9*(43), 27293-27304.
- Tian, H.*, Fürstenberg, A.*, and Huber, T. (2017). Labeling and single-molecule methods to monitor G protein-coupled receptor dynamics. *Chemical Review, 117*(1), 186-245.
- van Amerongen, R.*, Mikels, A.*, and Nusse, R. (2008). Alternative Wnt Signaling Is Initiated by Distinct Receptors. *Science Signaling, 1*(35), re9.
- van Unen, J., Stumpf, A. D., Schmid, B., Reinhard, N. R., Hordijk, P. L., Hoffmann, C., Gadella (jr.), T.W.J., and Goedhart, J. (2016). A new generation of FRET sensors for robust measurement of Gαi1, Gαi2 and Gαi3 activation kinetics in single cells. *PLoS One, 11*, e0146789.
- Veerapathiran, S., and Wohland, T. (2018). Fluorescence techniques in developmental biology. *Journal of Biosciences, 43*(3), 541-553.
- Venkatakrishnan, A.J., Deupi, X., Lebon, G., Tate, C.G., Schertler, G.F., and Babu, M.M. (2013). Molecular signatures of G-protein-coupled receptors. *Nature, 494*(7436), 185-194.
- Vilardaga, J.P.*, Bünemann, M.*, Krasel, C., Castro, M., and Lohse, M.J. (2003). Measurement of the millisecond activation switch of G protein-coupled receptors in living cells. *Nature Biotechnology, 21*(7), 807-812.
- Vilardaga, J.P., Bünemann, M., Feinstein, T.N., Lambert, N., Nikolaev, V.O., Engelhardt, S., Lohse, M.J., and Hoffmann, C. (2009). GPCR and G proteins: drug efficacy and activation in live cells. *Molecular endocrinology (Baltimore, Md.), 23*(5), 590-599.
- Vilardaga, J.P., Romero, G., Feinstein, T.N., and Wehbi, V.L. (2013). Kinetics and Dynamics in the G Protein-Coupled Receptor Signaling Cascade. *Methods in Enzymology, 522*, 337-363.
- Vinson, C.R., and Adler, P.N. (1987). Directional non-cell autonomy and the transmission of polarity information by the frizzled gene of Drosophila. *Nature, 329*(6139), 549-551.
- Vinson, C.R., Conover, S., and Adler, P.N. (1989). A Drosophila tissue polarity locus encodes a protein containing seven potential transmembrane domains. *Nature, 338*(6212), 263-264.
- Voloshanenko, O., Gmach, P., Winter, J., Kranz, D., and Boutros, M. (2017). Mapping of Wnt-Frizzled interactions by multiplex CRISPR targeting of receptor gene families. *FASEB Journal, 31*(11), 4832-4844.
- Wang, C., Wu, H., Katritch, V., Han, G.W., Huang, X.P., Liu, W., Siu, F.Y., Roth, B.L., Cherezov, V., Stevens, R.C. (2013). Structure of the human smoothened receptor bound to an antitumour agent. *Nature, 497*(7449), 338-343.
- Wang, W.*, Qiao, Y.*, and Li, Z. (2018). New insights into modes of GPCR activation. *Trends in Pharmacological Sciences, 39*(4), 367-386.

- Wang, Y. (2009). Wnt/Planar cell polarity signaling: a new paradigm for cancer therapy. *Molecular Cancer Therapeutics, 8*(8), 2103-2109.
- Weeraratna, A.T., Jiang, Y., Hostetter, G., Rosenblatt, K., Duray, P., Bittner, M., and Trent, J.M. (2002). Wnt5a signaling directly affects cell motility and invasion of metastatic melanoma. *Cancer Cell, 1*(3), 279-288.
- Wehrli, M.*, Dougan, S. T.*, Caldwell, K., O'Keefe, L., Schwartz, S., Vaizel-Ohayon, D., Schejter, E., Tomlinson, A., and DiNardo, S. (2000). Arrow encodes an LDL-receptor-related protein essential for Wingless signaling. *Nature, 407*(6803), 527-530.
- Willert, K., Brown, J.D.. Danenberg, E.. Duncan. A.W.. Weissman. I.L.. Reya. T.. Yates, J.R., 3rd, and Nusse, R. (2003). Wnt proteins are lipid-modified and can act as stem cell growth factors. *Nature, 423*(6938), 448-452.
- Wright, S.C.*, Alonso Cañizal, M.C.*, Benkel, T., Simon, K., Le Gouill, C., Matricon, P., Namkung, Y., Lukasheva, V., König, G.M., Laporte, S.A., Carlsson, J., Kostenis, E., Bouvier, M., Schulte, G., and Hoffmann, C. (2018). FZD_5 is a $G\alpha_q$-coupled receptor that exhibits the functional hallmarks of prototypical GPCRs. *Science Signaling*. [In Press].
- Wright, S., and Schulte, G. (2018). Frizzleds as GPCRs - more conventional than we thought!. *Trends in Pharmacological Sciences, 39*(9):828-842.
- Yang, Y., and Mlodzik, M. (2015). Wnt-Frizzled/planar cell polarity signaling: cellular orientation by facing the wind (Wnt). *Annual review of cell and developmental biology, 31*, 623-646.
- Yang, S., Wu, Y.*, Xu, T.H.*, de Waal, P.W.*, He, Y., Pu, M., Chen, Y., DeBruine, Z.J., Zhang, B., Zaidi, S.A., Popov, P., Guo, Y., Han, G.W., Lu, Y., Suino-Powell, K., Dong, S., Harikumar, K.G., Miller, L.J., Katritch, V., Xu, H.E., Shui, W., Stevens, R.C., Melcher, K., Zhao, S., and Xu, F. (2018). Crystal structure of the Frizzled 4 receptor in a ligand-free state. *Nature, 560*(7720), 666-670.
- Yu, J., and Virshup, D.M. (2014). Updating the Wnt pathways. *Bioscience Reports, 34*(5), e00142.
- Zhang, X., Zhao, F., Wu, Y., Yang, J., Han, G.W., Zhao, S., Ishchenko, A., Ye, L., Lin, X., Ding, K., Dharmarajan, V., Griffin, P.R., Gati, C., Nelson, G., Hunter, M.S., Hanson, M.A., Cherezov, V., Stevens, R.C., Tan, W., Tao, H., and Xu, F. (2017). Crystal structure of a multi-domain human smoothened receptor in complex with a super stabilizing ligand. *Nature Communications, 8*, 15383.
- Zhang, X., Dong, S., and Xu, F. (2018). Structural and druggability landscape of Frizzled G protein-coupled receptors. *Trends in Biochemical Sciences.* [In Press]
- Zeng, C.M., Chen, Z., and Fu, L. (2018). Frizzled Receptors as Potential Therapeutic Targets in Human Cancers. *International Journal of Molecular Sciences, 19*(5), 1543.
- Ziegler, N.*, Bätz, J.*, Zabel, U., Lohse, M.J., and Hoffmann, C. (2011). FRET-based sensors for the human M_1-, M_3-, and M_5-acetylcholine receptors. *Bioorganic and Medicinal Chemistry, 19*, 1048–1054.

* Contributed equally.

8. Curriculum Vitae

9. Acknowledgments

First and foremost, I would like to thank my first supervisor, Prof. Dr. Carsten Hoffmann, for giving me the great opportunity to do my PhD thesis in his group. His supervision during this time, and the constructive discussions and advice, helped me throughout this project. The beginning of the project was not easy, but when things do not work as expected, they end being definitely more interesting and worth doing.

I would also like to thank my second supervisor, Prof. Dr. Tobias Langenhan, for agreeing to be in my thesis committee, and for his feedback during our meetings.

I would also like to thank my third supervisor, Prof. Dr. Gunnar Schulte, for the valuable discussions and ideas for the project, and for his supervision during the time I spent in his lab. Also for sharing plasmids and the DVL KO cell line, which were used in this project.

Thank you to all the current and past members of AG Hoffmann, in particular to Dr. Benedikt Schmidt, Dr. Susanne Nuber and Nicole Ziegler, for their help at the beginning of my PhD. Special thanks to Cristina Perpiñá, for her constant support, the long but productive discussions, and for reviewing this thesis. Thanks also to Thea Maimari, for her help in writing the "Zusammenfassung", and for her support during this time. And thank you to Christine Salomon, for her assistance during these years.

I would also like to thank all the members of the WntsApp network. This project would not have existed as it is if it was not for all of you, the meetings, the scientific discussions, and of course the social part that came with them. It was an incredible experience. Thank you in particular to Jana Valnohova and Shane Wright, who were of great help during my research stay in their lab, and specially Jana for being so supportive. Thank you to Dr. Davide Proverbio and Dr. Teodor Aastrup for their assistance while performing experiments in Attana. Thanks also to Jakub Harnoš and Prof. Dr. Vitezslav Bryja, for sharing ideas, plasmids and reagents, and to Dr. Madelon Maurice, for the plasmid V5-mFZD$_5$, which is the basis of this project.

I would like to thank my family and friends, especially my parents, for their support from the very first moment. I would not be here if it was not for you. And my special thanks to Domingo, for your constant help and for being so caring and supportive, but most importantly, for following me in this adventure. It has been a long way, but as you told me once: "never stop dreaming, never stop believing, never give up, never stop trying, and never stop learning" (Roy T. Bennett).

Figure 28 and 29 are reprinted from ‘Structural Basis of Smoothened Activation in Hedgehog Signaling’, Huang et al., Cell 2018, Vol. 175(1), 295-297, with permission from Elsevier (required permissions for the use of these figures were obtained via RightsLink).